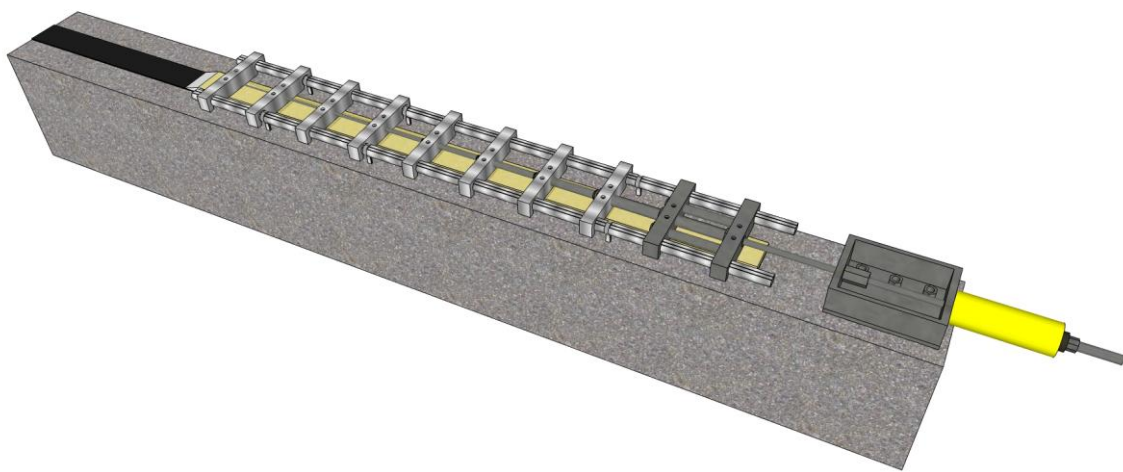


# CHALMERS



## A New Method for using Prestressed Fibre-Reinforced Polymer Laminates for Strengthening and Repair of Structural Members

*Master of Science Thesis in the Master's Programme Structural Engineering and  
Building Technology*

MARTIN FORNANDER, PATRIK NIHLMARK

Department of Civil and Environmental Engineering  
*Division of Structural Engineering*  
*Steel and Timber Structures*  
CHALMERS UNIVERSITY OF TECHNOLOGY  
Göteborg, Sweden 2013  
Master's Thesis 2013:124



MASTER'S THESIS 2013:124

# A New Method for using Prestressed Fibre-Reinforced Polymer Laminates for Strengthening and Repair of Structural Members

*Master of Science Thesis in the Master's Programme Structural Engineering and  
Building Technology*

MARTIN FORNANDER, PATRIK NIHLMARK

Department of Civil and Environmental Engineering  
*Division of Structural Engineering  
Steel and Timber Structures*  
CHALMERS UNIVERSITY OF TECHNOLOGY  
Göteborg, Sweden 2013

A New Method for using Prestressed Fibre-Reinforced Polymer Laminates for Strengthening and Repair of Structural Members

*Master of Science Thesis in the Master's Programme Structural Engineering and Building Technology*

MARTIN FORNANDER, **PATRIK NIHLMARK**

© MARTIN FORNANDER, PATRIK NIHLMARK, 2013

Examensarbete / Institutionen för bygg- och miljöteknik,  
Chalmers tekniska högskola 2013:124

Department of Civil and Environmental Engineering  
Division of Structural Engineering  
Steel and Timber Structures  
Chalmers University of Technology  
SE-412 96 Göteborg  
Sweden  
Telephone: + 46 (0)31-772 1000

Cover:

Illustration showing the prestressing device, the steel support box and the hydraulic jack mounted on a concrete beam.

Chalmers Reproservice / Department of Civil and Environmental Engineering  
Göteborg, Sweden 2013

# A New Method for using Prestressed Fibre-Reinforced Polymer Laminates for Strengthening and Repair of Structural Members

*Master of Science Thesis in the Master's Programme Structural Engineering and Building Technology*

MARTIN FORNANDER, PATRIK NIHLMARK  
Department of Civil and Environmental Engineering  
Division of Structural Engineering  
Steel and Timber Structures  
Chalmers University of Technology

## ABSTRACT

Strengthening and repair of bridges using adhered prestressed CFRP (Carbon Fibre Reinforced Polymers) laminates has many advantages compared to conventional strengthening methods using e.g. steel plates. The major drawback of prestressed CFRP laminates are the high shear stresses that arise near the laminate ends causing failure by plate debonding. This has traditionally been solved using mechanical anchors that require large modifications to the structure and time consuming inspections. To overcome this, a method where the prestressing force is introduced to the laminate in steps is developed. Experiments show that introducing the prestress in even steps over a distance of the laminate is an efficient way of eliminating the need of mechanical anchors.

A concept based on the theory of stepwise prestressing is further developed to enable convenient use outside of the test lab and to refine function and overcome practical issues. In order to develop the concept of stepwise prestressing, an in depth study of the behaviour of FRP strengthening systems is carried out. This includes identifying the parameters affecting the stress distribution and magnitude of the stresses along the bond line and the possible solutions to reduce the interfacial stresses. The main objective is to further develop and find practical ways of fulfilling the concept of stepwise prestressing.

The development of the prestressing concept will mainly be driven by FE-analyses using detailed models where the interfacial stresses are studied. This is necessary to identify and solve many of the problems that arise during the development of the concept. The theory of stepwise prestressing is proven to work and with the results of the FE-analyses, potential problem areas with the concept have been improved and several practical issues solved.

A working concept has been further refined and although it has been developed in several areas there is room for improvement. The many advantageous properties of prestressed CFRP strengthening are now available without the need of labour intensive mechanical anchors and time consuming inspections.

Key words: Strengthening, repair, FE-analysis, CFRP, stepwise prestressing, shear stress, peeling stress, mechanical analysis

# En Ny Metod för användning utav Förspända Fiberarmerade Polymer Laminat för Förstärkning och Reparation av Strukturella element

Examensarbete inom Structural Engineering

MARTIN FORNANDER

PATRIK NIHLMARK

Institutionen för bygg- och miljöteknik

Avdelningen för Konstruktionsteknik

Stål- och träbyggnad

Chalmers tekniska högskola

## SAMMANFATTNING

Reparations- och förstärkningsåtgärder av broar där förspända kolfiberlaminat används har flera fördelar jämfört med traditionella metoder där exempelvis stålskivor används. Metoden har dock en stor nackdel. Förspänningen av kolfiberlaminat ger upphov till höga skjuvspänningar i ändarna av laminatet. Dessa resulterar i brott i den svagare betongen. Detta har traditionellt lösts med hjälp av mekaniska ankare vilka kräver stora ingrepp på den ursprungliga konstruktionen och ofta tidskrävande inspektioner. För att undgå detta så har en metod där laminatet förspänns i flera steg utvecklats. Genom experiment har detta visat sig vara en effektiv metod att bli kvitt mekaniska ankare då förspänningskraften ökar stegvis över en längre sträcka av laminatet.

Ett befintligt koncept baserat på teorin om stegvis förspänning vidareutvecklas för att kunna tillämpas utanför testmiljön i labbet. Tekniken behöver förfinas och flera praktiska svårigheter klaras upp. För att kunna utveckla konceptet av stegvis förspänning så utförs en djupanalys av förstärkningssystem med fiberlaminat. Detta inkluderar de parametrar som påverkar spänningsfördelningen och spänningsamplituden längs gränsskiktet och de olika åtgärder som kan utnyttjas för att sänka denna. Huvudsyftet är att utveckla konceptet och hitta ett praktiskt sätt att uppföra stegvis förspänning.

Utvecklingen sker främst genom finita element analyser av detaljerade modeller där spänningar i gränsskiktet studeras. Detta är av stor vikt för att kunna identifiera och lösa de problem som uppstår under utvecklingen av konceptet. Teorin kring stegvis förspänning är bevisad att den fungerar och med hjälp av finita element analyser så har flertalet problemområden med konceptet förbättrats och många praktiska problem lösts.

Ett fungerande koncept har blivit vidareutvecklat och även om det på flera punkter blivit förfinat så finns det fortfarande utrymme för förbättring. Många av de fördelaktiga egenskaperna med förspända kolfiberlaminat är nu tillgängliga utan krav på mekaniska ankare eller tidskrävande inspektioner.

Nyckelord: Reparation, Förstärkning, kolfiber, stegvis förspänning, skjuvspänningar, normalspänningar, mekanisk analys

# Contents

1	INTRODUCTION	1
1.1	Background	1
1.2	Aim and objectives	5
1.3	Scientific approach	5
1.3.1	Literature study	5
1.3.2	Numerical modelling of the concept	5
1.3.3	Experimental verification of the concept	6
1.3.4	Analysis tools	6
1.4	Limitations	6
1.5	Outline of the thesis	6
2	GENERAL APPLICATIONS OF FRP MATERIALS	8
2.1	Materials in FRP composites and their properties	8
2.1.1	Fibres used in FRPs	8
2.1.2	Matrix material used in FRPs	10
2.2	Methods of manufacturing and installing different forms of FRPs	11
2.2.1	Manual methods	12
2.2.2	Semi-automated methods	12
2.2.3	Automated process	12
2.3	Properties of FRP composites	13
2.3.1	Mechanical properties of FRP composites	14
2.3.2	Glass transition temperature	15
2.3.3	Fatigue resistance	16
2.3.4	Moisture resistance	16
2.3.5	Fire performance	16
2.3.6	Exposure to ultraviolet radiation	17
2.3.7	Alkalinity and acidity	17
2.3.8	Temperature effects	17
2.3.9	Creep and relaxation	17
2.4	Properties of structural adhesives	17
2.4.1	Durability	18
2.4.2	Fatigue resistance of an adhesive joint	18
2.4.3	Creep behaviour	18
2.4.4	Fire performance	19
3	APPLICATIONS OF UNPRESTRESSED FRP COMPOSITES FOR STRENGTHENING AND REPAIR IN STRUCTURAL ENGINEERING	20
3.1	Introduction	20
3.2	Introduction of conventional methods of strengthening and repair	20
3.2.1	Strengthening and repair of concrete members	21
3.2.2	Strengthening and repair of steel members	22
3.3	Applications of FRP strengthening systems	23

3.3.1	Introduction to strengthening and repair with unprestressed FRP composites	23
3.3.2	Bonding of FRP composites	24
3.3.3	Application of FRP laminates	24
3.3.4	Flexural strengthening	29
3.3.5	Shear strengthening	30
3.3.6	Strengthening and confinement for compressive bearing capacity	30
3.4	Comparison of unprestressed FRP- and conventional- strengthening system	31
3.5	Stress analysis of adhesive joints	34
3.5.1	Definition of stress components	34
3.5.2	Distribution of stresses	35
3.5.3	Peeling stresses	36
3.5.4	Failure modes	37
3.5.5	Methods to influence stresses in adhesive joints	39
3.6	Critique of unprestressed FRP system	41
4	APPLICATIONS OF PRESTRESSED FRP LAMINATES	43
4.1	Introduction to prestressing	43
4.2	Prestressed CFRP laminates	44
4.2.1	Prestressing systems	44
4.2.2	Literature review of earlier experiments	46
4.2.3	Problem with prestressed laminates	48
4.2.4	Governing failure mode of prestressed laminates	49
4.2.5	Pre-stressing systems with mechanical anchors	50
4.3	Comparison of unprestressed systems with prestressed systems	52
4.4	Critique of prestressed systems with mechanical anchors	53
5	CONCEPT OF THE NEW PRESTRESSING METHOD	54
5.1	Concept of stepwise prestressing	54
5.1.1	Meier's technique based on the same principle	55
5.2	Description of the New Prestressing Method	56
5.2.1	Details of the concept	58
5.2.2	Advantages of the new technique	61
5.2.3	Application of the new technique	61
6	FE-MODELLING OF THE CONCEPT	63
6.1	Parametric study	63
6.1.1	Influence of different number of prestressing steps	65
6.1.2	Influence of adhesive stiffness	67
6.1.3	Influence of the stiffness of the CFRP laminates	68
6.1.4	Influence of different tab spacing	69
6.1.5	Conclusions from the parametric study	70
6.2	FE-model of the concept without the prestressing device	71
6.2.1	Shear stress in the middle of the adhesive layer	74



6.2.2	Axial force in the laminate and effect of GFRP and tapering	74
6.2.3	Shear stress in the concrete beneath the adhesive	75
6.2.4	Stress in the adhesive between the CFRP and GFRP	76
6.2.5	Stress in the GFRP and steel plate in the middle of the GFRP	76
6.2.6	Stress in the steel nuts and steel plate	77
6.2.7	Changes made to the concept	79
6.3	FE-model of the concept with the prestressing device	80
6.3.1	Removing the nuts on one side of the tabs in the device	81
6.3.2	Changing the first two tabs from aluminium to steel	81
6.3.3	Three springs	83
6.3.4	Difference between locked and free ends of guiding bars	86
6.3.5	Effect of stiffness of the guiding bars	87
6.3.6	Effect of stiffer GFRP laminate	88
6.3.7	The final resulting shear stress distribution	90
6.4	Modelling of details of the concept	92
6.4.1	Temporary prestressing support	92
6.4.2	Holdings for the guiding bars	94
6.4.3	Aluminium tabs	95
7	EXPERIMENTAL VERIFICATION OF THE PRESTRESSING DEVICE	96
7.1	Experiments carried out in advance at Chalmers	96
7.1.1	Effect on Serviceability Limit State	97
7.1.2	Efficiency of strengthening and failure mode	98
7.1.3	Improved stiffness	98
8	DISCUSSION	99
9	FINAL REMARKS	101
9.1	Conclusions	101
9.2	Suggestions on future research	102
10	REFERENCES	104

APPENDIX A	Derivation of formulas for calculation of interfacial shear stress in the adhesive, axial force in the laminate, and bending moment of the strengthened beam
APPENDIX B	Calculations of a reinforced concrete beam strengthened with CFRP laminate
APPENDIX C	Hand calculations for the temporary prestressing support
APPENDIX D	Photographs and results from the experimental verification of the prestressing device

## Preface

In this thesis project, a new technique for prestressing fibre-reinforced polymer laminates for strengthening and repair of structural members has been developed. To verify the technique, a prototype of the prestressing device was manufactured to prestress a carbon fibre laminate and bond it to a concrete beam. The tests have been carried out from June 2013 to July 2013. The work is a part of a European research project (PANTURA) concerning strengthening and repair of bridges. The project has been carried out at the Department of Structural Engineering, Steel and timber Structures, Chalmers University of Technology, Sweden.

All parts of the project have been carried out with Dr. Reza Haghani as supervisor and examiner and the tests were carried out in the laboratory of the Department of Structural Engineering at Chalmers University of Technology. We would like to express our sincere gratitude and appreciation to Dr. Reza Haghani for his guidance, knowledge, and understanding during the project work. Additionally, our thanks go out to Mohammad Al-Emrani, Mohsen Heshmati, and Nils Nilsson for their interest, ideas, and contributions to the project.

Finally, we extend our appreciation to all researches and laboratory staff at the Department of Structural Engineering at Chalmers University of Technology for their professional conduct and for providing a nurturing work environment.

Göteborg september 2013

Martin Fornander, Patrik Nihlmark

# Notations

## Roman upper case letters

$A_b$	Cross-sectional area of the beam
$A_f$	Cross-sectional area of fibres
$A_g$	Cross-sectional area of the gross cross-section
$A_l$	Cross-sectional area of the laminate
$A_s$	Cross-sectional area of the tensile reinforcement
$A'_s$	Cross-sectional area of the compressive reinforcement
$E$	Modulus of elasticity
$E_b$	Modulus of elasticity of the beam
$E_f$	Final modulus of elasticity of the composite
$E_{fibre}$	Component modulus of elasticity of the fibres
$E_{matrix}$	Component modulus of elasticity of the matrix material
$E_l$	Modulus of elasticity of the laminate
$F_{fp\ max}$	Maximum prestressing force in laminate
$G_a$	Modulus of rigidity of the adhesive
$I_b$	Second moment of area of the beam
$I_g$	Moment of inertia of gross cross-section
$L$	Length of the laminate
$M$	Bending moment in the laminate
$M_b$	Bending moment in the beam due to prestressing
$P_0$	Initial prestressing force in the laminate
$P_{max}$	Full prestressing force in the laminate
$P_l$	Prestressing force in the laminate after bonding and releasing
$V_{fibre}$	Fibre volume fraction of the composite
$T_g$	Glass transition temperature

## Roman lower case letters

$b_l$	Width of the laminate
$d$	Distance from extreme compression fiber to centroid of tension reinforcement
$e$	Eccentricity from the interface between the laminate and the adhesive and the middle of the laminate
$e_p$	Eccentric distance from the bottom of the beam
$f_{F,max}$	Failure point for the fibre
$f_{m,max}$	Failure point of the matrix material
$h_s$	Height of the beam

$k$	Ratio of depth of neutral axis to reinforcement depth measured from extreme compression fibre
$r_g$	Cross-section radius of gyration
$t_a$	Thickness of the adhesive layer
$y_1$	Distance from neutral axis to outermost compressed fibre
$y_2$	Distance from neutral axis to outermost tensile fibre

### Greek lower case letters

$\alpha_1$	Maximum angle of the force development in the laminate
$\alpha_2$	Maximum angle of the force development in the laminate with stepwise prestressing
$\beta$	Factor for the relation between the slope of the axial force in the laminate and shear stress in the adhesive
$\sigma$	Stress level
$\varepsilon$	Strain level
$\varepsilon_{F,\max}$	Failure strain of the fibre
$\varepsilon_{m,\max}$	Failure strain of the matrix material
$\gamma$	Shear strain
$\tau$	Shear stress level
$\sigma_x$	Stress level
$\sigma_y$	Stress level
$\tau_{xy}$	Shear stress level
$\delta_s$	Displacement in the outermost fibres of the beam lower flange
$\delta_l$	Displacement in the laminate
$\omega$	Constant

### Abbreviations

°C	Degree Celsius
A-glass	Alkali-lime glass (window glass)
AR-glass	Alkali-resistant glass
E-glass	Electrical glass (most commonly used glass fibre)
S-glass	Structural or high-strength glass
A	Area
AFRP	Aramid Fibre-Reinforced Polymer
CAE	Complete Abaqus Environment
CFRP	Carbon Fibre-Reinforced Polymer
E-modulus	Young's modulus, modulus of elasticity
EB	Externally Bonded
EC	EuroCode
EMPA	Swiss Federal Laboratories for Material Science and Technology
FE	Finite Element
FRP	Fibre-Reinforced Polymer
G	Giga-

GFRP	Glass Fibre-Reinforced Polymer
h	hour
HM	High-Modulus
HS	High-Strength
k	kilo-
LVDT	Linear Variable Differential Transformer
M	Mega-
m	meter
m	milli-
N	Newton
NSMR	Near Surface Mounted Reinforcement
Pa	Pascal
PAN	Poly-Acrylo-Nitrile
PANTURA	A research project
PVC	Poly-Vinyl-Chloride
RC	Reinforced Concrete
ROBUST	A research project in the United Kingdom
RTM	Resin Transfer Moulding
UHM	Ultra-High-Modulus
UV	Ultra-Violet







# 1 Introduction

## 1.1 Background

At the present, Fibre-Reinforced Polymer (FRP) composites are widely used for strengthening and repair of existing structures [1]. They are also used in entirely new structures made completely from FRP, as well as structural elements in composite structures, i.e. hybrid structures of, for example, steel, concrete, and FRP. Examples of structures that have been made of FRP are bridge decks, bridge enclosures, and fairings. FRP composites are used to strengthen structures with insufficient capacity in bending, shear or compression.

One of the challenges ahead of road authorities and bridge owners at present is to keep bridges in service for current traffic demands at an acceptable safety level. Important reasons for upgrading of bridges include aging and deterioration, increasing traffic demands in terms of axle load and traffic intensity and higher safety demands. The majority of railway bridges in Europe are old [2]. Of all bridge types surveyed between 2003 and 2006, only about 11% are less than 20 years old, 22% are between 20 and 50 years old, 31% are between 50 and 100 years old, and 35% are older than 100 years. More detailed statistics on the age profile of different bridge types, from the European research project PANTURA, can be seen in Table 1.1.

Table 1.1 Age profile of railway bridges in Europe [2].

Bridge type	<20	20-50	50-100	>100
Concrete	25%	55%	16%	4%
Metallic	10%	22%	40%	28%
Arches	1%	1%	34%	64%
Steel/concrete composite	25%	33%	35%	7%

Furthermore, higher traffic demands are expected in the future and the railway traffic have increased over the last decades, see Figure 1.1.

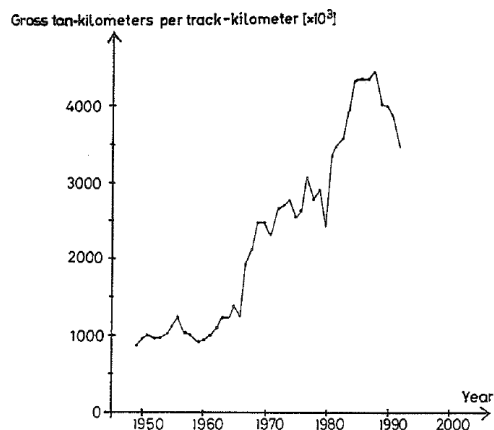


Figure 1.1 Graph showing the increasing railway traffic in Europe [3].

Another goal in Europe is to increase the maximum axle traffic load to 33 tons. However, many of the existing bridges today are only designed for a maximum of 18 tons, meaning there is a need for strengthening of those bridges [2]. Also, the fact that more and more high speed trains are used the dynamic load on the bridges are increased. Demand of higher safety is also a factor which increases the need for strengthening and repair.

Due to that the traffic intensity is increasing, the demands from clients has become stricter and above all they require a strengthening method that is non-disruptive to the traffic, meaning that it should be quick and easy to apply [2]. The method should also be durable and require minimal maintenance during the structures remaining service life.

The number of reinforced concrete structures that reach the end of their service life is increasing as a result of a more widespread use of de-icing salts, environmental factors causing deterioration of concrete and reinforcement and an increase in applied loads [4]. The majority of these structures are in dire need of replacement or rehabilitation and the deterioration may have made the structures obsolete functionally and even structurally lacking. Often, the only feasible solution to replacement of these structures is strengthening – which is a rather cost-effective alternative.

There are a number of upgrading, including strengthening and repair, techniques for concrete and steel bridges [2]. Some of these methods for concrete and steel structures are described in Chapter 3, Section 3.2.

One of the most common techniques for strengthening and repair of concrete and steel bridges is to use steel plates added to the weak parts of the structure in order to increase the bending and shear resistance of the structure and stabilize it against different types of instability [2]. Using steel plates, for strengthening and repair purposes, involves several difficulties. Such as the compatibility of old and new steel, unintended contact of old and new steel, and durability issues are important considerations when this method is used [5]. Furthermore, extra maintenance is needed for the new steel plates including surface preparation, painting and regular inspections. The extra maintenance adds to the costs and complications of this traditional method. Additionally, there are several practical difficulties with the method due to the material properties of steel. The high density of steel makes it difficult to handle the plates on the installation site and usually heavy lifting machinery is needed for this purpose. The plates are often cut in limited lengths, for transportation purposes, which necessitate splicing – this causes problems of joining the plates, which is mostly done by on-site welding, and creating poor fatigue details. These considerations are time-consuming and labour intensive and without them problems such as, e.g., lowered bond strength due to corrosion at the steel/adhesive interface might occur.

Bonding FRP laminates to exposed faces of concrete members is a non-corrosive, efficient, and light-weight alternative to other rehabilitative and strengthening methods [6]. Therefore, as an alternative to strengthen concrete structures with steel plates, FRP laminates and sheets have been used as they provide a solution to durability problems caused by corrosion of steel [7]. Since FRPs are well suited to strengthen deteriorated structures due to their advantageous characteristics, the use of FRP strengthening in civil engineering has correspondingly grown rapidly in recent

years [4]. The strengthening of weakened concrete members with FRPs is becoming a more and more promising and effective solution.

The use of FRPs in strengthening applications was suggested in the mid-1980s as a replacement for steel plates [5]. The suggestion was prompted due to the rather significant shortcomings of using steel plate bonding some of which have been mentioned in previous paragraphs. FRPs, however, have a high strength-to-weight ratio, a low maintenance cost, good fatigue properties, and a high resistance against corrosives such as alkalis, salts, and acids under a wide range of temperatures [4], [5]. In comparison to a steel strengthening system, an equivalent FRP system requires much fewer resources to install and being that it consists of a non-corrosive material it's a more durable solution [6]. The non-corrosive characteristic of FRP is its most significant advantage. However, a disadvantage is that the material cost of FRP is comparatively high. Nevertheless, FRP composites often prove to be the most economical choice because of the dramatic reduction of labour costs, mainly due to the quick and easy application of the FRP [4], [6]. As a result, the use of FRPs can greatly reduce the overall costs of a project and minimize traffic disruptions due to the quick application.

The method of strengthening structures with FRP composites has been investigated experimentally and thus there have been guidelines and codes published addressing the technology [6]. Many structures of different materials (steel, iron, concrete, masonry, and timber) have been successfully strengthened throughout the world with Carbon FRP (CFRP) composites.

The most important problem in CFRP laminate bonded beams is the high stress concentration at the area close to the laminate end which usually triggers debonding of the laminate at this location [8]. Studies show that debonding often takes place far before the ultimate strength of the laminate is reached (at around a utilization ratio of 50%) which makes the method somewhat expensive from an economical point of view with regard to the high cost of CFRP materials.

FRP composites that are unprestressed, also called passive strengthening technique, cannot support the dead load of a structure [4], [7]. They solely provide resistance and support to added live loads applied after bonding of the FRP. Studies have shown that unprestressed FRP when bonded to a damaged concrete member on the tensile face, will enhance the flexural strength of the member [4]. On the other hand, the behaviour at failure can become more brittle and in zones of high shear concentration, peeling and delamination of the FRP can occur. Information about peeling and delamination may be found by the reader in Chapter 3, Section 3.5.

Strengthening structures by applying external prestressing on passively bonded FRP laminates is a new innovative area that has emerged [6]. In comparison to the study of unprestressed FRP for strengthening of concrete members, only recently has the application of prestress been studied [7]. The technique of prestressing FRP is referred to as active strengthening technique [4]. This method combines the advantages with external prestressing to the benefits of the unprestressed FRP laminate system [6]. The FRP laminates used in the prestressing method is of the same materials which are used in the previous method (strengthening with unprestressed FRP), i.e. has the same advantageous characteristics such as being non-corrosive and lightweight. In comparison with unprestressed FRP, which may fail prematurely by peeling, the prestressed FRP utilize a greater part of the tensile capacity and can attain the full tensile strength, thereby using the material more efficiently [4].

Both dead and live loads carried by a structure may be supported by prestressed FRP [4]. Before additional deformations occur in a structure, prestressed FRP contribute to the load carrying capacity. A few systems to prestress laminates have been devised for flexural strengthening, and also for shear strengthening and confinement [6]. Furthermore, three different field applications have been completed of the prestress technology. The reader is directed to Chapter 4, Section 4.2.1, for more detailed description of the three different systems of prestressing.

By prestressing FRP laminates and bonding them to a concrete beam on the tension face the deflection is limited, the cracks may be controlled and as a result the durability of the concrete is improved [7]. The deterioration of the concrete is directly related to the crack widths and their propagation and growth with time. Hence, the serviceability of a beam is improved by delaying the onset of cracking and providing crack control by reduction in crack widths [4]. Additionally, the durability is improved since the moisture access is limited to the adhesive layer and to the concrete because existing cracks in the structures may be closed by using prestress. Compared to concrete beams strengthened with unprestressed FRP, the ultimate loads in beams strengthened with prestress have been shown to attain a higher value since the failure mode may change and premature failure modes may be prevented [4], [7]. Moreover, a weakened concrete structure may have suffered a loss of internal prestressing, and by strengthening with prestressed FRP the prestressing to the internal reinforcement can be restored (by shifting the load and giving the internal reinforcement time to recover).

Even though there are many advantages with strengthening by bonded prestressed FRP composites, some of which have been mentioned in the previous paragraph, there is a problem at the end zones, or anchorage zones, because of the high stress concentration accumulated there [7]. The strengthening with prestressed FRP technique may be made more efficient by prestressing before bonding to the concrete surface using a suitable anchorage system [4]. FRP laminates shear off at the end zones even with a low level of prestressing, if special anchoring isn't used.

The problem of failure may be solved in a few different ways [7]. By using end anchors the problem of failure may be solved. Peeling failure may be prevented by increasing or decreasing the layers of FRP, by successively cutting the FRP along the beam, or by geometry changes of the FRP at the anchorage zone. All techniques mentioned reduce the magnitude of normal and shear stress concentrations at the end of the FRP laminate. By using end anchorages when strengthening beams with prestressed FRP composites, higher loads are achieved and a more ductile behaviour is exhibited.

A method which gradually prestress the FRP laminate has been developed by Meier in 2001 [7]. This method use heating elements that cure the epoxy quicker without decreasing the overall thickness of the FRP, which reduces the prestress force gradually to zero at the end of the FRP laminate. Risk of shearing is thereby prevented and the need of tensioning heads or anchorage devices is eliminated. The method is however cumbersome and impractical due to the complications induced by the heating moment of the procedure.

Based on the idea of Meier to use stepwise prestressing a new technique is developed that eliminates the shortcomings of the Meier method. The new method could be carried out without limitations in number of steps and could be performed with or

without fast curing. It introduces a novel way of introducing the prestressing force to the laminate which eliminates the need for mechanical anchorage.

## **1.2 Aim and objectives**

The Master's thesis aim to develop a stepwise prestressing system of bonded CFRP laminates for strengthening and repair of concrete and steel structures that eliminate the need for mechanical anchorage, thereby removing the shortcomings involved in other stepwise prestressing systems. The system will be developed with regard to requirements from clients and site conditions. The thesis is performed in cooperation with the European project PANTURA for Tenroc Technologies and Trafikverket.

The objectives of this thesis are:

1. In depth study of the behaviour of FRP strengthening systems such as force transfer mechanisms and failure modes in unprestressed and prestressed systems. This includes identifying the parameters affecting the stress distribution and magnitude of the stresses along the bond line.
2. Identification of possible solutions to reduce the interfacial stresses in the bond line.
3. Identification of possible practical ways to fulfil step 2.

## **1.3 Scientific approach**

### **1.3.1 Literature study**

The thesis starts with a state-of-the-art literature study of existing unprestressed and prestressed FRP systems with focus on their advantages and disadvantages. In order to study strengthening systems with FRP laminates the literature study begins by examining different FRP materials and their properties (Chapter 2). Thereafter, the study examines the application of existing unprestressed and prestressed FRP strengthening systems (Chapter 3 and Chapter 4 respectively).

### **1.3.2 Numerical modelling of the concept**

Numerical modelling of the concept is performed to evaluate suggestions for improvement which, in turn, are derived from the client needs, requirements and demands.

A parametric study on a 2D FE (Finite Element)-model of a concrete beam prestressed with a CFRP laminate is performed to investigate the effect of the following factors:

- the E-modulus of the adhesive,
- the E-modulus of the CFRP laminate,
- the thickness of the CFRP laminate,
- the different tab spacing's of the new strengthening technique.

See Chapter 6, Section 6.1 for the parametric study.

The parametric study is followed by a 3D FE-analysis of the concept with stepwise prestressing without the prestressing device attached (Chapter 6, Section 6.2). The analysis establishes various stresses in the different components of the concept and concludes by presenting changes made to the concept based on the resulting stresses.

The numerical modelling continues with analysing a 3D FE-model of the concept with the prestressing device attached (Chapter 6, Section 6.3). This is a more refined model which is used to examine what effects factors such as, e.g., the material of the tabs and amount of springs between the tabs have on the stress distribution. The main purpose of this analysis is to investigate these effects in order to find a solution that reduces the high interfacial shear stresses at the end of the laminate. The analysis is concluded with the final resulting shear stress distribution.

Finally, numerical modelling is done on the temporary prestressing support, the holders for the guiding bars and the aluminium tabs in order to check the stresses and adjust the dimensions and properties of these components accordingly (Chapter 6, Section 6.4).

### **1.3.3 Experimental verification of the concept**

The concept is verified experimentally by performing experimental investigations as well as studying and comparing with previous laboratory test results.

Based on earlier experiments carried out at Chalmers, the existing concept will undergo refinement and modifications to improve upon and develop the system so it will be possible to use in practise.

### **1.3.4 Analysis tools**

The numerical FE-modelling and analysis of stresses and strains of the prestressing concept is performed with the commercial software Abaqus CAE version 6.11-3. Results from the Abaqus numerical analyses have been compiled, organised and illustrated graphically using Microsoft Excel. Calculations done in Appendix B have been performed with MathCAD 15. Illustrations of the concept were drawn in AutoCAD, Google Sketch Up, and Microsoft Visio.

## **1.4 Limitations**

The thesis is limited to studying the strengthening and repair of concrete and steel beams with CFRP laminates. Specifically, the flexural strength of a concrete beam strengthened with a CRFP laminate is examined. Shear strengthening and confinement with CFRP is mentioned but not investigated to any further extent. The authors limit themselves to study CFRP laminates and no other types of CFRP composites such as sheets or other types of FRP materials.

The experimental verification of the concept is to be performed on one reinforced concrete beam, however results from previous experiments performed at Chalmers will be included and studied in the thesis.

## **1.5 Outline of the thesis**

The chapters 2, 3 and 4 encompass the literature study. The outline for the literature study have been chosen to emphasize a logical flow of information with regard to the

application of unprestressed and prestressed FRP strengthening systems so to enable comparisons and conclusions to be drawn between the two as well as between the new prestressing method.

Chapter 2 presents general information about FRP. More specifically, Chapter 2 introduces the different constituents in FRP composites, the characteristics of the materials, and the FRP composites themselves. Additionally, the application of the different FRP composites in civil and structural engineering is presented. A special focus is placed on CFRP, due to its favourable properties for prestressing.

Chapter 3 explains how unprestressed FRP composites are used for strengthening and repair works in structural engineering. Chapter 3 ends by analysing and critically reviewing the problems with the unprestressed strengthening systems.

Chapter 4 begins with an introduction to the application of prestress to FRP laminates; the advantages and disadvantages of adding prestressing to FRP laminates before bonding them to structural members. Specifically, the drawbacks of using mechanical anchors are emphasised in this chapter.

Chapter 5 describes the background, theory and concept of the new method of prestressing CFRP laminates. The chapter also explains how the method is used in practise to get the desired stepwise prestressing and the associated practical issues.

Chapter 6 presents the results from the FE-modelling and describes the different models and the process in which they change and become more refined depending on the results. The chapter ends by describing the modelling of the details of the prestressing device.

Chapter 7 concerns the experimental verification of the concept. By studying and comparing previous tests done in literature and at Chalmers, the theory of stepwise prestressing, and FE-analyses verify whether the new concept is viable, efficient and practical.

In Chapter 8 the results of the study is discussed.

The thesis is concluded in Chapter 9, where conclusions are drawn whether the study has fulfilled the aim and objectives of the thesis. Finally, suggestions for future research are presented.

## 2 General Applications of FRP Materials

This chapter presents general properties and characteristics of the materials used when strengthening and repairing with FRP composites. This includes properties of fibres, resins, composites and structural adhesives as it is very important that the correct material is used to ensure and maximize the service life requirements. The focus is on carbon fibres and CFRP, as almost 95% of all strengthening applications are carried out with CFRP due to its superior properties with regard to strength and stiffness, and aptitude for prestressing. Aramid and glass fibres are also mentioned.

### 2.1 Materials in FRP composites and their properties

A composite material is composed of two or more different constituents with, usually, significantly different properties [1]. To be defined as a composite material the combined properties of the constituents must produce a material with characteristics different from the individual components. Furthermore, the components should remain separate and distinct within the finished structure.

Composite materials is not a new idea; mud straw bricks are an example of an application at a very early age [9]. The straws contribute with tensile strength and bind the mud together while the mud contributes with compressive strength. Like the mud bricks, FRPs consist of fibres and a matrix material, i.e. a binding material. The fibres contribute with stiffness and strength while the matrix material binds the fibres together and protects them against degradation and wear.

#### 2.1.1 Fibres used in FRPs

There are three different types of fibres commonly used in civil engineering; carbon, aramid and glass fibres [10]. The main fibres used in structural engineering are carbon and glass fibres and for strengthening purposes almost 95% are carbon fibres [11]. For strengthening of structures in bending using prestressed FRPs, carbon fibres are used for their suitable properties such as high strength and stiffness. Typical properties for the different fibres are presented in Table 2.1.

Table 2.1 Typical properties of reinforcing fibres [12].

	Carbon fibre			Aramid fibre	E-Glass fibre
	High-strength (HS)	High-modulus (HM)	Ultra-high-modulus (UHM)		
Modulus of elasticity [GPa]	230-240	295-390	440-640	125-130	70-85
Strength [MPa]	4300-4900	2740-5940	2600-4020	3200-3600	2460-2580
Strain to failure [%]	1.9-2.1	0.7-1.9	0.4-0.8	2.4	3.5
Density [kg/m <sup>3</sup> ]	1800	1730-1810	1910-2120	1390-	2600



				1470	
Coefficient of thermal expansion (parallel to fibre) [ $10^{-6}/^{\circ}\text{C}$ ]	-0.38	-0.83	-1.1	2.1	4.9

### 2.1.1.1 Carbon fibres

Carbon fibres have high strength, high stiffness and they are light-weight [12]. They have a low thermal expansion but a high electrical conductivity.

There are different types of carbon fibres which are categorized depending on the manufacturing process [12]:

- High-strength (HS),
- High-modulus (HM),
- Ultra-high-modulus (UHM).

Generally, carbon fibres with a higher stiffness have lower tensile strength and vice versa [12]. UHM carbon fibres are very brittle and therefore CFRP composites require special care when handled.

Carbon fibres are manufactured from mainly two raw materials. About 90% of the carbon fibres are manufactured from poly-acrylonitrile (PAN) and the rest is made from rayon or petroleum pitch [1], [13]. With the PAN precursor material, i.e. starting with a PAN fibre, a round cross-section fibre is manufactured by spinning of the original precursor fibre with a yield of only 50%. The PITCH precursor fibres are derived from petroleum, asphalt, coal tar and polyvinyl chloride (PVC). With the PITCH precursor the yield is much higher; however the produced fibres are of uneven quality from batch to batch. The pitch precursor is invariably used to produce UHM fibres. In the process of making the fibres there are four steps which includes a stabilization process at  $200^{\circ}\text{C}$  - $300^{\circ}\text{C}$ , a carbonation process at temperatures above  $800^{\circ}\text{C}$  and a graphitization process at temperatures above  $2000^{\circ}\text{C}$ . HS and UHM fibres are produced in the same way although the ultra-high stiffness fibres are heat treated (the graphitization process) at a higher temperature.

### 2.1.1.2 Aramid fibres

In the 1980s the first prestressing tendons were manufactured with aramid fibres, usually presented under their commercial names; Kevlar and Twaron [13], [14]. Today very few manufacturers produce them. Aramid fibres have high toughness and are not brittle in non-composite form as carbon- and glass- fibre, but they exhibit other weaknesses. The combination of their relatively high price, low compression and shear strength, difficulty in processing, low resistance against ultraviolet (UV) radiation and moisture has made the fibres less attractive for structural engineering [9], [14].

### 2.1.1.3 E-glass fibres

E-glass fibres are the most commonly used glass fibre but there are also A-glass, AR-glass and S-glass [1]. A-glass (window glass) and AR-glass (alkali resistant glass) are used for specialized products in structural engineering and S-glass (extra high-strength glass) is usually used in aerospace technology. E-glass fibres are used for a lot of different structural components including reinforcement bars for concrete, FRP strengthening fabrics and FRP structural profile shapes. Glass fibres are the least stiff

and strong compared to aramid- and carbon- fibres, but they are the cheapest. The E-Glass fibres are weak against highly acidic or alkaline environments and are also susceptible to creep.

### 2.1.2 Matrix material used in FRPs

The matrix material, or the resin, is the constituent that holds the fibres together, fixes them in place, and provides the integrity of the composite material [12]. One of the most important functions of the matrix is to transfer force between the fibres, but it also has to protect the fragile fibres against wear, impact and environmental degradation.

The properties of the resin affect the properties of the final composite [12]. The different types of resins available all have different properties regarding stiffness and strength as well as heat, fire and chemical resistance, affecting the durability of the composite. The most usual matrix materials and some of their properties are presented in Table 2.2.

Table 2.2 Typical properties of resins [12].

	Epoxy	Polyester	Phenolic	Polyurethane
Modulus of elasticity [GPa]	2.6-3.8	3.1-4.6	3.0-4.0	0.5
Tensile strength [MPa]	60-85	50-75	60-80	15-25
Strain to failure [%]	1.5-8.0	1.0-2.5	1.0-1.8	10
Poisson's ratio	0.3-0.4	0.35-0.38	not available	0.4
Density [kg/m <sup>3</sup> ]	1110-1200	1110-1250	1000-1250	1150-1200
Coefficient of thermal expansion [10 <sup>-6</sup> /°C]	30-70	30-70	80	40

#### 2.1.2.1 Epoxy resins

Epoxy resins have qualities including high specific strength, good dimensional stability, high temperature resistance and good resistance to solvents and alkalis [12]. Additionally, they exhibit a toughness that is superior to a lot of other civil engineering polymers. Epoxy resins have good adhesion to most materials and exhibit a low shrinkage, usually 2-3%, during polymerization [9]. One drawback is that they often have a limited resistance against acids [12]. Most pre-cured CFRP composites are made with epoxy resins and they are also used extensively for dry sheets and fabrics acting as both adhesive and resin [14].

#### 2.1.2.2 Polyester and vinyl ester resins

Polyester resins, compared to epoxy resins, are cheaper and easy to process and they are frequently used as resins for larger pultruded structural profiles, see Section 2.2.3 for an explanation of the pultrusion method, and pre-formed FRPs [14]. The mechanical

properties though, are not as good as epoxies and the curing is highly exothermic and thus experience significant shrinkage. Vinyl esters are closely related to the polyester resins but with better temperature stability and environmental resistance, although they also suffer from significant curing shrinkage [12]. Polyester resins are being replaced more and more by vinyl ester resins which have superior resistance against alkaline environments. Vinyl ester resin is often called modified epoxy resin or epoxy vinyl ester resin because it is a hybrid of an epoxy and a polyester resin [14].

### **2.1.2.3 Phenolic resins**

Phenolic resins have advantageous properties with respect to fire [12]. They have a high-resistance and emit a low amount of toxic fumes and smoke during fire. However, they have a low toughness and are more hygroscopic than other resins, and therefore absorbed moisture will evaporate during fire resulting in severe damage to the bond. The use of phenolic resins for FRP products are limited and they are used particularly in FRP strengthening strips for timber structures and in walkway gratings for offshore platforms [14].

### **2.1.2.4 Polyurethane resins**

Polyurethane resins come in several different formulas and are generally a bit weaker than epoxies [14]. On the other hand they have a high tolerance against chemicals and an adequate resistance against moisture, nevertheless they suffer from extensive curing shrinkage, creep and moisture movements [12].

## **2.2 Methods of manufacturing and installing different forms of FRPs**

The final properties of FRPs are heavily dependent on the manufacture process [12]. The manufacture process of FRPs can be organised into three basic techniques:

- Manual methods,
- Semi-automated methods ordered,
- Automated methods.

The fibres can be arranged in several layers with different direction to achieve desired properties [13]. Unidirectional FRP laminates have their fibres arranged mainly in one direction making them highly anisotropic, while sheets or yarns are woven with the fibres arranged perpendicular to each other. Moreover, the fibres can also be placed in multiple directions, for example at 0°, 30°, 60°, 90° to achieve an quasi-isotropic behaviour or be placed randomly to achieve an isotropic behaviour [12], [13].

There are larger components like beams and bridge-decks manufactured in FRPs, but the different forms of FRPs generally used for strengthening are [15]:

- Sheets made like fabrics consisting of dry fibres,
- Pultruded composite laminates,
- Pre-impregnated sheets and laminates,
- Reinforcement bars,
- Tendons for prestressing.

### 2.2.1 Manual methods

There are three main types of manual methods [1]:

- The wet lay-up method,
- Pressure bag method,
- Vacuum assisted method.

The wet lay-up method is a simple method used to laminate the composite material directly to the structure [1]. The thin sheets or fabrics of dry fibres are formed by wetting the fibres with a polymer, which then can be applied or wrapped onto the structure. A mould can also be used to acquire a desired shape of the composite material to fit the structure.

Both the pressure bag method and the vacuum assisted method are similar to the ordinary wet lay-up method [1]. The difference is that after applying the composite fibres to the structure, pressure is put on the top of the sheets or fabrics by pressure bags or by vacuum. These methods allows for a higher fibre/polymer ratio than the regular wet lay-up method.

### 2.2.2 Semi-automated methods

The semi-automated methods are simplified versions of the manual methods with the difference that they have been refined to make the installation simpler and to ensure a better end result [12].

Vacuum infusion method is similar to the wet-layup method [1], [12]. Dry FRP sheets or mats are stacked onto the structure and then covered by a diffusion membrane and a vacuum bag membrane. The vacuum makes the vacuum bag seal around the edges and simultaneously infuses resin to impregnate the dry mats.

The resin transfer moulding (RTM) process use thermosetting resin injected into a fibre pre-form placed in a two-part closed mould [1]. The resin is then infused into the mould with pressure or vacuum. This method enables the making of large, complex, high-performance structures with good surface finish on both sides.

Low temperature moulding prepregs comes in several designs consisting of HM or UHM carbon fibre sheets pre-impregnated with an epoxy resin which are pre-cured under vacuum consolidation and elevated temperature [1], [12]. These can later be post-cured to a higher temperature.

### 2.2.3 Automated process

The automated methods are used to manufacture structural elements with the highest performance under fully controlled circumstances [1]. Different methods are used to get different structural shapes.

Filament winding is used to manufacture pipes and “other cylindrical cross-sections” where high strength is needed [1], [12]. The method is based on winding continuous fibres around a rotating mandrel. The fibres are fed through a traversing bath of active resin or, if pre-impregnated reinforcement is used, through a hot roller and then rolled onto the mandrel. After the completion of the initial polymerisation, the composite is removed from the mandrel and left to cure at a temperature of around 60°C for 8 hours.

The pultrusion method is an automated closed mould method where continuous fibres are impregnated and drawn through a heated mould manufactured to a desired shape [1], [12]. The pull speed and temperature in the mould has to be at certain levels and carefully calibrated to ensure a product of good quality. A high fibre/resin ratio can be obtained using the pultrusion method.

### 2.3 Properties of FRP composites

The final properties of a FRP material are governed by the combined properties of both the matrix material and the fibres [9], see Figure 2.1.

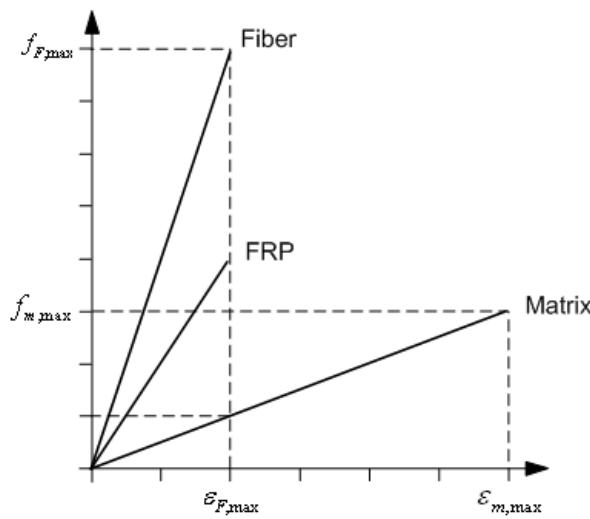


Figure 2.1 Stress-strain relationships for fibre, FRP, and matrix [9].

The different fibre ratios in the composite varies between different manufacturing methods; from around 25-35% for manual layup methods to 50-70% for pultruded profiles [10]. Consequently, the properties of the composite are considerably affected depending on method of manufacture. Furthermore, automated and semi-automated manufacturing methods contribute to the quality of the FRP since they produce FRPs with less variability and defects compared to manual methods [9]. Typical differences dependent on manufacturing process is displayed in Table 2.3.

Table 2.3 Effect of manufacturing process on typical UHM carbon fibre laminates [9].

Process	Fibre volume fraction	Void content	Stiffness parallel to the principal fibre direction [GPa]
Hand lay-up	0.4	Up to 5%	230
Vacuum infusion	0.54	<1%	310
Prepreg	0.60	1-2%	360

The direction of the fibres is another way to alter the properties [12]. Unidirectional composites have their fibres placed in one direction which gives the composite different properties in transversal and longitudinal direction, with the stiffest and strongest behaviour in the direction of the fibres. Several layers of unidirectional composites can be arranged with different number of layers and with the fibres at different angles to each other to give desired properties to the final composite. Thus, it is possible to combine different fibres with different matrices and arrangements to attain desired final properties. The straightness of the fibres also influence the final composite and is easier to control with the automated product, e.g. with pultrusion. Additional factors affecting the properties of composites are the temperature and duration of the cure cycle where a higher temperature and longer curing times usually results in better mechanical properties of the final composite. Moreover, defects like fibre breakage, voids, fibre disbands, and unplanned fibre folds, naturally influence the final strength and stiffness of the composite. Typical properties of CFRPs with epoxy matrix material are presented in Table 2.4.

*Table 2.4 Typical mechanical properties of long directionally aligned epoxy fibre composites (with a fibre weight fraction of 65%) [1].*

Fibre	Relative density	Tensile strength [MPa]	Tensile modulus [GPa]	Flexural strength [MPa]	Flexural modulus [GPa]
Carbon (PAN)	1.6	2689-1930	130-172	1593	110.0
Carbon (PITCH)	1.8	1380-1480	331-440	-	-

The reader is directed to Section 2.1.1.1 for explanation of PAN and PITCH carbon fibres.

### 2.3.1 Mechanical properties of FRP composites

As mentioned in the previous section, the mechanical properties depend on a number of factors. To determine the stiffness of the composite in the fibre direction the “rule of mixture” applies [12]:

$$E_f = E_{fibre} \cdot V_{fibre} + E_{matrix} \cdot (1 - V_{fibre}) \quad (2.1)$$

The reader is referred to the Notations at the beginning of the Thesis (after the Preface) for information pertaining to the terms in equation (2.1).

While the stiffness is dependent on the thickness of the composite, this method can only be applied where the thickness can be controlled, e.g. for pultruded profiles where control over the thickness is relatively accurate [12]. If the composite is built up in-situ, e.g. by hand lay-up, the thickness can be rather varying and thus other methods would have to be considered. For that case the properties of the resin can be ignored, the fibre properties need only be considered.

Composites are usually anisotropic, which means that their properties vary with the loading angle against the fibres [12]. The stiffness set against the angle between load- and fibre- direction is illustrated in Figure 2.2.

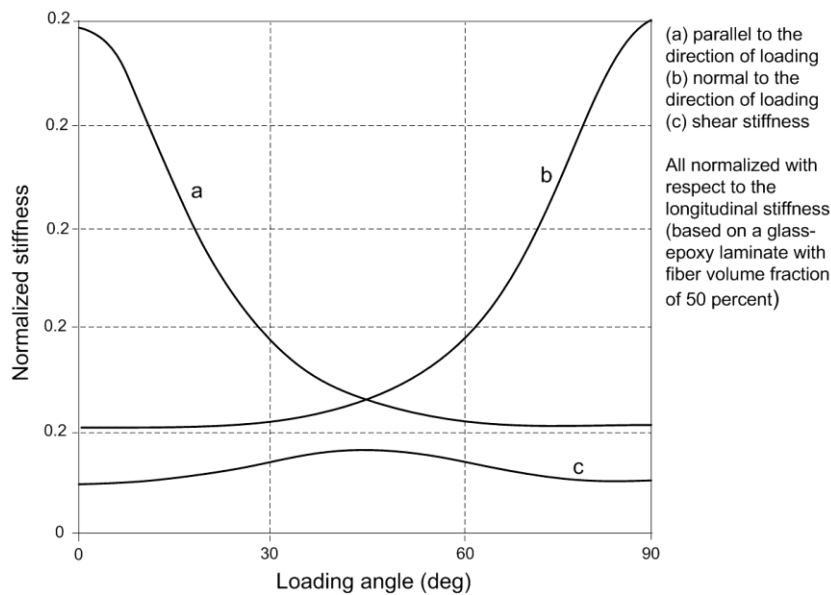


Figure 2.2 Variation of the unidirectional laminate stiffness with direction of loading [12].

The mechanical properties of composites are affected by several factors during the manufacturing process [12]:

- Thickness and volume fraction of the laminate
- Orientation of the fibres
- Straightness of the fibres
- Temperature and duration of the cure cycle
- Incidence of fibre breakage, voids, fibre disbands, unplanned fibre folds, and other defects
- The glass transition temperature

### 2.3.2 Glass transition temperature

All resins softens with increased temperature and polymers that are tough and strong at 20°C can become weak and soft at 100°C [13]. Therefore, a temperature of particular interest to structural engineering is the glass transition temperature ( $T_g$ ).

Above the transition temperature, amorphous polymers such as epoxies and vinyl ester resins, which are used frequently in structural engineering, change their structural behaviour drastically; their stiffness decrease and their volume is also affected, as illustrated in Figure 2.3. When the temperature is above the transition temperature the additional energy provided is enough to soften the bond between the polymeric chains and thus make them more flexible. This can lead to a large reduction in load-carrying capacity of the FRP composite.

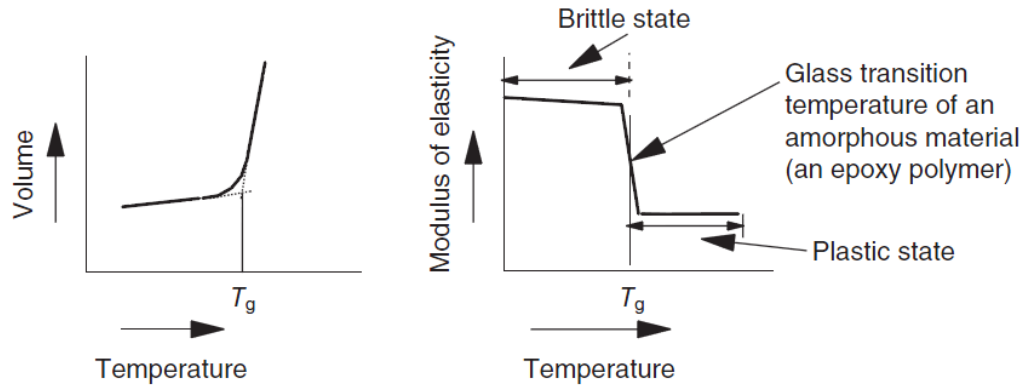


Figure 2.3 Effects of the glass transition temperature [16].

Due to the decrease in load-carrying capacity and to avoid premature debonding failure, it is important that the service temperature is kept well below the glass transition temperature. If the strengthened member is to be subjected to high temperature it is vital to ensure that the FRP composite used as well as the adhesive used have a high transition temperature. There are some resins that can be post-cured by heat-treatment to increase the transition temperature.

### 2.3.3 Fatigue resistance

The fatigue resistance of FRP composites is larger than for metallic structures, but this is only valid for the material [11]. However, joints, connections, and anchorage details are local stress-raisers and are more susceptible to fatigue. Consequently, these details have to be designed with care to avoid high levels of stress and possible fatigue damage.

Based on earlier test results and studies it has been confirmed that a raised temperature and more moist conditions will affect the fatigue life negatively [9]. CFRP composites are the least susceptible to fatigue among the different FRP composites.

### 2.3.4 Moisture resistance

Almost all materials used in structural engineering, including FRP composites, are affected negatively by moisture [9]. Compared to steel that might rust, concrete that can carbonate and wood that rots, it's the resin chains in FRPs that are susceptible to moisture ingress which can cause them to split. The extent of the absorption is affected by both the temperature and the type of resin, and two immediate effects are a reduction of the glass transition temperature and a stiffening of the resin. Resins are continuously modified to increase their in-service performance and also additives can be added to affect their properties [1]. These modifications will affect the durability of the FRPs.

### 2.3.5 Fire performance

The fire performance of FRP composites is dependent on the choice of fibre and matrix material, thus can be tailored to reach an adequate performance [12]. Considerable research has been carried out on the subject since many FRP materials are used for ships and offshore platforms where fire regulations are strict. FRPs have a low thermal conductivity, they absorb heat energy, and the surface combustion zone



acts as a protective layer, delaying the spread of heat through the material. They also contain high ratios of fibres which are incombustible.

The fire performance of FRPs is often governed by the adhesive due to its lower glass transition temperature [9]. Appropriate measures for fire protection should be used.

### **2.3.6 Exposure to ultraviolet radiation**

Polymers degrade by the UV radiation of sunlight [1]. The degradation makes the resins more brittle and gives them a slight discoloration. The rate of degradation is dependent on which type of resin that is used, the fibre content, and the fibre orientation [9]. The degradation of the resin can be solved by adding additives to stabilize the epoxy polymers so that they can withstand UV radiation, and while the additives have a little effect on the discoloration there is no indication of mechanical degradation of the epoxy polymers [1].

### **2.3.7 Alkalinity and acidity**

FRP composites, unlike other construction materials, do not suffer from “rust” which makes them attractive where corrosion is concerned, and in corrosive environment [1]. The resistance against alkalinity and acidity for FRPs depends on both the fibres and the resin of the composite. Carbon fibres are resistant against alkaline and acid and there have been several studies proving that CFRP composites have high resistance against both alkalinity and acidity given that a suitable resin is used.

### **2.3.8 Temperature effects**

The coefficient for thermal expansion is negative for CFRP composites as opposed to most conventional materials, e.g. concrete and steel [12]. As a result, large differences in thermal strain between the strengthening CFRP composite and the strengthened substrate can occur, thus special care is required in design to avoid high thermal stresses in the adhesive bond.

### **2.3.9 Creep and relaxation**

The polymeric matrix materials are susceptible to creep but the fibres, carbon fibres, are not [12]. Since FRPs used for strengthening usually contains high rates of unidirectional fibres, the resulting creep is insignificant.

FRP composites can fail suddenly by creep rupture if they are subjected to constant loads over a long time; this is called the endurance time [17]. A higher load will result in shorter endurance time and the environmental situation will affect the endurance time as well, e.g. high acidity and alkalinity, high humidity, and freeze-thaw cycles.

Both Aramid FRP (AFRP) and Glass FRP (GFRP) show significant loss of tensile strength under constant loading over time while CFRP show only a slight loss [11], [18].

## **2.4 Properties of structural adhesives**

Depending on which method of strengthening with CFRP that's employed, different types of adhesives can be used [12]. If manual lay-up is used, the adhesive is also the resin for the composite fibres, and if pre-formed FRP composites are used the composite has to be attached to the structural element using a separate adhesive.

Several of the different resins used in FRPs are also available as adhesive to apply pre-formed FRPs to the existing structure.

The difference between the resins and the adhesives is that the adhesives need to be able to cure at in-situ, which often includes exposure to low temperature compared to the possibilities of higher controlled temperature while curing the resins in a factory [12]. Moreover, the viscosity of the epoxy that serves as both adhesive and resin is low in order to have good wetting properties, compared to epoxy used as adhesive exclusively, which have higher viscosity and often contains inorganic fillers such as clays or silica sand [14].

Epoxies are the most used structural adhesives [12]. There are several different epoxies, both single component and two component epoxies. The single component epoxies have a longer pot-life but requires higher temperature to cure, while the two component epoxies cure at ambient temperature but have a pot-life of only 20-90 minutes; so if large areas are to be covered it has to be planned carefully [10], [12].

The behaviour of structural joints depend not only on the properties of a given adhesive but also heavily on the interface of the substrate and the composite [12]. The presence of voids and defects in the surfaces as well as contaminations in the adhesive greatly influence the behaviour of the joint.

The properties and structural behaviour of the adhesives are in most cases almost the same as for the matrix material, since they can, e.g. with the wet lay-up method, serve as both matrix and adhesive [12]. Nevertheless, there are some differences, e.g. the difference between two epoxies could be that the epoxy acting as a matrix can be cured under controlled conditions at an elevated temperature while the adhesive may have to cure at significantly lower temperature.

#### **2.4.1 Durability**

The most critical factor in terms of durability of adhesives is subjection to humid environments resulting in moisture ingress [12]. The moisture ingress can lead to plasticization of the adhesive and cause it to hydrolyse, crack, or attack the interface by displacing the adhesive.

It is important to choose a proper adhesive for given circumstances since there are epoxies which are more susceptible to moisture ingress than others [12]. Under moist conditions, an adhesive with good moisture resistance should be chosen to resist chloride attacks and degradation due to freeze-thaw cycles.

#### **2.4.2 Fatigue resistance of an adhesive joint**

The adhesive is more susceptible to fatigue than FRPs, although it can be a lot better than a riveted joint [12]. Fatigue damage appears at points with high stress concentrations, therefore the geometry of the joint is crucial for the fatigue resistance.

Both large scale tests and small scale tests on steel girders have been carried out on fatigue performance of adhesive joints [12]. The results showed no sign of fatigue damage after 10 million cycles of cyclic loading.

#### **2.4.3 Creep behaviour**

The temperatures polymeric adhesives typically are exposed to are frequently close to or coincide with their viscoelastic phase, i.e. the region of/near? the glass transition temperature [12]. The combination of this fact with permanent loading will result in

significant creep deformation. Sustained loading will eventually lead to creep rupture of the adhesive, thus setting a limit to the service life of the adhesive.

In the majority of the strengthening cases with FRP composites the permanent stress in the adhesive will be low [12]. Although, if load-relief jacking is used or if a prestressing force is induced into the FRP, the stress in the adhesive will be higher. Loading history as well as temperature and moisture will affect the magnitude of creep, and it is important that the temperature is kept well below the glass transition temperature for the adhesive.

#### **2.4.4 Fire performance**

The performance of structural members strengthened with FRP composites is often governed by the fire performance of the adhesive [12].

The adhesives that emit the least toxic fumes are acrylics and some epoxies [12]. The adhesives having the most favourable fire-resisting properties are the two-part cold-cured epoxies. They are stable at relatively high temperatures and self-extinguishing if the source of ignition is removed, moreover they emit small amounts of toxic fumes and smoke.

### **3 Applications of Unprestressed FRP Composites for Strengthening and Repair in Structural Engineering**

This chapter introduces conventional ways of strengthening and repair of structural members in concrete and steel and strengthening with FRP composites. How FRP composites can be used for strengthening and repair, and the application process is described. Advantages with the use of FRP composites instead of conventional are presented as well as the main disadvantage of bonded FRP laminates and their corresponding failure modes.

#### **3.1 Introduction**

A large number of structures today are in need of either a higher capacity than they were designed for or they have been damaged and lost part of their design capacity [1]. There are several different reasons governing the need of strengthening and repair of structures, including; increased load, change in structural behaviour, material deterioration, and fatigue. Additionally, hazardous events such as impact, fire, and vandalism add to the need. As a result, the field of strengthening and repair of structures has become a major area in civil engineering while this is often a lot less expensive than to replace the old structure with a completely new one.

Usually this kind of strengthening and repair is collectively called “retrofitting applications”, as they are used in existing structures and not in the construction of new structures [14]. Strengthening is when the capacity or performance of an existing structure needs to be improved. The reason for this could be one of many, e.g. higher safety regulations, increased live- or dead loads or to reduce displacements. In the case when a structure needs repair the original capacity usually has been reduced of deterioration and needs to be restored. It could be deteriorated due to environmental effect, e.g. corrosion of reinforcing steel, damage in service or if it wasn't constructed in a proper way.

All structural problems have more than just one solution [12]. In the end it is the least expensive one that is considered the best solution at the point where a decision is made. It is important to remember that the whole structural life cost should be included in “least expensive”, i.e. it should include future maintenance costs, all consequential traffic disruptions etc. and not just the initial build cost.

#### **3.2 Introduction of conventional methods of strengthening and repair**

There are several conventional ways of strengthening structures of both concrete and steel. What they all have in common is that they can be replaced by a similar method using FRP materials and gaining from their benefits. Between the methods used for members of concrete or steel there are of course differences but they build on the same principle. The conventional way of strengthening beams are to attach steel plates or concrete and reinforcement to the webs or flanges as can be seen in following figures. This is done to increase the cross-sectional area and by doing this increase

bending stiffness and strength, compressive and shear capacity or increasing the fatigue life.

### 3.2.1 Strengthening and repair of concrete members

Concrete beams can be strengthened or repaired for bending stiffness or strength using conventional methods in several different ways, as illustrated in Figure 3.1 [19]:

- Mounting steel plates externally as additional reinforcement, which is the method closest related to FRP plate bonding. The steel plates can be either bolted or adhered to the concrete beam.
- Adding layers of reinforcement and cover it with new concrete.
- Strengthening with near surface mounted reinforcement.

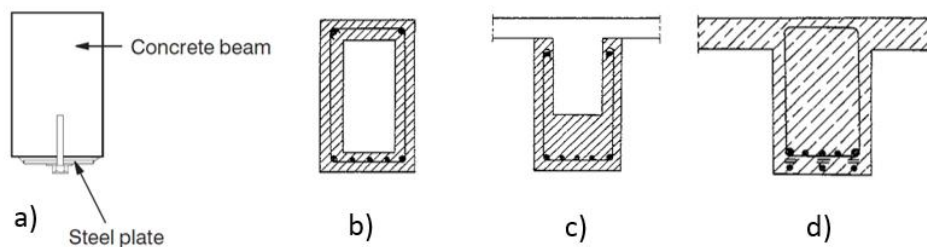


Figure 3.1 Example of concrete beams strengthened using conventional methods, a) with steel plate, b) and c) with additional reinforcement covered with new concrete and d) with near-surface-mounted reinforcement [19].

Strengthen concrete beams in shear can be achieved by using steel wraps as seen in Figure 3.2. The reinforcement has to be covered, e.g. with concrete, to protect it against corrosion.

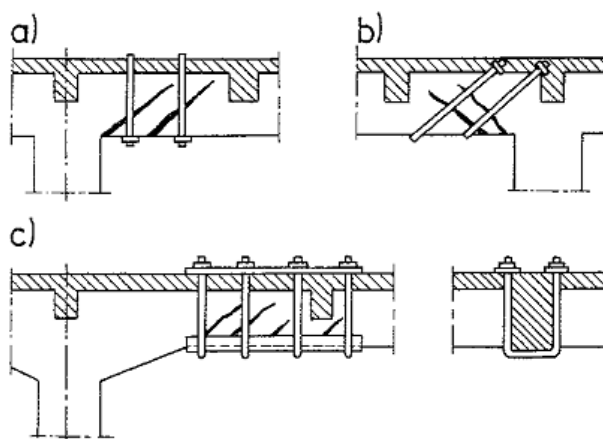


Figure 3.2 Example of a concrete beam with additional shear reinforcement [19].

Columns of concrete can be strengthened by adding steel reinforcement and covering it with a concrete layer, called jacketing. This process starts by adding steel connectors to be able to fasten the new stirrups and bars. A mould is placed around the column and filled with concrete, see Figure 3.3.

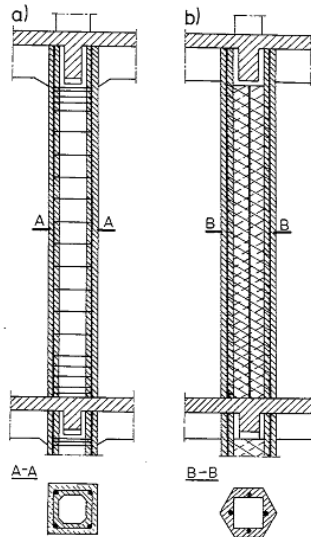


Figure 3.3 Concrete columns strengthened with concrete jacketing [19].

### 3.2.2 Strengthening and repair of steel members

To steel members steel plates are attached usually by riveting, bolts or welds. The plates added to the cross-section increase the area and so forth the stiffness and capacity in bending, shear or compression. The principles of the techniques are alike but there are some differences. If bolts or rivets are used drilling is needed which will affect the cross-section area as well as result in local stress raisers. A couple of strengthened cross-sections are shown in Figure 3.4.

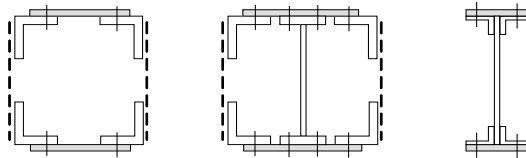


Figure 3.4 Strengthening structural members by bolting steel plates [20].

Welds on the other hand is one of the weakest details in terms of fatigue strength and the weldability of older steel structures is somewhat limited and can result in damages to the strengthened structure during strengthening process. Cross-sections strengthened with welded steel plates are shown in Figure 3.5.

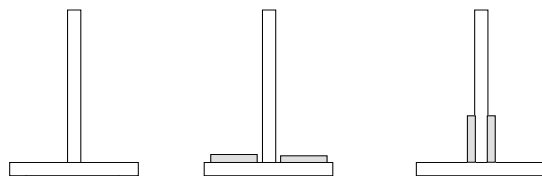


Figure 3.5 Strengthening the bottom flange of an I-girder using welded steel plates [20].

### 3.3 Applications of FRP strengthening systems

#### 3.3.1 Introduction to strengthening and repair with unprestressed FRP composites

In a similar way to the conventional strengthening methods, especially using steel plates, FRP laminates, plates and fabrics can be used for strengthening and repair. A few different structural elements that can be strengthened by FRPs are illustrated in Figure 3.6.



Figure 3.6 Different possibilities and areas where FRPs can be used for strengthening [10].

The most significant advantages of FRP laminates are their light weight and non-corrosive properties [6]. Compared to a steel plate of the same strength it can be up to six times thinner and as it has a much lower density it will also be a lot lighter. A typical increase in bending strength from a 1-mm-thick FRP plate could increase the load bearing capacity of a 18.0 m long beam with 23% and correspondingly up to over 69% for a 3 mm thick plate. Furthermore, researchers have concluded that the increase in strength for a pre-damaged and pre-loaded beam compared to undamaged beam is similar, although with a decrease in stiffness in the pre-damaged beams.

The construction industry is conventional and often cautious with new methods and materials [13]. This is understandable due to problems with earlier materials. For example, concrete deteriorate in many more ways than what was widely appreciated only 30 years ago. At the same time durability and maintenance implications of a solution is much more important today. There is always a risk with a new method because there is no long track record of successful projects. The risk has to be estimated and handled, a process that is much easier with advanced technology. Finite element modelling has made it possible to both predict and solve possible problems of advanced structures.

The ROBUST project have made an considerable amount of testing to prove the strength, fatigue and durability of the FRP materials [13]. There have been far more research on the field of FRP bonding than on steel plate bonding, which was enough to accept it as a strengthening method. Technically, the step to using FRP plates instead of steel plates is a lot smaller than the initial step of the technique of external reinforcement.

The durability and performance of fibres, adhesive and matrix materials have been proven and the risks have been minimized by the work done today [13]. Also the knowledge on fatigue, creep and different failure modes is a well-documented area [14]. Even if it is not possible to claim that the any of the methods for construction or repair involving structural analysis and deterioration mechanisms is completely understood, FRP composite plate bonding has been sufficiently researched to be able to use it with confidence. The versatility and advantages of FRP plates over steel plates presented above provide opportunities for strengthening and repair which were not possible before. It is important to ensure that these applications are carried out in an appropriate manner and that bad detailing and lack of experience put the benefits of the material at risk.

### **3.3.2 Bonding of FRP composites**

To be able to transfer loads through a component consisting of several members, the members have to be joined in some way [9]. Two main methods for joining composites are mechanical joining with bolts or rivets or adhesive bonding. Adhesive bonding is used in several engineering fields today including aerospace, automotive and construction and has many advantages to bolted or riveted connections, to name a few:

- Outstanding fatigue resistance.
- Suitable for joining dissimilar materials.
- Relatively high stiffness.
- For certain applications it's the only practical method.
- Can reduce manufacturing costs.
- Ease of application in comparison to other joining methods such as bolting and riveting.

Using bolts or rivets with fibre composites can be problematic as the composites used in this kind of applications often have a unidirectional behaviour with very low fibre-density in the transverse direction of the load. This makes them weak in this direction and as tensile stresses are induced in the transversal direction of the fibres it creates a ripping effect.

### **3.3.3 Application of FRP laminates**

In order to get a strong connection between the substrates, the adhesive has to get a good bond with the surface of each substrate [1]. In the case where the substrate is a lot stronger than the adhesive it is important that the adhesive bond is not the weakest link and that the adhesive strength determines the strength of the bond. In order to get such a bond it is important that the application of the laminate is carried out in a proper way. This preparation is crucial for the final result of the strengthened beam. The surface of the strengthened member has to be roughened up and cleaned to get rid of all dust and dirt and then prepared with a primer to get a more suitable surface and filling cavities that would require large amounts of adhesive and would affect the behaviour of the joint [4]. The laminate also needs to be cleaned from possible dirt, dust and grease using acetone or similar to wipe the laminate surface [1].

In Table 3.1 and Table 3.2 the general steps in the application of FRP composites is described for both concrete and steel, as well as illustrated in Figure 3.7 and Figure 3.8.



### 3.3.3.1 Application of FRP laminate on concrete beams

Table 3.1 The basic steps to apply bonded FRP laminate systems to concrete beams [19].

Step	Description
1	<i>Repair of the corrosion.</i> FRP laminates should not be applied to the structure that contains corroded reinforcing steel. The expansive forces associated with the corrosion process are difficult to determine and could compromise the structural integrity of the externally applied FRP system.
2	<i>Injection of cracks.</i> The cracks that are larger than 0.25mm should be pressure injected with epoxy resin. If the structure is situated in aggressive environment smaller cracks may also require injection or sealing to prevent corrosion of existing steel reinforcement.
3	<i>Surface preparation.</i> Dust, dirt, oil, curing compound, existing coatings, cement layer and any other matter that could interfere with the bond of the FRP system to the concrete should be removed. Surface preparation can be accomplished using abrasive or water and sand-blasting techniques. If the FRP laminate is wrapped around the corners of rectangular cross section, the corners need to be rounded to prevent stress concentrations in the FRP system and voids between the FRP system and the concrete.
4	<i>Application of primer.</i> It should be applied to all areas on the concrete surface where the FRP system is to be placed. The primer should be placed uniformly on the prepared surface at the manufacturer's specified rate of coverage. The applied primer should be protected from dust, moisture, and other contaminants prior to applying the FRP system. (a)
5	<i>Application of putty.</i> Bug holes and voids should be filled with epoxy putty; also roughened corners should be smoothed with putty. (b)
6	<i>Preparation and application of first layer of saturator/adhesive.</i> The saturator/adhesive should be prepared based on the manufacturer's recommendations. In the case of two-component adhesives, attention should be paid to the correct ratio and mixing speed. The saturating resin should be applied uniformly or "roof-shaped" to all prepared surfaces where the system is to be placed. (c)
<b>Wet layup system/Pre-cured system</b>	
7	<i>Application of fibre sheet.</i> The fibres can also be impregnated in a separate process using a resin-impregnating machine before placement on the concrete surface or can be directly put on the surface with the use of roller. The Pre-cured system like: shells, strips, and open grid forms are typically installed with an adhesive. In next step entrapped air between layers should be released or rolled out before the resin sets. Sufficient saturating resin should be applied to achieve full saturation of the fibres. (d)

8	<i>Application of next layers of fibre sheet.</i> Second layer of saturating resin/adhesive is placed more or less after 30 minutes after application of first layer of fibre. The thickness of the second layer should be similar to the first one and varied circa 0.4-0.5mm.
<b><i>Prepreg system</i></b>	
7	<i>Preparation and application of pre-impregnated fibre sheet.</i> Dry fibre sheet is impregnated in a separate process with a use of impregnation machine. Pre-pregs can be stored in refrigerator in temperature -20°C. Before application fibre sheet need to reach a room temperature. (e)
8	<i>Application of vacuum bag and curing.</i> To remove the entrapped air and achieve uniform integrated material the vacuum bag can be installed and the pressure is applied. Prepreg systems should be cured at an elevated temperature. Usually a heat source is placed around the column for a predetermined temperature and time schedule. Temperatures are controlled to ensure consistent quality.
9	<i>Application of optional topcoat.</i> In order to enhance corrosion resistance external layer of topcoat can be applied.

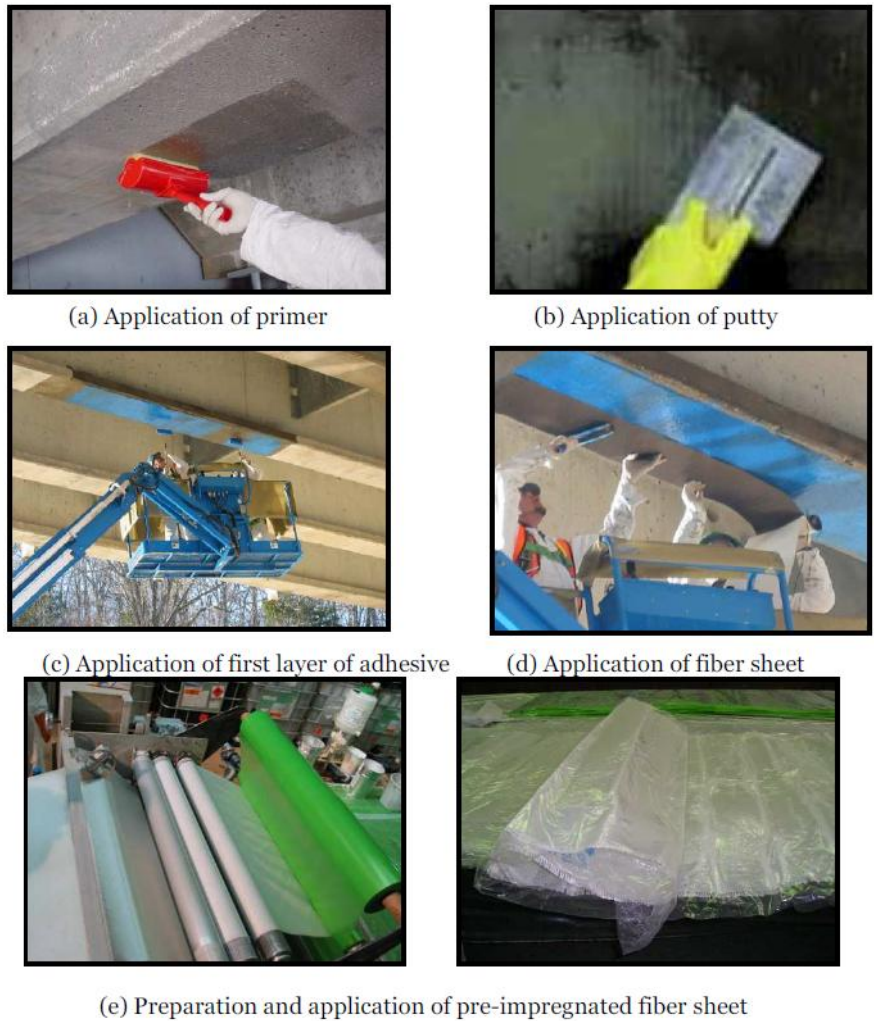


Figure 3.7 Application steps for FRP composites on concrete structures [19].

### 3.3.3.2 Application of FRP laminate on steel beams

Table 3.2 The basic steps to apply bonded FRP laminate systems to steel beams [9].

Step	Description
1	<i>Surface preparation.</i> To ensure a good bond the first and maybe the most important step is to remove any dust, paint or contamination from the surface. The recommended method of doing this is sand blasting followed by a chemical cleaning of the surface using a suitable solvent, e.g. acetone.
2	<i>Application of primer.</i> To enhance the chemical bond between the adhesive and the metallic surface a primer is used. The application of primer should take place shortly after blasting to prevent possible corrosion of the surface (a).

3	<p><i>Preparation of laminates.</i> To enhance the bond between the laminate and adhesive layer the laminates have to be prepared by cleaning them of potential dirt. Some laminates are equipped with protective peel plies which should be removed before application. Otherwise, laminates should be prepared by slight sanding followed by cleaning with a suitable solvent, e.g. acetone.</p>
4	<p><i>Preparation of adhesive.</i> The adhesive should be prepared based on the manufacturer's recommendations. In the case of two-component adhesives, attention should be paid to the correct ratio and mixing speed.</p>
5	<p><i>Application of the adhesive.</i> After curing the primer layer and completing steps 3 and 4, the adhesive is applied. Depending on the accessibility of the metallic or concrete surface, the adhesive can be applied to either the FRP laminate or directly to the substrate. Care should be taken in order to avoid defects in the adhesive layer, e.g. air bubbles.</p>
6	<p><i>Application of laminate.</i> After completing step 5, laminates should be carefully placed on the structure. It is important to complete this step before the pot life of the adhesive is reached. Care should be taken in order to keep the laminates and the adhesive layer clean during this step. Any displacement of the laminate during the curing time should be avoided (e).</p>



Figure 3.8 Preparation and installation of CFRP laminates on a steel beam [9].

### 3.3.4 Flexural strengthening

Strengthening of members in bending is the most common way to strengthen structures with FRP composites [10]. To date the most common composite used for strengthening is CFRP used as unprestressed laminates bonded to the tension face of the strengthened beam. The principle is the same as for strengthening with steel plates. The FRP laminates or sheets, which are unidirectional with the fibres parallel to the tensile force i.e. axial direction, are attached to the tension face of a beam to increase the inertia of the cross-section and stiffen the beam, see Figure 3.9. When using this method to strengthen elements, special attention is needed in design in order to cope with the high stresses along the bond line between the concrete and FRP. Apart from that the design may follow the well established procedures for reinforced concrete structures [6].

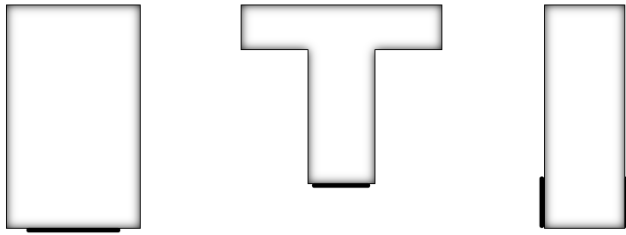


Figure 3.9 Concrete cross-sections strengthened in bending with FRP laminates.

### 3.3.5 Shear strengthening

The shear capacity of a beam can be increased by bonding FRP laminates to the web of the beam prepared [1]. It has been shown that the best way of strengthening where the shear capacity increases most is with the fibres perpendicular to the beam axis and the FRP fabrics or laminates should be wrapped over the full depth of the strengthened member. This is because the sheets or fabrics need a certain bond area to be able to develop full tensile strength of the fibres, although it is possible to just cover the sides but it may not be as effective, see Figure 3.10 [21].

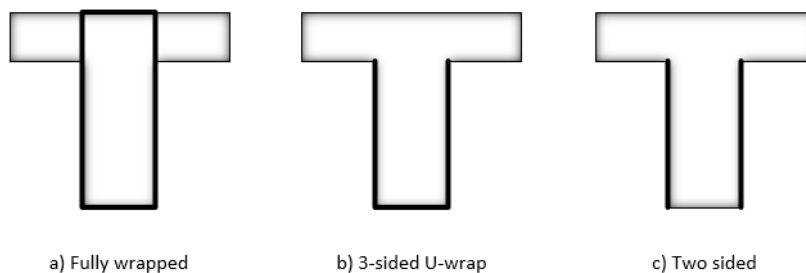


Figure 3.10 Concrete cross-sections strengthened in shear with FRP.

The effect of inducing a prestressing force in the shear reinforcing FRP laminates has been studied and turned out to be an effective way of shear strengthening prepared [1]. It resulted in a change in behaviour of the beam from a brittle failure to a ductile failure mode and increased the capacity due to higher aggregate interlock, delaying the initiation of shear cracking and improved the concrete compressive strength.

The use of externally bonded FRPs for shear strengthening have not been as wide of a field of research as for flexural strengthening [10]. This could be because of the fact that the shear failure behaviour is more complex.

### 3.3.6 Strengthening and confinement for compressive bearing capacity

A column is a structural element which is loaded mainly in its longitudinal direction where this load is considerably larger than loads in any other direction [10]. To increase the capacity of a column the most efficient way to do this without increasing the cross-section is to apply a confining pressure. This is achieved with lateral reinforcing steel in reinforced columns. When the axial strain increases the lateral confining pressure increases because of expansion of the concrete, the Poisson's effect. This effect can be achieved with FRP sheets or jackets, see Figure 3.11, and can be carried out using one of several methods. Several studies show that FRP materials are very effective for both circular and rectangular cross-sections [22].

When retrofitting a column for a certain failure mode another failure mode can become the governing one and has to be taken into account.

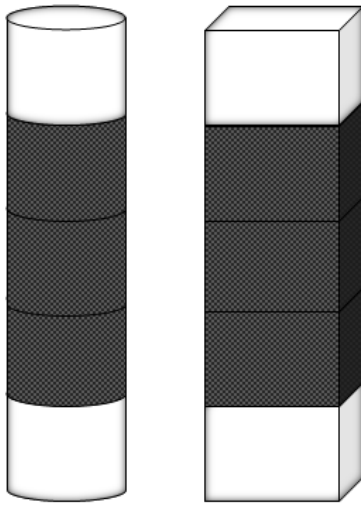


*Figure 3.11 Compressive strengthening of columns using FRP sheets.*

Wrapping is the most usual strengthening method with FRP's [10]. Unidirectional thin sheets or fabrics are wound around the column with their fibres transverse to the loaded direction. Usually they are installed by wet layup where the dry fibres either are pre-wetted close to or at the site or by rolling a layer of resin onto the column before placing the dry fibres on top of the wet resin and then roll one more layer of resin on top of the fibre sheets. It is important that all the fibres are thoroughly wetted and that no air voids are trapped between the FRP sheets and the strengthened column. This method is useful if there are a small number of columns and it is easy to handle on site when no special equipment is needed. It is also easy to cope with different shapes of columns.

Another method is filament winding which is using computerized automatic special equipment which yarns the FRP material around the column [10]. It requires that the shape and size of the column is of the ordinary kind because of the need of fit with special equipment. The quality of the result is high and it is not labour intensive.

A third method to strengthen columns is by using pre-fabricated shells. The advantage of this is that the FRP's shell can be produced under controlled conditions and a high quality is assured [10]. The pre-fabricated shells are either delivered in two halves or a longitudinal cut is made through the shell to make it possible to fit around the column. This method is very useful when there are a high number of columns with the same dimensions that needs to be strengthened.

### **3.4 Comparison of unprestressed FRP- and conventional-strengthening system**

The most obvious conventional solution to compare against FRP plate bonding is steel plate bonding [9]. These two methods have a lot in common, but it is important to remember that FRP materials give new opportunities and enables new technical solutions.

There are several advantages with FRP materials compared to conventional steel plate bonding [9], [13]. General advantages of FRPs light weight and high strength which apply for both strengthened concrete and steel beams are:

- Tailor made FRP materials: The possibility to design the FRP plates with constituents to meet certain requirements and obtain a specified stiffness and strength. FRP plates are likely to have an ultimate strength which is at least three times the strength of steel.
- Low weight of FRP plates: FRP composites have a density which is around 20% of the density of steel. This in combination with its high ultimate strength can result in that the weight of a FRP plate is less than 10% of a steel plate of similar strength. Large savings of time and labour for both transport and installation of the plates can be obtained due to this fact. The FRP plates does not need any support to keep them in place during installation, as steel plates need, because they are light enough to be held in place by the adhesive.
- Transportation of plates: The low weight makes it possible for one man to carry a 20 m long composite plate. The FRP plates are also possible to bend into as small coil as 1.5m in diameter, this makes it possible to transport large amounts of strengthening plates in a small car. Their flexibility also makes it possible to operate in confined spaces.
- Versatility: Because of the steel plates high weight they cannot be transported and handled in long pieces and thus they have to be connected with lap plates. FRP composite plates come in almost infinite length and it is possible to fix in layers to suit existing requirements and they can also be applied in several directions crossing each other by adjusting the adhesive thickness.
- Surface preparation of plate: Plates which will be adhered to the strengthened beam needs surface preparation. A steel plate needs to be grit blasted and thereafter protected until shortly before installation, this has to be done carefully and is labour intensive. The FRP plates may be produced with a protective strip which is peeled off right before application.
- Reduced mechanical fixing: As the composite plates are a lot thinner than the steel plates, the peeling stress will be greatly reduced. This reduces the need of fixing compared to steel plates. Improved headroom as well as better appearance is also achieved with the thinner FRP plates.
- Dead weight: The heavy steel plates will influence the dead weight of the beam and this can result in a need of even larger plates. The serviceability of the strengthened beam may also be affected in a negative way. Foundations, bearings and joints will have to withstand the increased load as well and may be necessary to modify to ensure sufficient capacity of these.

FRP plate materials have superior durability over conventional steel plates but maybe the most advantageous property is their ability to be non-corrosive [6]. Also they have been proven to be more cost effective in the long-term. Durability properties that are advantageous with FRP compared to steel are [13]:



- Durability of strengthening system: Plates of steel are susceptible to corrosion, especially if they are fixed to a cracked chloride contaminated concrete beam. This will greatly affect the bond between the plate and the adhesive if the steel plate is adhered to the beam. FRP plates will not have this problem.
- Galvanic corrosion: There may be galvanic corrosion if the steel of the strengthened member and the strengthening steel plate is incompatible; they have a difference in electrode potential. This results in increased inspection- and maintenance costs.
- Fire-resistance: The thermal conductivity of FRP composites is lower than for steel. This will isolate the adhesive from heat in case of a fire and make it sustain its strength for a longer time.
- Reduced risk of freeze-thaw: There is a risk that water is trapped behind a plate strengthening system. If the installation of the plates is performed in a correct manner there should not be a problem with this but in case something goes wrong the adhesive can be damaged. The isolating factor of the FRP material compared to steel will make the risk of freeze/thaw damage smaller and if there is damage to the adhesive it is a lot easier to localize by just tapping the plates. With steel this is a lot harder to localize.
- Maintenance costs: Plates out of steel will have to be maintained by painting them and secure that they won't corrode. This will often include a lot of work with supports and traffic interruptions. FRP plates will not need this kind of maintenance and will reduce the whole life cost of the system.
- Reduced construction period: The construction time for strengthening with FRP plates instead of steel plates is usually a lot less. The possibility of using mobile platforms to install FRP plates makes it practical to confine work within limited workspace and night-time working.
- Possibility to prestress: The possibility to prestress FRP plates gives a new level of opportunities that can't be achieved without prestressing; closing or reducing crack widths, increase shear strength, the ability to replace lost prestressing etc.

When steel plates are welded to the strengthened steel beam there are several other disadvantages with the weld itself and results from the welding process [9]:

- Fatigue performance: If the steel plates are used to strengthen a steel beam by welding the plate. A weld is one of the weakest details by means of fatigue strength. It could be necessary to use a thicker plate just to be able to reach the fatigue strength required for the strengthened member.
- Damage from welding: The strengthened steel beam is often damaged by the welding done to attach the strengthening steel plate. This could lead to a premature failure of the beam.
- Weldability: Older structures that are constructed of steel with high rates of carbon may suffer from poor weldability and in these cases other joining

methods have to be used. Welding in steel with high carbon content can lead to premature fracture during welding.

The principle of bolted or riveted plates is the same as for welded steel plates and thus they suffer from the same disadvantages except for that the fatigue strength is better [9]. It requires that holes for the bolts are predrilled in the steel beam which decreases the cross section area of the beam. Special attention is needed to ensure that no slip occurs between the connected members to avoid that the bolts and holes experience non-uniform stress distribution. This would give local stress raisers and reduce the fatigue performance. To guarantee that there is no slip, friction connections are recommended. Surface preparation and tightening of the bolts require extra care to ensure that the connection fulfils the requirements. As mentioned earlier the limited length of steel plates makes it necessary to splice them to get larger lengths.

There are of course possible disadvantages with FRP composite plate bonding but there are measures to be taken in order to minimize these [9]:

- Cost of plate material: FRP materials are more expensive than conventional materials but as the market and demand grow for FRP materials the prices will go down. Although, it is the total cost of the strengthening that matters including the cost for e.g. labour and traffic disruption fees. It has been shown that in the cases where FRP materials have been used, the total cost is already lower than for conventional methods and this is without including future savings for maintenance.
- Mechanical damage of FRP: FRP is more susceptible to impact damage, e.g. a distinct hit with a sharp object. In public environments where the risk of vandalism or accidental damage is higher there could be necessary to add a protection layer on top of the FRP. On the other hand, FRP is easier to repair than e.g. steel. The damages are easier to localize and it is possible to replace a small part of the FRP by cutting out the damaged length of the FRP and add a new plate bonded on top of the old plate with an appropriate anchorage length.

## 3.5 Stress analysis of adhesive joints

While there are several advantages with FRP plates and adhesive bonding, the load transfer mechanism in adhesive joints potentially give rise to a new problem [9]. A definition of stress components and stress concentrations along the adhesive bond is presented below together with potential failure modes and measures to influence the stress components.

### 3.5.1 Definition of stress components

An adhesive joint between structural elements basically transfer the load with shear deformation [9]. This generates mainly two stress components along the joint, shear stress ( $\tau$ ) and normal stress ( $\sigma$ ), see Figure 3.12. The normal stress is developed from load eccentricity and is also called peeling stress as it acts perpendicular to the adhesive.



Figure 3.12 Illustration of shear and normal stresses in the adhesive layer [9].

### 3.5.2 Distribution of stresses

Peeling and shear stresses are caused by forces acting perpendicular and parallel respectively to the adhesive joint line [9]. The stress distribution in the adhesive is dependent of the strain in the substrate and the laminate. Close to the laminate end where no force has been transferred from the substrate the difference in strain is large and this results in large shear stresses. The peeling stress, which is a secondary effect of the shear action, is also largest close to the edge of the laminate and is the result of the eccentricity between the middle of the laminate and the laminate-adhesive interface.

The normal stress and strain are related to each other by the stiffness of the material, as equation (3.1) show.

$$\sigma = E \cdot \varepsilon \quad (3.1)$$

The relation of shear stress and strain is given in equation (3.2).

$$\tau = G \cdot \gamma \quad (3.2)$$

The shear stress reduces along the adhesive as bond as the force is transferred from the substrate to the laminate [9]. The result of this is that the shear stress decreases with increased distance from the laminate end. To understand how the shear and peeling stress is developed along the bond line it is helpful to study Figure 3.13.

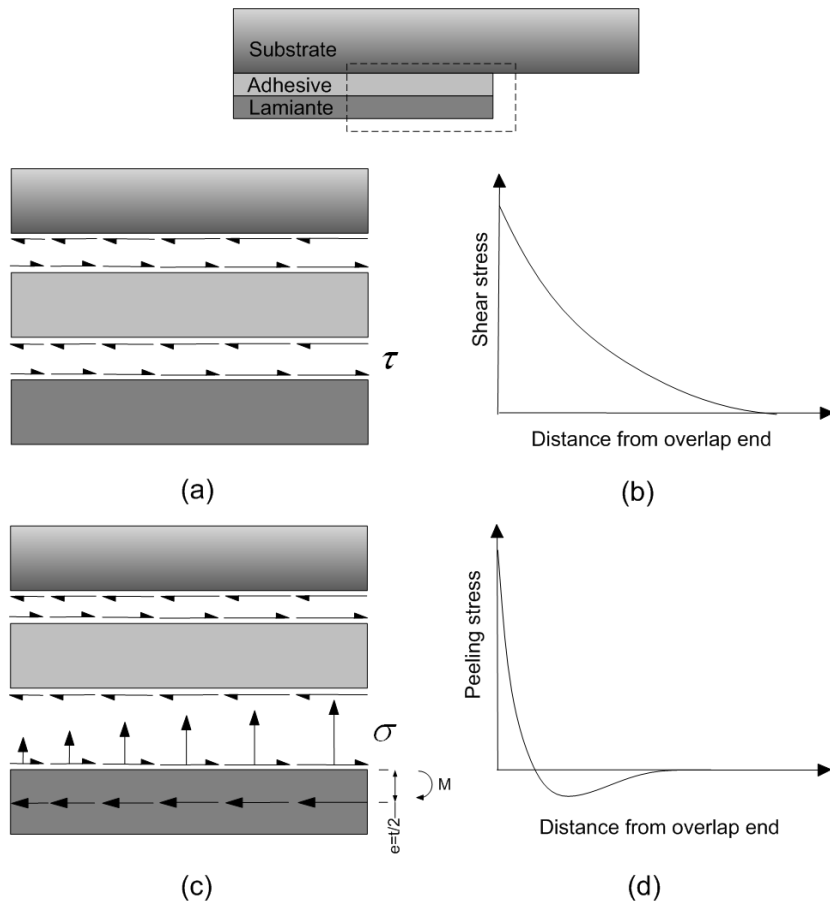


Figure 3.13 Formation of (a) shear and (b) peeling stresses in adhesive joint [9].

### 3.5.3 Peeling stresses

The peeling stress is the normal force acting perpendicular to the adhesive, this force is a result of the bending moment acting on the laminate trying to bend it [9]. The bending moment is a result of the eccentricity and magnitude between the force, i.e. axial force in the mid-laminate, and the interface between the laminate and the adhesive. The peeling stress is self-balancing and the resulting peeling force along the total length of the bond line should be zero. In Figure 3.14 this is illustrated with the theory of a beam on an elastic foundation, with the springs representing the adhesive and the beam representing the laminate. Tensile forces are induced in the springs close to the end while compressive forces are acting on the springs at a greater distance.

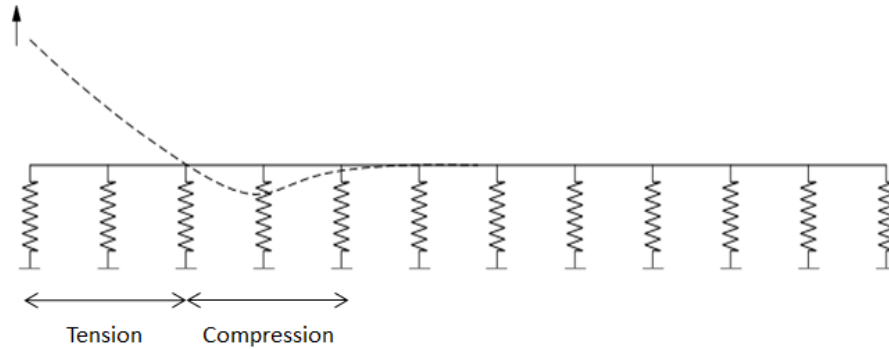


Figure 3.14 Illustration of peeling stress pattern in the adhesive joint using beam on elastic foundation analogy [9].

These stresses can be induced by other factors than mechanical loading, which is the most common load, such as thermal loading [9].

### 3.5.4 Failure modes

Depending on the sectional design of the strengthened beam there are several potential failure modes. The potential failure modes differ if the strengthened beam is made of concrete or if it is made of steel, this especially for the governing modes, as a result of their large differences in material properties.

#### 3.5.4.1 Failure modes of strengthened concrete members

The failure modes of concrete are usually governed by its low tensile strength. Hereafter is a list of the potential failure modes of flexural strengthened concrete members [10], [22]–[24]. It should be emphasised that the optimal design of a strengthened concrete beam is to have yielding of the reinforcement steel closely followed by concrete crushing leaving the FRP laminate intact.

- Yielding of reinforcement followed by FRP fracture: This failure mode is governing when the ratios of steel reinforcement and FRP are unusually low and the tensile failure strain of FRP is low.
- Yielding of reinforcement followed by concrete crushing.
- Concrete compressive crushing: Occurs when the reinforcement ratio, steel and/or FRP, is high.
- Peeling in concrete (see Figure 3.15): The high shear and peeling stresses near end of the laminate combined with the low tensile strength of concrete may cause premature separation of concrete cover. Failure initiates at a crack near the end of the laminate. This crack propagates through the concrete up to the reinforcement layer where it causes peeling of the concrete cover.

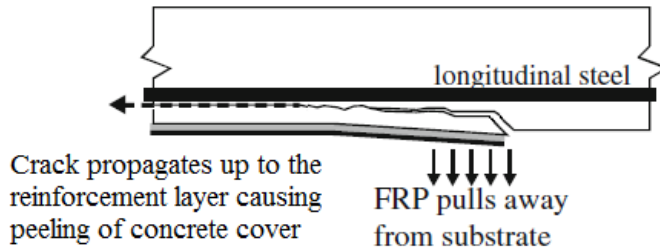


Figure 3.15 Peeling of concrete cover due to crack propagation initiated by high shear stresses [23].

- FRP plate debonding (see Figure 3.16): This failure mode is initiated by either shearing of the concrete near the concrete-adhesive interface, at inclined cracks caused by the vertical or horizontal opening of inclined shear cracks or flexural cracks [23], [24]. The crack then propagates towards the end of the laminate.

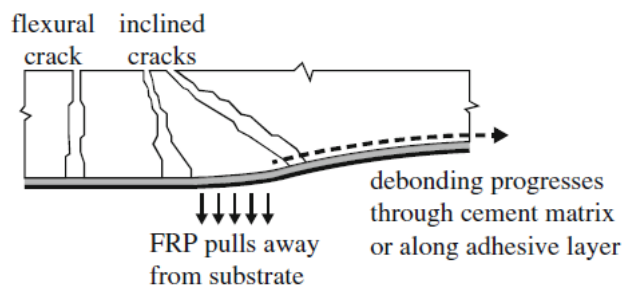


Figure 3.16 FRP plate debonding caused by shear or flexural cracks [23].

- Debonding at the interface of the laminate and concrete (see Figure 3.17): This failure mode is initiated by high interfacial shear stresses that exceed the weakest constituent materials strength, which is usually concrete [23]. Consequently, a thin layer of concrete remains bonded to the laminate surface. This failure mode can also appear at flexural cracks, in areas of concrete unevenness or due to imperfect bonding.

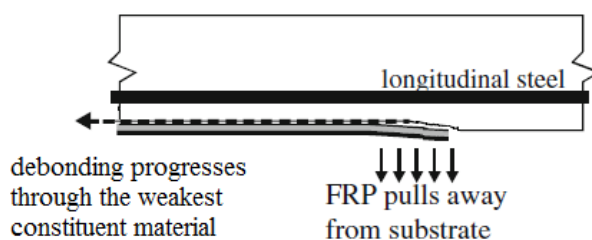


Figure 3.17 Debonding at the interface of the laminate and the concrete [23].

The first three failure modes of the listed above are classic failure modes which can be analysed using the conventional methods for flexural behaviour of reinforced concrete [22]. However, due to the low tensile strength of concrete the three latter failure modes, debonding and peeling failure, are the absolute most probable [10], [24]. Appendix B contains calculations to estimate the required amount of CFRP laminate to reach a desired strength capacity of a reinforced concrete beam. It also predicts the governing failure mode depending on cross-section properties. The calculations in the appendix can further be used for more detailed calculations of prestressed CFRP laminates following the principles of prestressed concrete.

#### **3.5.4.2 Failure modes of strengthened steel beams**

If the strengthened beam is made of steel, the failure modes caused by the typical characteristics of concrete are non-existent. This is because the large difference in properties between concrete and steel. The low tensile strength of concrete and the presence of cracks often is the governing factor of failure for concrete. For steel beams strengthened in bending the following failure modes apply [20]:

- Cohesive failure of the adhesive layer: This failure mode is governed by the strength of the adhesive.
- Delamination the FRP laminate: This failure mode is characterized by failure of the composite matrix material bonding the fibres together.
- Debonding along the interface between the adhesive and -the substrate or -the laminate. Good bond strength is crucial for this mode of failure.
- Yielding of the metal substrate.

The most favourable failure mode is laminate rupture where the full capacity of the laminate has been utilized [20]. This failure mode requires that none of the above mentioned failure modes take place and to avoid them special attention is needed to take care of high shear and peeling stresses near the laminate ends.

As an earlier governing failure mode is being strengthened the failure mode of the strengthened beam can change to a completely different failure mode [12]. Of that reason it is important to also keep other failure modes in mind, those not in direct connections with the strengthening laminate, e.g. global or local buckling.

#### **3.5.5 Methods to influence stresses in adhesive joints**

There are several factors that influence the magnitude of the shear and peeling stresses of adhesive joint [9]. The thickness of both the adhesive layer and the laminate as well as the modulus of elasticity of both materials has a great impact on the stresses. Another way to lower the high peak stresses at the end of the laminate without changing materials is to modify the end of either or both the laminate of/and the adhesive. This can be done in several different ways, see Figure 3.18, with fillets, by tapering or with mechanical dampers.

The use of more ductile adhesives leads to weaker bonds but larger failure strains [23].

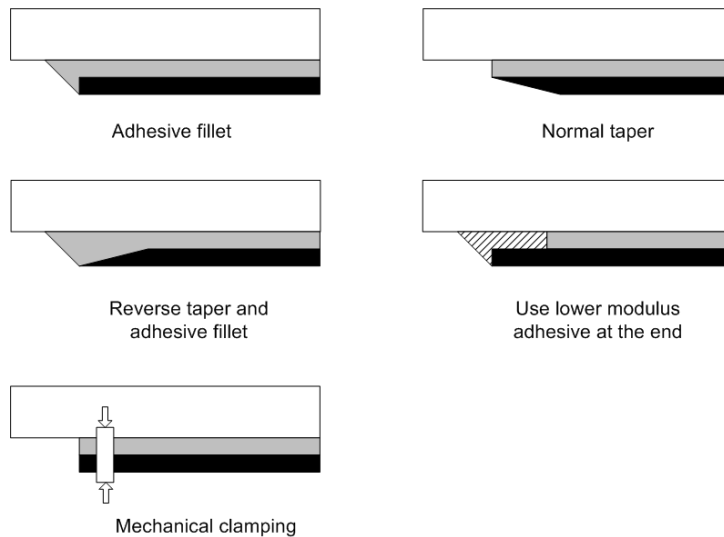


Figure 3.18 Different methods used to reduce stress concentration at the end of adhesive joints [12].

Modifying the end of the joint by changing the geometry can be an effective way of reducing high stress concentrations [9]. Several different configurations of different geometries have been studied and analysed and the idea is to create a more successive transition of the force from the laminate to the substrate [12]. This is typically done by tapering the laminate and/or the adhesive in order to get a successive increase of stiffness. More configurations of fillets and tapering and combinations of them are shown in Figure 3.19, and their expected result regarding shear and peeling stresses are presented in Figure 3.20.

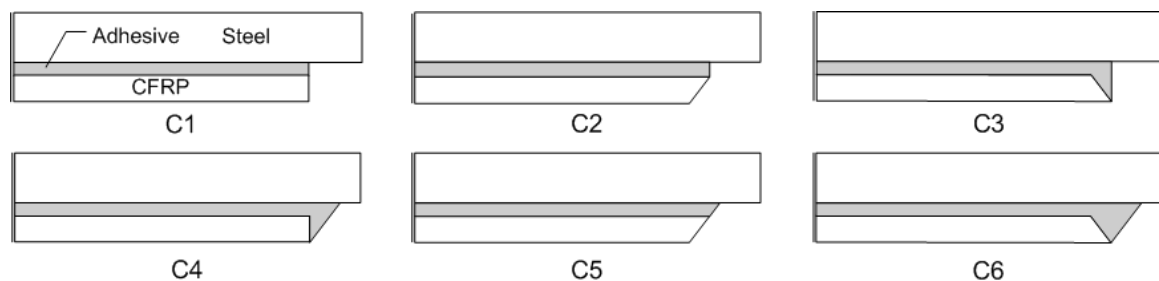


Figure 3.19 Different geometric modifications of adhesive joints: C1: basic configuration, C2: normal taper, C3: reverse taper, C4: adhesive fillet, C5: normal taper and adhesive fillet, C6: reverse taper and adhesive fillet [9].



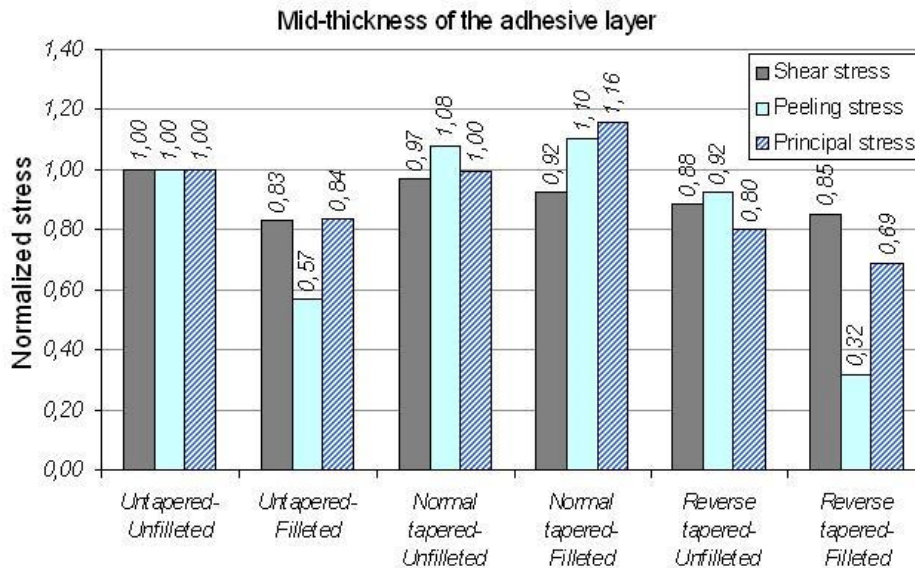


Figure 3.20 Bar diagram showing how the shear stress and peeling stress in the adhesive layer is influenced from tapering and filleting [20].

### 3.6 Critique of unprestressed FRP system

Despite the above stated advantages of FRP strengthening there are factors that needs to be improved with the method.

Experimental studies of beams strengthened with unprestressed CFRP fails when only 10-20% of the ultimate strength in the laminate is reached [25]. However, two other studies show that the strengthened beam fails at 30-50% [26], [27].

During investigations on unprestressed FRP plates the failure is brittle fracture and the failure mode is often debonding of the laminate [6], [13]. This is caused by failure in the concrete leading to separation of the concrete cover.

Several studies have been carried out to design an anchoring system so that the problem with peeling failures of the laminates can be avoided [6]. These include both mechanical anchors, bolted and glued angled plates, and transversally wrapped FRP sheets around the web of the beam. Bolted anchors eliminate the problem with FRP laminate separation but premature failure is still observed due to shear cracking making the concrete cover below the internal steel reinforcement to separate. The bolted anchors do provide a significant improvement to the composite action also after separation of the laminate. The wrapped FRP anchors changed the failure mode from premature laminate debonding to tensile failure of the laminate and this behaviour is expected according to [23]. Beams with anchors show a more ductile behaviour than beams without them. But even when solving the problems stated above using anchors the utilized potential of the unprestressed FRP laminates compared with their high initial cost is too low, i.e. benefits within service state are poor.

While the effectiveness of the strengthening method with unprestressed laminates has been proven, there are disadvantages involved in this method, especially compared to prestressed FRP laminates. By prestressing the laminates it is possible to utilize the full capacity of the laminates. Even though the problem with debonding can be solved

with special external stirrups or anchorages, it can be retarded or even eliminated if a prestressing force in the order of 20% of ultimate load is applied in the laminate. Also, the use of unprestressed laminates can only support the additional live loads and will not affect the deflection, cracking load and crack-widths due to the dead-weight [13], [28]. Studies show that the flexural strength is enhanced by the addition of laminates but the failure mode can become brittle often due to de-lamination or peeling of the laminate in the high shear zones near the laminate ends. To gain the greatest advantage and to be able to fully utilize the potential of bonded of CFRP the laminates have to be prestressed. Prestressing will improve the serviceability and further improve ultimate capacity of strengthened structures in several ways and will be presented in the next chapter.

## 4 Applications of Prestressed FRP Laminates

The following chapter will treat the concept of prestressing and will emphasise the advantages adopting the technique but it will also handle the problem that arises within the field of prestressed bonded laminates. As the concept and main focus is on flexural strengthening of concrete beams the remainder of this report will only treat concrete and steel members will not be further discussed. Although, the principle and the concept will work just as well on steel beams but it will need modifications to handle the problems with mounting and installing the device prior to prestressing. Also, as strengthening of steel beams using prestressing techniques is less beneficial compared with concrete beams and the fact that most of the structures in need of strengthening is made of concrete justifies where the focus is placed.

### 4.1 Introduction to prestressing

Prestressing is a common technique used in several fields of civil engineering today, generally for the improvement of flexural stiffness of beams and bridges [29]. The technique is based on applying a compressive normal force into the beam, either internally or externally, in order to give initial compressive and tensile stresses. These stresses, or initial upward cambering, will counteract the bending that occurs when an external load is applied. Figure 4.1 illustrates the basic principle of an externally bonded prestressed laminate. In the second step the laminate is prestressed and applied to the beam and in the third step where the force is released the upward cambering effect is obtained.



Figure 4.1 The principle steps in prestressing.

Prestressing is primarily used in order to improve serviceability of strengthened structures but there are several benefits with prestressing [6], [28]:

- Reduce crack widths and delay onset of cracking,
- Relieve stress in the internal reinforcement and delays yielding,
- Possibly control the crack distribution,
- Increasing the stiffness and reduce and limit deflections,
- Fatigue failure is resisted by induced compressive stress,
- Further increase the load bearing capacity of reinforced concrete beams,
- Higher utilization of both concrete and FRP,

- Replace lost prestress in internal reinforcement,
- Increase shear capacity by the compressive stresses induced in the beam.

## 4.2 Prestressed CFRP laminates

When strengthening a structure using regular unprestressed CFRP laminates, only the deflection and stresses from the additional load will be reduced [2]. By adding a prestressing force into the CFRP laminate the material will be used more efficiently because a larger part of the laminates capacity is utilized. Prestressing also improve the structural capacity in service state as it reduces initial deflections and lower the stresses. This will improve fatigue life of details subjected to tensile loading. For concrete structures the induced prestressing force improves a number of factors including unloading of reinforcement, closing or delaying crack propagation and improving the durability.

The resulting initial stress distribution due to the prestressing force can be seen in Figure 4.2.

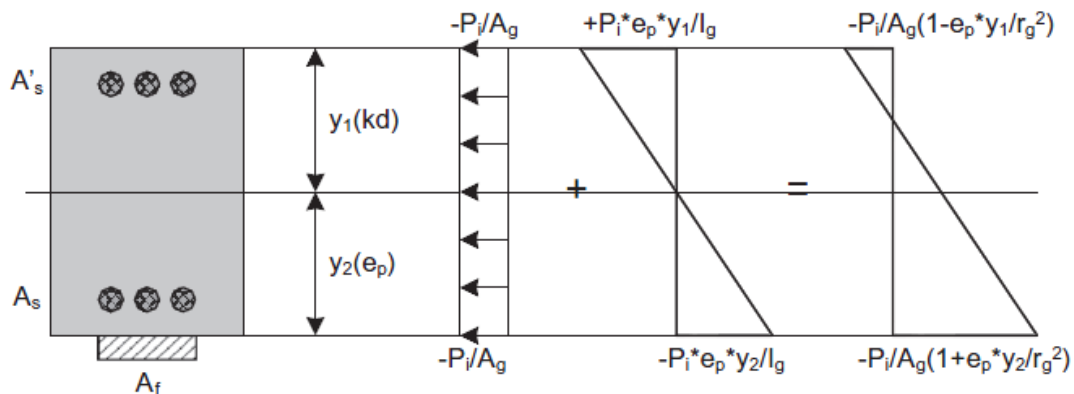


Figure 4.2 Stress distribution in a section strengthened by prestressed FRP [30].

### 4.2.1 Prestressing systems

In general there are three different methods that are used to externally prestress and bond FRP laminates and these are presented in this section.

#### 4.2.1.1 Cambered beam system

The cambered beam system is a way of prestressing the laminate by using hydraulic jacks to lift the beam at mid-span and counteract the deflection caused by self-weight [6]. The FRP-laminate is then attached to the beam in its elevated position and a prestressing force is induced upon release of the hydraulic jack, the sequence of events can be seen in Figure 4.3. This method can only produce a small amount of prestressing force and it requires a large effort to lift the beam at mid-span. It has been shown that this method is very material inefficient and there is an extensive risk of damaging and overstressing the beam at the same time.

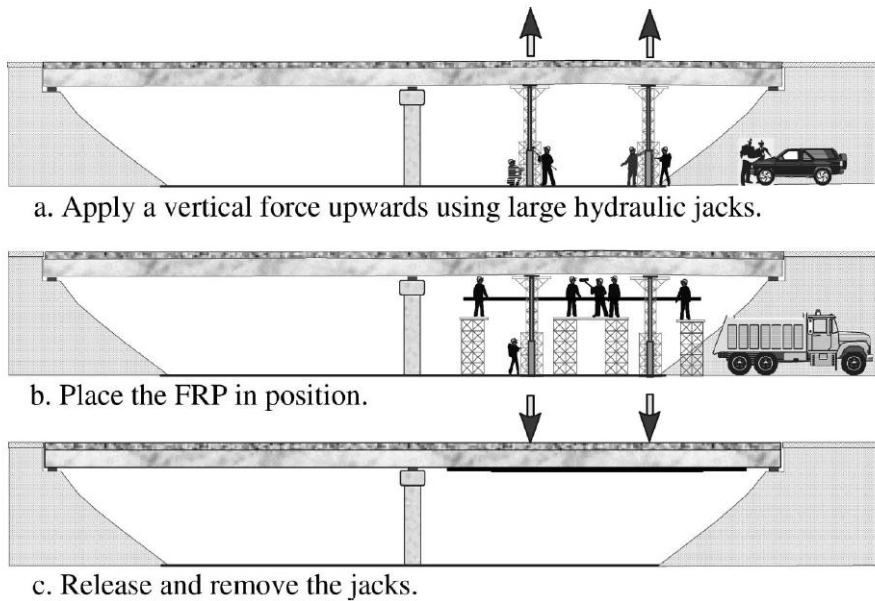


Figure 4.3 Cambered beam system [6].

#### 4.2.1.2 Tensioning against an independent beam system

This method of prestressing is using an external steel frame to prestress the CFRP laminates [6]. The laminates are anchored to the jacks with steel plates and when the laminates are tensioned they are bonded to the strengthened beam with an adhesive. When the adhesive is fully cured the external prestressing force is reduced gradually and the laminates are cut at the ends, see Figure 4.4. This method is tested in laboratory on smaller scale beams, but at a larger scale beams and for field applications specialized equipment is needed.

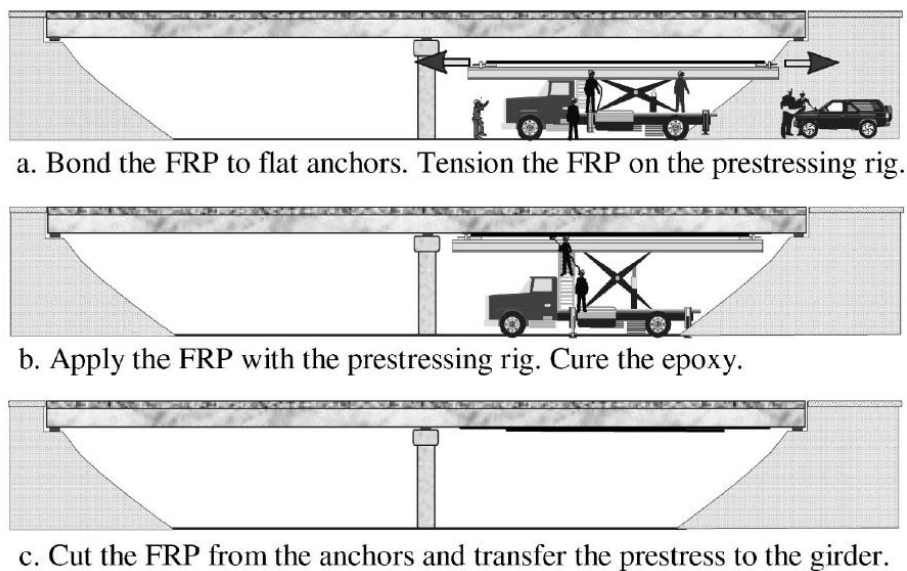


Figure 4.4 Tensioning against an independent beam [6].

#### 4.2.1.3 Tensioning against the strengthened beam

The third method is using the strengthened beam to pre-stress the laminate. The laminate is anchored to the pre-stressing device at both ends and separate permanent

anchors are mounted to the strengthened beam [6]. The laminate is then pre-stressed by pulling the anchors attached to the laminate reacting to the anchors that are fixed permanent on the strengthened beam, see Figure 4.5.

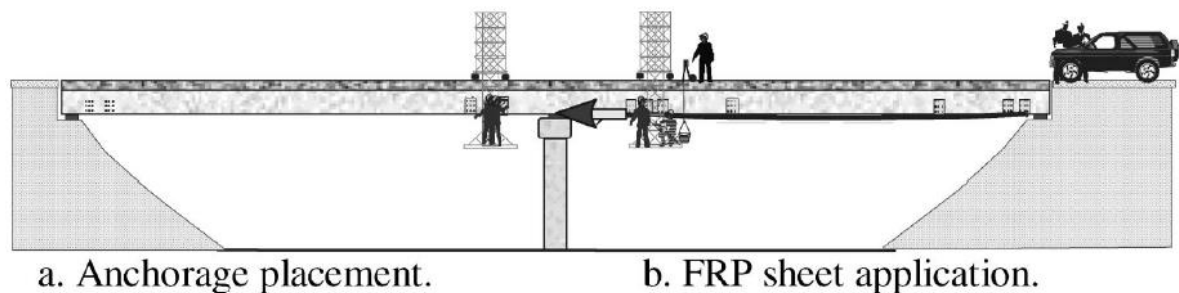


Figure 4.5 Tensioning against the strengthened beam [6].

#### 4.2.2 Literature review of earlier experiments

The idea of prestressing FRP laminates arises already in the early nineties and a lot of different experiments have been carried out since then. Triantafillou developed an analytical model in 1991 where the problems with high shear stresses near the ends were investigated and possible solutions were discussed [5]. It was concluded that there may be necessary to use mechanical anchors to be able to utilize the advantages with the method. In 1992 the same Triantafillou carried out successful experiments on small plain concrete beams with prestressed laminates. It showed that the strengthened concrete beams exhibited great stiffness, strength and ductility characteristics as long as the ends of the laminates were sufficiently anchored.

In strengthened concrete beams with CFRP laminates prestressed to 50 and 75% of their tensile strength, the higher prestressing failed earlier due to the low tensile strain capacity left in the laminate after prestressing [22].

During the nineties many experiments were carried out with different methods and varying results, but all with promising results about what was achievable with prestressed laminates [6].

Several experiments with different prestressing levels have all indicated that cracking load and flexural strength increased with increased prestressing level [13], [25], [26].

[25], measured large increases in both cracking load and yield load for the internal reinforcement. Prestress levels, actual at testing, varied between 31 and 51% and the increase in cracking load and yield load compared to a non-strengthened control beam was 30% to 105% and 70% to 145% respectively. The load bearing capacity increased in the range of 60% to 130% over the non-strengthened beam. Beams with non-prestressed laminates were also included in this test and displayed improvement over the non-strengthened beam but not significant in service state, although the load bearing capacity improved with 60% over the non-strengthened beam.

[27] also investigated different and prestressing levels, 0% to 60%, and varied the number of laminates for the non-prestressed beams. The experienced improvements are similar to the ones in [25] experiment the same year but also concluded that increasing the amount of CFRP also increase the strengthening efficiency with an

increase of 40-60% for a single laminate and 100% for double laminates compared to a non-strengthened beam.

Another similar experiment was carried out where the highest prestressing was 70% of the laminates ultimate strength [30]. For this beam the increase in cracking load and steel yielding load was 235% and 186% respectively but as the failure mode was brittle with laminate rupture without any signs of delamination the study concluded that a prestressing of maximum 50% is recommended to have a safety margin of certain ductility.

S Hong and S-K Park, 2012, also concluded that the prestressing level should be kept at a certain level in order to not have any problems with brittle failure [31]. The level that was recommended in this report was 40%.

All experiments carried out have been using mechanical anchors of some kind and the most recent experiments all use anchors similar to the anchor systems available on the commercial market. These recent experiments are also based on the technique of prestressing against the strengthened beam but several of the experiments during the nineties used the technique where the laminate is prestressed against an independent beam system [22].

The above mentioned results are to prove the efficiency of prestressed laminates with regard to serviceability state and ultimate capacity, however there are also experiments on other aspects in terms of performance of prestressed laminates.

[4] investigated how prestressed laminates were affected by temperature by testing concrete beams strengthened with prestressed laminates which had been subjected to room and low temperature (+22°C and -28°C) prior to testing. The results showed that there were no signs, negligible, of difference between the beams and concluded that it should be possible to strengthen and repair using this method despite if the environments reach extreme low temperature. In the same study the effect of long-term loading, approximately one year, was investigated and the average long-term loss was 11% in room temperature and 4.5% due to low temperature. The low temperature loss was recovered when the low temperature beam was subjected and heated to room temperature again. A prediction of a 5% long-term loss after 50 years was made and this indicates that this could be interpreted into the design.

Wen-Wei Wang, 2012, investigated prestress loss by monitoring the loss depending on initial anchor set, relaxation of CFRP and creep and shrinkage of the concrete [32]. It was concluded that the initial loss caused by anchor set was 12.6-18.2% and that the combined loss caused by CFRP relaxation and concrete creep and shrinkage only 2.3-3.9%. The losses due to relaxation of the laminate occur after 100 h and after this the relaxation is negligible. The adhesive bond line between laminate and concrete is predicted to give an impact on the prestress loss which is 170% larger than the loss from laminate relaxation and this is therefore of greater importance than losses in the laminate.

The difference between bonded and un-bonded laminates has also been investigated. [26] concluded that bonded laminates compared to un-bonded laminates had a slightly higher cracking load as well as yielding load and ultimate load. The beams with bonded laminates also showed a more ductile behaviour, however when [27] investigated the same parameter the result was the other way around and the un-bonded system showed a more ductile behaviour.

The literature studied covered many of the subjects involved when working with strengthening with CFRP materials. They all emphasize the many beneficial properties CFRP materials exhibit and the potential of prestressed CFRP.

### 4.2.3 Problem with prestressed laminates

The problem with prestressed bonded laminates is the high shear stresses at the ends of the laminates which are too high for the tensile strength of the concrete making it debond [33]. The shear stress is directly related to the difference in strain between the laminate and the substrate. To be able to understand what parameters that affect the shear stress, the main expressions are presented in equations (4.1) to (4.5). The whole derivation of the expressions describing the shear stress, the axial force and the bending moment can be found in Appendix A.

The shear stress can be described by the relation between the strain in the laminate and the concrete:

$$\tau(x) = \frac{G_a}{t_a} (\delta_l(x) - \delta_b(x)) \quad (4.1)$$

Shear stress along the bond line with x as the distance along the beam starting from the middle can be calculated using this expression:

$$\tau(x) = \frac{G_a P_0}{t_a A_l E_l} \frac{\sinh(\omega x)}{2\omega \cosh\left(\frac{\omega L}{2}\right)} \quad (4.2)$$

Where the constant  $\omega$  as following:

$$\omega^2 = \frac{G_a}{t_a} \left( \frac{b_l}{A_l E_l} + \frac{b_l}{A_b E_b} + \frac{b_l h^2}{4I_b E_b} \right) \quad (4.3)$$

Axial force in the laminate is found with this expression:

$$P_l(x) = \frac{P}{A_l E_l} \left[ 1 - \frac{\cosh(\omega x)}{\cosh\left(\frac{\omega L}{2}\right)} \right] \frac{1}{\left( \frac{1}{A_l E_l} + \frac{1}{A_b E_b} + \frac{h^2}{4E_b I_b} \right)} \quad (4.4)$$

And the distribution of bending moment along the strengthened length of the beam becomes then:

$$M_b(x) = -P_0 \frac{h}{2} \frac{\left[ 1 - \frac{\cosh(\omega x)}{\cosh\left(\frac{\omega L}{2}\right)} \right]}{\left( 1 + \frac{A_l E_l}{A_b E_b} + \frac{A_l E_l h^2}{4E_b I_b} \right)} \quad (4.5)$$

From the derived equations it is possible to determine the parameters that affect the shear stress in the adhesive and the axial force in the laminate, and how they affect.



There are several parameters that can be changed to influence the interfacial shear stress [33]:

- Shear stiffness of adhesive,
- Thickness of adhesive,
- Stiffness of laminate,
- Thickness of laminate.

The result of a higher adhesive shear stiffness is that the anchorage length of the prestressing force decreases [33]. This decrease of the anchorage length will increase the interfacial shear stresses. However, by increasing the thickness of the adhesive the interfacial shear stresses are reduced. This parameter is coupled with the adhesive shear stiffness as it is a part of the ratio  $G_a/t_a$  in equation (4.1). In contrary with the effect of increased adhesive shear stiffness the increase of the laminate axial stiffness will result in a decrease of the interfacial shear stresses. This is due to the fact that the initial strain required to reach a desirable prestressing force in a stiffer laminate will be lower. However, increasing the laminate stiffness will result in a larger loss of prestressing force due to initial or long term deformations. Increasing the thickness of the laminate has the same effect as increasing the stiffness of the laminate and hence the same effect on the shear stress and the increased prestressing losses.

#### 4.2.4 Governing failure mode of prestressed laminates

It has been mentioned earlier that shear crack debonding failure can be delayed or prevented with a prestressing force of 20% of the laminates ultimate strength. Although when the laminates are prestressed with a force of approximately 5% of the laminate ultimate tensile strength the laminate shear off at the laminate end due to high shear stresses [6], [22]. The shear stresses could be as high as 100MPa at the very end of the laminate if a prestressing force of 20ton is used; this is illustrated in Figure 4.6.

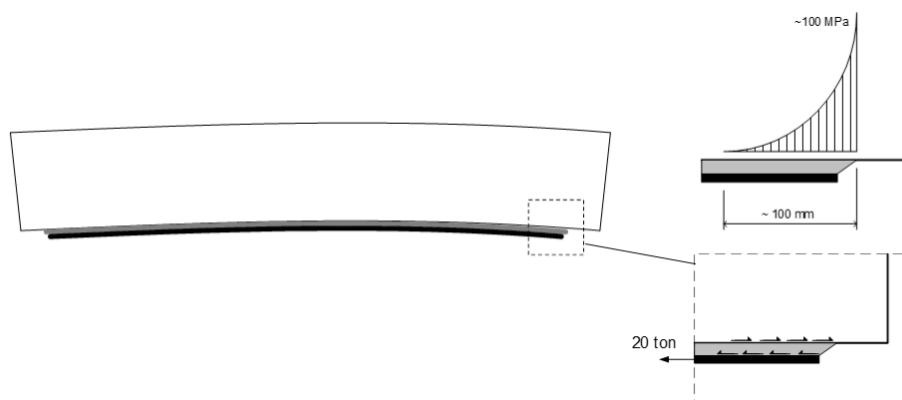


Figure 4.6 Illustration of the high shear stresses at the end of adhered prestressed laminates.

Other than the earlier mentioned methods to affect the high shear stresses, there are methods which can be used to reduce the risk of peeling failure by reducing the magnitude of normal and shear stress concentrations at the ends of the prestressed laminate, or by reducing the prestress level in the laminate at the location of termination [6]. This can be achieved by:

- Terminating the FRP laminates successively,
- Increasing or decreasing the number of FRP laminates,
- Changing the laminate geometry at the anchorage zones.

However, even though these measures lower the shear stresses at the bond interface, they will only increase the possible prestressing force by a small margin and larger reductions of the shear stress concentrations has to be done.

As the typical shear strength of the adhesive is around 25MPa and of the concrete around 3MPa, the failure will be initiated in the weaker of these two materials. This is clear in Figure 4.7, showing the typical debonding failure and where this problem is solved with anchors which are the typical way of solving this problem today.



*Figure 4.7 Laminate debonding caused by high shear stresses at the laminate end as a result of prestressing [34].*

## **4.2.5 Pre-stressing systems with mechanical anchors**

### **4.2.5.1 Commercial prestressing systems**

There are a number of different commercially available prestressing systems on the market. What they all have in common is that they use some kind of mechanical anchors.

The Sika LEOBA prestressing system is based on using temporary as well as permanent mechanical anchors [35], [36]. These anchors are attached to an anchor plate which is located in a cavity in the concrete, see Figure 4.8. This cavity has to be cut out of the concrete. The anchor plate is used as a base plate to transfer the force from the anchor to the concrete. The CFRP laminates are prestressed using a hydraulic jack and the temporary anchorage is blocked with locking screws. Permanent anchors are then installed with both bolts and adhesive and when the adhesive has fully cured it is possible to remove the temporary anchors and solely rely on the permanent anchors.



Figure 4.8 Tension head with temporary anchors and permanent anchor block from the Sika LEOBA system [36].

The Sika StressHead system [35], [36]. With this system the CFRP laminates are prepared with the elliptically shaped Sika StressHead. A hole is drilled in the concrete where a steel framework is placed using the hole as an anchor point. The steel framework is used to prestress the laminates with a hydraulic jack and after the prestressing the StressHead is blocked with a mechanical anchor, see Figure 4.9.



Figure 4.9 To the left is a picture of the Sika StressHead system installed with the permanent mechanical anchor locking the StressHead in place, and to the right is two pictures of the steel framework [36].

S&P is another company that provides a prestressing system for CFRP laminates [35]. This system is, like the Sika systems, based on using mechanical anchorage. The CFRP laminates are prepared with a special anchorage element consisting of two steel plates and one cylindrical element that are fixed to the laminates. The laminates are then prestressed using a hydraulic jack and when the adhesive has cured the jack can be removed and the anchorage is secured.

Similarly to the previous mentioned systems, Neoxe prestressing system uses mechanical anchors [37]. CFRP strips with steel plates mounted on both ends are prestressed using a hydraulic jack. At one of the ends, the steel plate anchor is bolted to the strengthened beam and at the other end of the plate a temporary anchor is mounted with a device for the hydraulic jack, sees Figure 4.10. The CFRP strip is then prepared with an adhesive as well as the concrete surface. After jacking the CFRP strip to desired prestressing force the end with the temporary anchor is permanently anchored by using bolts.

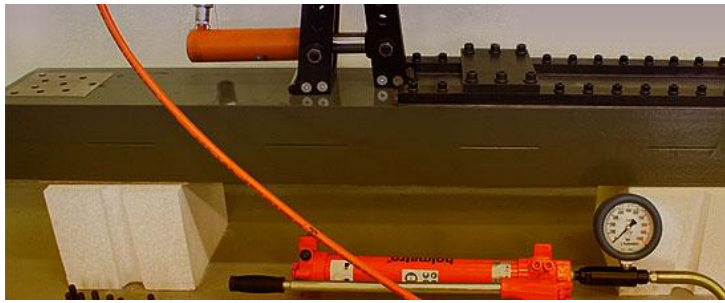


Figure 4.10 The Neoxe prestressing system with hydraulic jack and temporary anchor [37].

### 4.3 Comparison of unprestressed systems with prestressed systems

There are several advantages to prestress the CFRP-laminates compared to using unprestressed laminates [6]. Unprestressed laminates have been widely used for strengthening with the only advantage over prestressed laminates that it is less labour-intensive. Prestressing the laminates not only utilizes a significantly larger amount the laminates capacity it also increases the serviceability performance which the unprestressed laminates lack the ability to do. By prestressing the laminates the failure mode often change from peeling failure or delamination to rupture of the FRP laminate itself, given that the laminate is properly anchored. The combination of the high efficiency of external prestressing, light-weight material and its superb durability strengthening using prestressed FRP laminates has become one of the most promising solutions today.

Figure 4.11 show a load-deflection graph over the typical behaviour of strengthened beams compared to an unstrengthened beam. It clearly illustrates the benefits of FRP strengthened concrete and especially in using prestressed laminates.

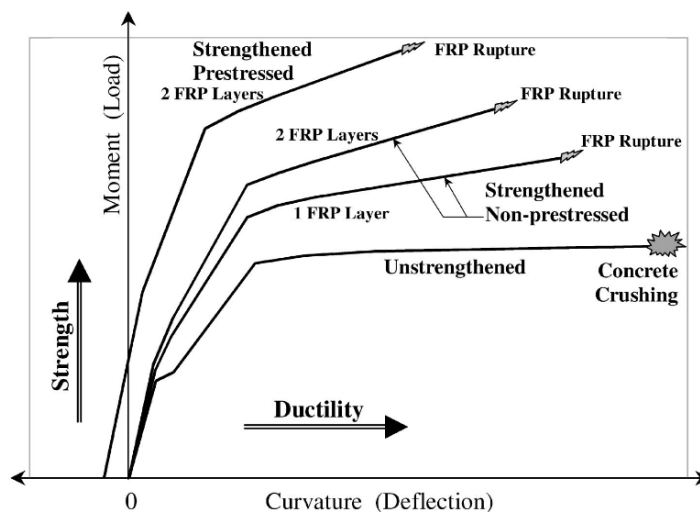


Figure 4.11 Typical load-deflection curves that emphasize the advantages of prestressing FRP laminates for concrete beams [6].

## 4.4 Critique of prestressed systems with mechanical anchors

The problem with debonding of laminates in the high shear stress zones near the ends is often solved with mechanical anchors. Although, that solution has several drawbacks:

- Often complicated with the need of large modifications of the strengthened member; Parts of the member need to be cut out and removed to fit anchors and bolts may have to be fixed in place with mortar or adhesive.
- Costly to manufacture, install and inspect; Manufacturing often needs to be specific for the strengthened structure with small dimensional tolerances.
- Time-consuming with several steps including preparation, cutting and drilling, of the strengthened member and injection of bolts for both temporary and permanent anchors.
- Anchors are aesthetically displeasing, often ugly and visible and if covered they build a lot more which affects the free height and the possibility for inspection.
- The clamping force has to be able to be constant over a long time, if it some part of it is lost the laminate can slip and the shear stresses will become large and failure of the bond is likely
- The mechanical anchors are susceptible to corrosion caused by moisture and dust accumulation. Galvanic corrosion may take place if metal anchors are used to repair members of dissimilar metal.
- Inspection is needed regularly and if they are covered to withstand the risks of environmental and impact damage they are very hard to inspect.
- Drilling holes required for installation of mechanical anchors situated in high moment areas create new fatigue-prone points in steel structures. Often, the strengthening purpose is to enhance the fatigue life, hence causing new problems.

## 5 Concept of the New Prestressing Method

In this chapter, the author's intent to introduce the new prestressing method by background information, including the concept of stepwise prestressing, followed by more elaborate descriptions on how the design of the proposed prestressing concept have been established. Specifically, how results from analyses performed in Abaqus have influenced and changed the design of the system but also describing how the theory is to be realised in practise.

A large part in the development of the concept has been carried out with FE-analysis in Abaqus. The goal with the FE analyses is to identify which parameters that influences, i.e. adds to, the problem definition and reshape/design the prestressing device in light of the results. Hopefully, the results will indicate where improvements can be made so the device may be as optimized as possible. Analysis based on a more advanced model in Abaqus to analyse the shear stress and axial force response in (Chapter 6, Section 6.3).

### 5.1 Concept of stepwise prestressing

With the above stated argument on why it would be beneficial to be able to apply prestressed laminates for strengthening without the need of mechanical anchors a method based on the ideas of Meier is developed, see Section 5.1.1.

The concept of stepwise prestressing is based upon applying the prestressing force to the laminate at several locations to build up the force in steps. This is done to distribute the prestressing force over an increased length of the laminate. As mentioned earlier, in Chapter 4, Section 4.2.3, there is a direct relation between the difference of the substrate displacement and the laminate displacement and the shear stress. By applying the prestressing force in several steps, the difference in displacement is also reduced and hence the shear stress, see Figure 5.1. The slope of the axial force curve corresponds to the shear stress and a lower slope would be beneficial and is therefore desirable.

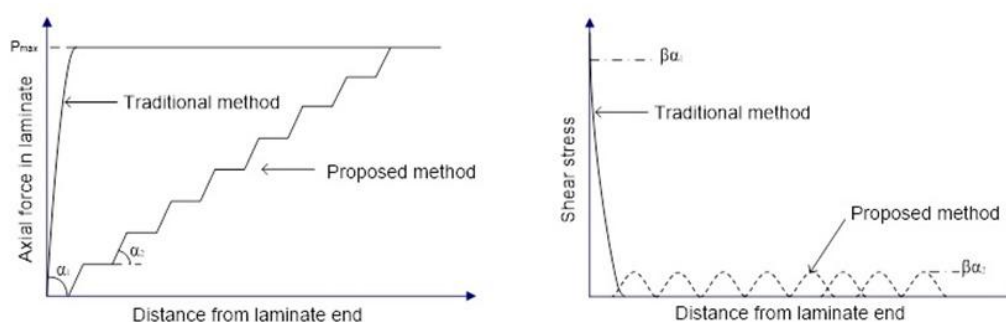


Figure 5.1 The principle of the stepwise prestressing method compared to the traditional method.

The optimum way to get an even shear flow through the adhesive layer and in the concrete the force in each step should be equally large, see Figure 5.2. The number of steps and the distance between these points can be altered to control and optimize the shear flow along the bond line.

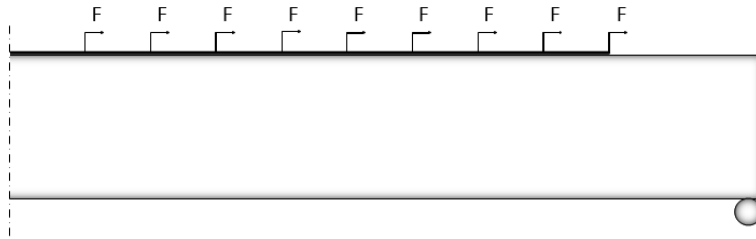


Figure 5.2 The optimal way to prestress stepwise is with equal magnitude and spacing between each step.

### 5.1.1 Meier's technique based on the same principle

Professor Urs Meier and his team at the Swiss Federal Laboratories for Material Science and Technology (EMPA) have been working on a technique which is based on the same concept; to stepwise decrease the prestressing force towards the ends of the laminates to reduce the high shear stress concentrations [38]. Meier's method is using the adhesives curing temperature to achieve this effect. The laminate is prestressed, with a prestressing device capable of adjusting the prestressing force, and applied to the beam, see Figure 5.3. The centre of the laminate and adhesive is then heated with heat elements to cure the adhesive. When the adhesive in the middle of the beam has fully cured, the prestressing force is lowered and the heat elements are moved on step towards the ends of the laminates.

There are, however, limitations in how the technique can be used in practise.

- Higher prestressing force would need more steps which also would need more time.
- An advanced prestressing device is needed as it has to be able to adjust the prestressing force and also release an exact amount of the force in each step.
- Pot life of adhesive limits the number of steps and may affect the resulting bond if adhesive is partly cured while adjusting the prestressing force.
- Time-consuming as the work process includes several steps to complete each laminate and the need to carefully monitor the process.
- The temperature has to be controlled to ensure fully cured adhesive in each step and at the same time not cure adhesive that is supposed to be uncured during a certain step.
- Laminate needs to be pressed against the substrate and the heating element has to have full contact so that there is no risk of uneven curing.

As mentioned earlier the clients in Europe request a solution which is fast to apply, durable and cost-effective and that is what make it necessary to improve upon the technique Meier developed.

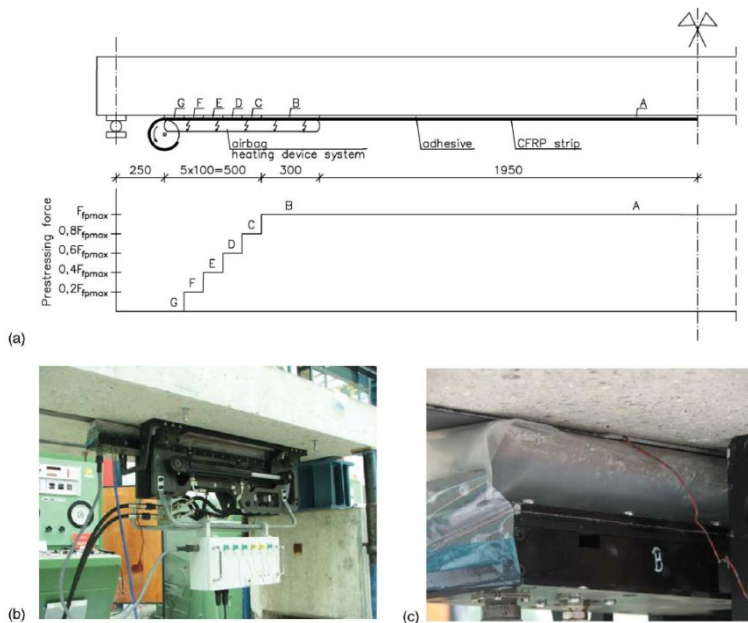


Figure 5.3 The stepwise prestressing technique of Meier: (a) principle prestressing device system and (b) airbag to keep pressure on laminate [28].

Compared to the technique developed by Meier, the concept developed at Chalmers will be easier to use and handle and will be more versatile. The prestressing force will be applied in one phase and it will not have to be adjusted during the process. Without heating elements that have to be moved and controlled to keep the right temperature for the right amount of time the whole prestressing process will be a lot simpler. It will not be limited by pot life and it will not matter how long the beam is, it will work in the exact same manner either way. With Meier’s technique, strengthening of long member will be problematic because of the required heat source to cure the adhesive.

## 5.2 Description of the New Prestressing Method

The technique is based on the prestressing method “Tensioning against the strengthened beam”. This is in accordance with all other commercial methods on the market and it has the advantage that it is versatile and will fit on most structures and won’t have any limitations in terms of length of the strengthened member.

All developments of the system are based on a first prototype here at Chalmers which have been used to carry out experiments on concrete beams. This prototype was not designed for usage more than in the lab where special measures in terms of mounting the system and modifying of the strengthened member are possible.

The prestressing system contains several different parts; a prestressing device, guiding bars, temporary supports, and a hydraulic jack. The temporary supports are used during the prestressing phase to anchor the prestressing force and the guiding bars are used to keep the device in place and will be removed after the prestressing is done.

One device has to be mounted to each end of the laminate to achieve the stepwise effect at both ends but the prestressing force is only applied at one end while the other end is passive and kept fixed using a temporary support of the same kind.



The device is designed with a number of tabs which are connected to each other with steel rods acting as springs to serve as the dividing element of the prestressing force, see Figure 5.4. The tabs in the device are then bolted to the laminate.

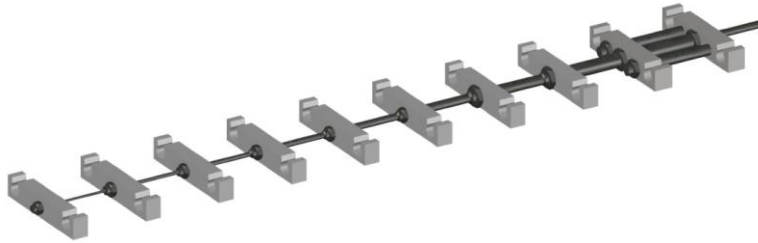


Figure 5.4 The prestressing device used to prestress the laminate in several steps.

When the system is mounted and the adhesive has been applied to the laminate as well as the substrate the full prestressing force is applied to the device. The force is applied with a hydraulic jack that is connected to the prestressing device, which will distribute the force in several steps, see Figure 5.5.

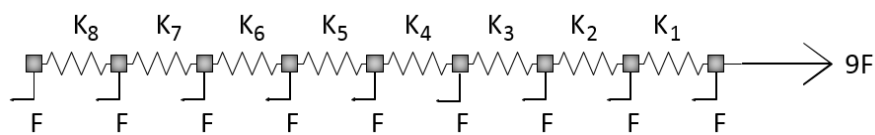


Figure 5.5 Concept of the prestressing device which use springs to equally divide the force.

The full system, including the device, guiding bars, temporary supports and hydraulic jack, mounted to a concrete bridge is shown in Figure 5.6 to give a clear picture of what it will look like. The prestressing force is applied at the right-hand side in the figure where the hydraulic jack is located while the other side is passive. When the prestressing force is applied the jacking rod is locked in the temporary support with a nut and the hydraulic jack can be removed.

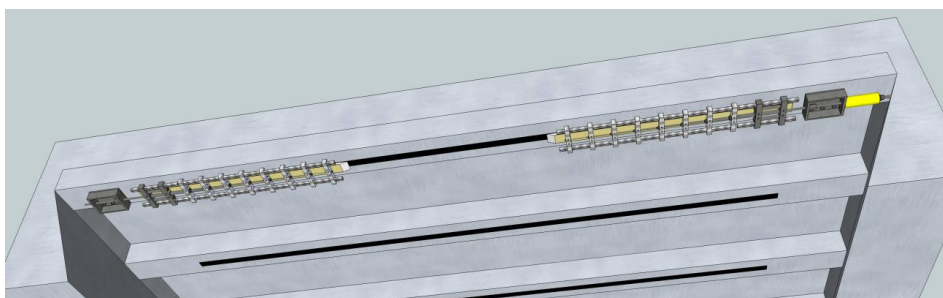


Figure 5.6 The system applied on a model concrete bridge.

When the adhesive has cured the device, the guiding bars and the temporary support is removed from the structure leaving only the thin laminate left on the structure.

### 5.2.1 Details of the concept

In order to make the system fulfil requirements as “ease of use” and “time-efficient” details has to be designed and thought through. This is to reduce the number of steps involved in the prestressing-phase and the ability to mount the system onto the strengthened structure with minimum effort but without jeopardize safety.

After the experimental study (Chapter 7) it was concluded that the possibility to mount the steel tabs with adhesive directly onto the laminate was not possible as they sheared off at a prestressing force lower than intended. With bolts combined with adhesive it was possible to achieve a higher prestressing force but not enough. It was decided that a layer of GFRP with a thickness of 15mm and built in nuts attached on top of the CFRP would be a good solution to transfer the force. As the GFRP would yield at the point where the nuts are placed a solution with a steel plate attached to the nuts to distribute each load step over a larger area in the GFRP. A test of how much this solution would contribute to the shear stress distribution was carried out with the same shell model as used in the parametric study, but with nine steps and a tab spacing of 150mm. The result was very good. The GFRP plate made the anchorage length larger and therefore a larger distance between the tabs was chosen to lower the stresses even more.

In order to mount the CFRP laminate to the device, a GFRP plate is adhered to the top of the CFRP, as stated above. Inside the GFRP plate a steel plate with attached steel nuts is molded. This steel plate is there to both keep the nuts in place during manufacturing and to distribute the load in the GFRP and the nuts are there for the attachment of the device, see Figure 5.7.

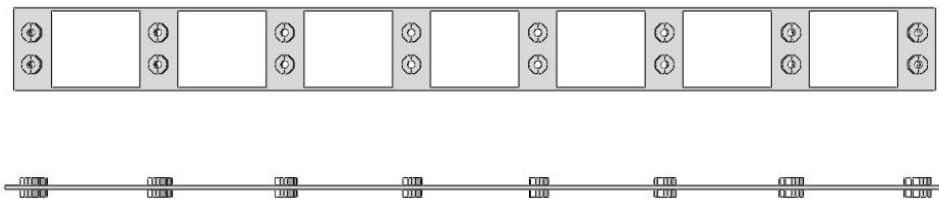
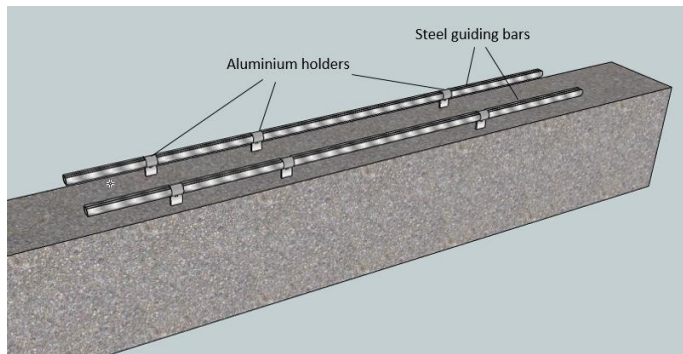


Figure 5.7 The steel plate with nuts which is embedded in the GFRP laminate.

To keep the prestressing device in place and at an even distance from the concrete surface two steel guiding bars are mounted to the beam. These guiding bars are hold in place with six holders, see Figure 5.8, that are split in two pieces just to make it possible to mount the guiding bars in them. The holders are possible to adjust to get the correct and even distance between the device and the beam. This is to both keep the device aligned which is crucial to not get any extra eccentricity to the load when prestressing and to get an even thickness of the adhesive layer. It is done by using double tapered bolts, right hand thread at one side and left hand thread on the other, so when screwing the bolts they will either contract or detract. To be able to reach these screws holes are drilled through the holders as well as the steel guiding bars making it possible to adjust the height of each holder when everything is in place.



*Figure 5.8 The guiding bars mounted to the concrete beam using six adjustable holders.*

The tabs on the device have notches which has the same diameter as the guiding bars mounted on the beam. To be able to mount the device to the guiding bars they have been chamfered so that it is possible to install them and when they are in place, the guiding bars can be turned 90 degrees so that the tabs are locked in place, see Figure 5.9.

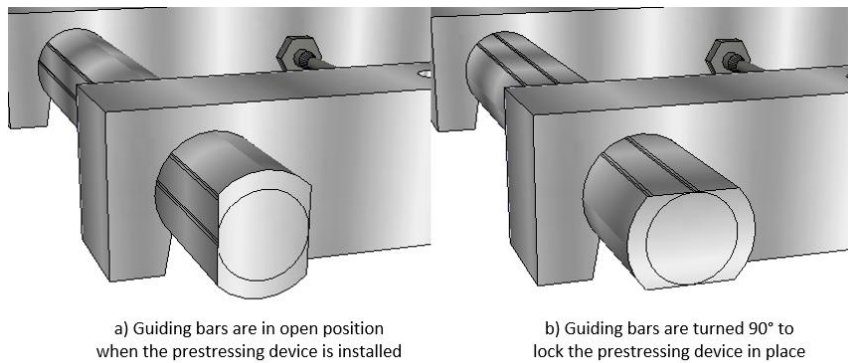


*Figure 5.9 The locking mechanism in both a) opened and b) closed position. It makes it possible to mount the guiding bars without the device attached.*

As the tabs, all but the two first, are of the same width as the holders it is important that they are made to same dimensions as the steel guiding bars so that they are able to run free past the holders without the risk of get stuck. The edges of both the guiding bars and the holders are therefore smoothed to further decrease this risk, see Figure 5.10.

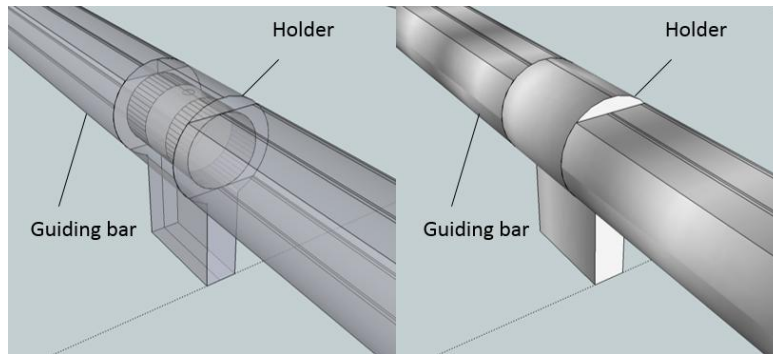


*Figure 5.10 The guiding bars and the holders must have the same diameter and smooth edges to make it possible for the tabs to slide past the holders.*

The prestressing jack is anchored against a support. This support is made like a small box that is mounted to the beam in advance using six bolts. As can be seen in Figure 5.11, the prestressing bar runs through the support box and uses the walls as support for both the hydraulic jack and the locking nut. When the hydraulic jack has reached the full prestressing force the prestressing bar will be locked in place by tightening the nut so that the jack can be demounted and used for the next laminate.

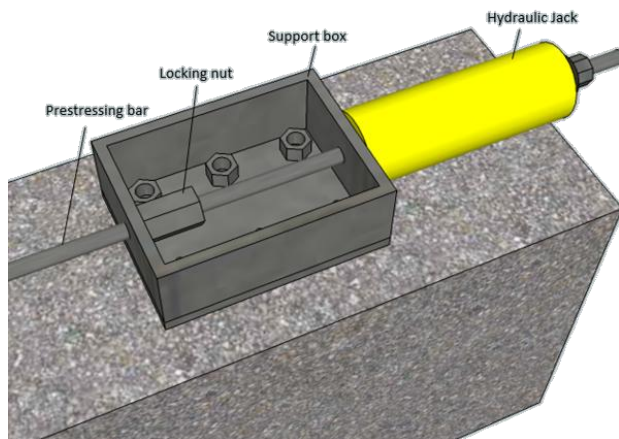


*Figure 5.11 Support box with prestressing bar and hydraulic jack.*

The bolts used to mount the temporary support are of the kind that can be removed and reused. Also, the holes in the box are made elongated (elliptic) to create a margin to allow height adjustment of the support.

When the adhesive have fully cured the nut holding the prestressing bar is released and due to the design of the device all tabs will release at the same time with the same pace. This is achieved by having the steel springs connected as one solid piece with the tabs only locked in place at one side so that the steel spring can move freely upon release, see Figure 5.12. In this way there will be no stresses left in the spring at release that could be transferred to the laminate which could be both destructive and risky.

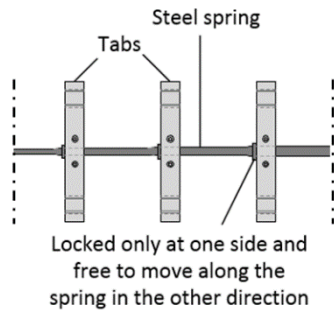


Figure 5.12 Part of the prestressing device with tabs, spring and how it is locked at only one side of each tab by metric nuts.

## 5.2.2 Advantages of the new technique

In comparison with prestressing systems utilizing mechanical anchorage the proposed method and developed system has a number of advantages or rather don't share several of the limitations that those systems have.

- Mechanical anchors can be difficult to use in narrow spaces since they require a comparatively large height.
- Mechanical anchors are often regarded as aesthetically unpleasant and they increase the cross-section even more if they are to be covered.
- Require more bolts and deeper penetration into the substrate, which may affect the durability of the substrate negatively.
- The clamping force has to be able to be constant over a long time, if it some part of it is lost the laminate can slip and the shear stresses will become large and failure of the bond is likely.
- The mechanical anchors are susceptible to corrosion and thus require regular inspection. Furthermore, if they are covered they are hard to inspect.

As this method should be an improvement of the method developed by Meier the limitations of his method stated above has been the starting point of where focus has to be put. Compared with Meier's method, there are several improvements:

- A higher prestressing force distributed over more steps, the prestressing force is high enough to fully utilize the capacity of the laminate but still retain ductile behaviour.
- Using a regular hydraulic jack to prestress the laminate in one single stage eliminating the need for precise adjustment.
- Pot life of adhesive will not be a limit or a problem.
- Time and labour efficient as the work process contains one prestressing stage and no heating elements have to be moved or adjusted.
- The adhesive cures evenly and in accordance with manufacturer's specifications and there is no need to worry about insufficient heat.

## 5.2.3 Application of the new technique

The following list comprehensively describes the application process step by step for the developed prestressing system.

1. The CFRP laminate is equipped with a GFRP plate that has a built in steel plate which makes it possible to attach the device and also to spread the load over a larger area to avoid high stresses in the GFRP plate.
2. The concrete beam and CFRP laminate is prepared and cleaned according to Table 3.1 in Chapter 3, Section 3.3.3.1.
3. The temporary supports are mounted to the beam in an aligned position using laser/ropes/levels. They are first attached using only two, out of a total four bolts per support leaving room for adjustments. When they are aligned the two remaining holes are drilled in the concrete and remaining expanders are mounted.
4. After that the temporary supports are applied the guiding bars are mounted. These have to be completely straight and aligned with each other so that there won't be an issue with high friction between the tabs and the bars. To mount them six holes are drilled in the concrete and threaded anchors are fastened into the concrete using a pattern to get them in the exact right positions. The guiding bars are then adjusted to be straight using a level and with help of right and left threaded bolts which are used to attach the bars to the anchors.
5. The device is mounted to the CFRP laminate with the bonded GFRP layer. Adhesive is mixed and applied to the laminate and the concrete beam to ensure a good bond and then the device with the mounted laminate is attached to the guiding bars.
6. Using a hydraulic jack the laminate is prestressed to desired prestressing force and when it is reached a locking nut is used to lock the prestressing bar in place allowing the hydraulic jack to be removed.
7. When the adhesive has cured the nut is loosened to transfer the prestressing force into the beam and the device, the guiding bars and the temporary support is dismantled from the concrete beam. The GFRP plate can also be removed from the CFRP as its only task is to transfer the prestressing force from the device to the CFRP laminate.

## 6 FE-Modelling of the Concept

In order to understand and to improve the prestressing system the FE-program Abaqus CAE is used to analyse the prestressing system. This is carried out mainly in three larger FE-models to improve the function of the system and some smaller models to ensure and design details of the concept which are necessary for practical reasons. Since some parts of the concept are already manufactured and some parts are manufactured during the project, dimensions and properties are changed through the project based on the findings, while some parameters are fixed.

### 6.1 Parametric study

A parametric study has been carried out in Abaqus CAE. This is done to investigate the behaviour of the CFRP laminate, as well as the maximum value of the shear stress distribution in the adhesive layer along the bond line between the laminate and the concrete beam. A two-dimensional FE-model with shell elements is made based on the geometry seen in Figure 6.1 and is shown in Figure 6.2. Symmetry conditions are utilized at the centre of the concrete beam. The base dimensions of the included members are found in Table 6.1. All materials have elastic material response and the concrete and the steel have an E-modulus of 25 GPa and 210 GPa respectively. The adhesive and CFRP laminate have a variable stiffness and is found in Table 6.2.

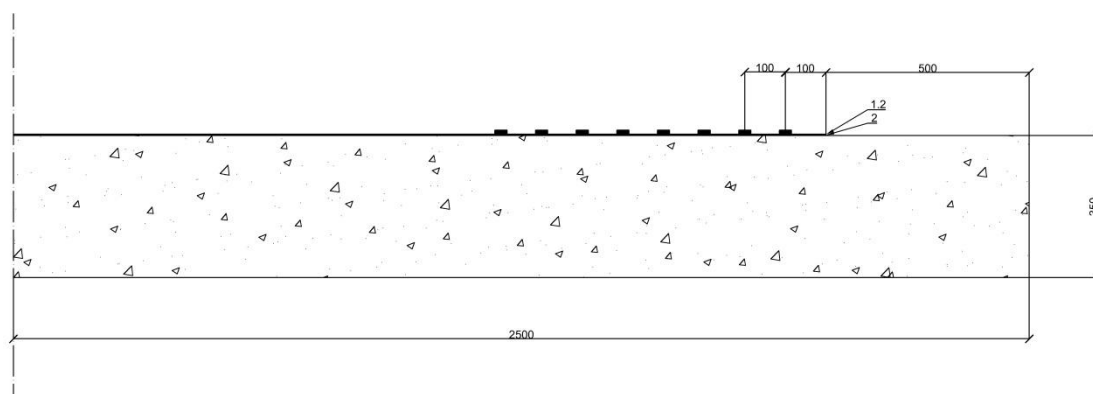


Figure 6.1 Dimensions of the parts in the FE-model (view from the side).

Table 6.1 Dimensions of the parts in the FE-model.

Parts	Dimensions [mm]
Concrete	2500, 350, 250 (length, height, width)
Adhesive	2, 50 (height, width)
CFRP laminate	1.2, 50 (height, width)
Steel tabs	30, 10, 50 (length, height, width)

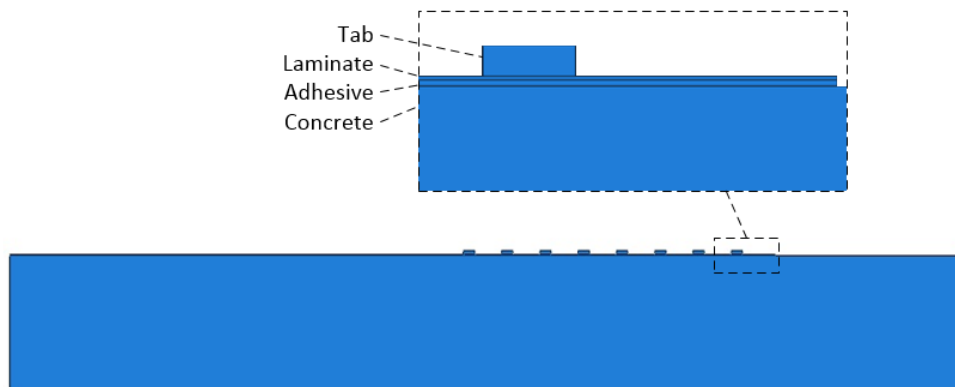


Figure 6.2 2D-shell element FE-model of the beam used in parametric study.

As the prestressing force is applied in steps with the help of steel tabs mounted on top of the laminate, steel tabs are modelled and the prestressing force is applied as a pressure on one side of each tab. A total force of 100kN is applied which is divided over the actual number of steps in each analysis.

All analyses in the parametric study are based on the properties in Table 6.2. The values in bold are the default values and they are used when the parameter is not the alternating one. The first parameter analysed is number of steps to which also gives the default value for this parameter while the other default values are decided in advance.

Table 6.2 Values of the different parameters that were analysed in the parametric study, default values are marked in bold.

Parameter	Varying values
Number of steps	1, 2, 3, 4, 5, 6, 7, <b>8</b> , 9, 10 [steps]
E-modulus Adhesive	4.5, 5.3, 6.2, <b>7.0</b> [GPa]
E-modulus CFRP laminate	150, <b>200</b> , 250, 300 [GPa]
Distance between steel tabs	50, 75, <b>100</b> , 150, 200 [mm]

The analysis is made in three steps. In the first step the prestressing force is applied and the adhesive layer between the CFRP and the concrete beam is deactivated to simulate its properties before curing. In the second step the adhesive is activated with its cured properties in order to simulate a fully cured adhesive and finally in the last step prestressing force is deactivated simulating the release of the prestressing force.

Basically what is interesting is the resulting shear stress distribution in the adhesive, but also the axial force in the laminate. These results are extracted from the analyses by creating a path running through the middle the adhesive and the laminate in the model respectively.



The following analyses in Sections 6.1.1 to 6.1.3 are based on “default” properties and only the parameter studied in each section is changed while the others are fixed, as stated in Table 6.2.

### 6.1.1 Influence of different number of prestressing steps

The concept with stepwise prestressing is based on stepwise tensioning with the tensioning force ranging from nil at the end of the laminates to maximum force after a certain number of steps. In Figure 6.3 it is possible to see the difference in shear stress distribution in the middle of the adhesive along the bond line with different number of steps.

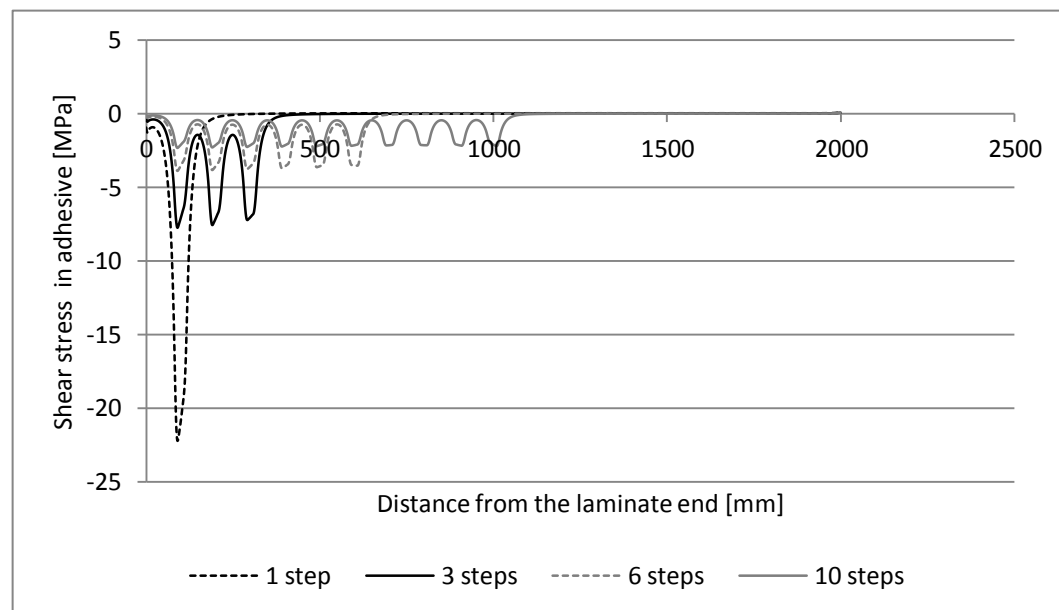


Figure 6.3 The shear stress distribution in the adhesive layer with different number of steps.

To continue with the parametric study a number of steps which is in the region of an acceptable level of maximum shear stress is chosen. A shear stress below 3MPa seems reasonable which corresponds to at least eight steps. Of that reason the rest of the analyses in the parametric study are carried out using eight prestressing steps. Figure 6.4 shows the influence of number of steps (or tabs of the device) on the maximum shear stress in the adhesive layer.

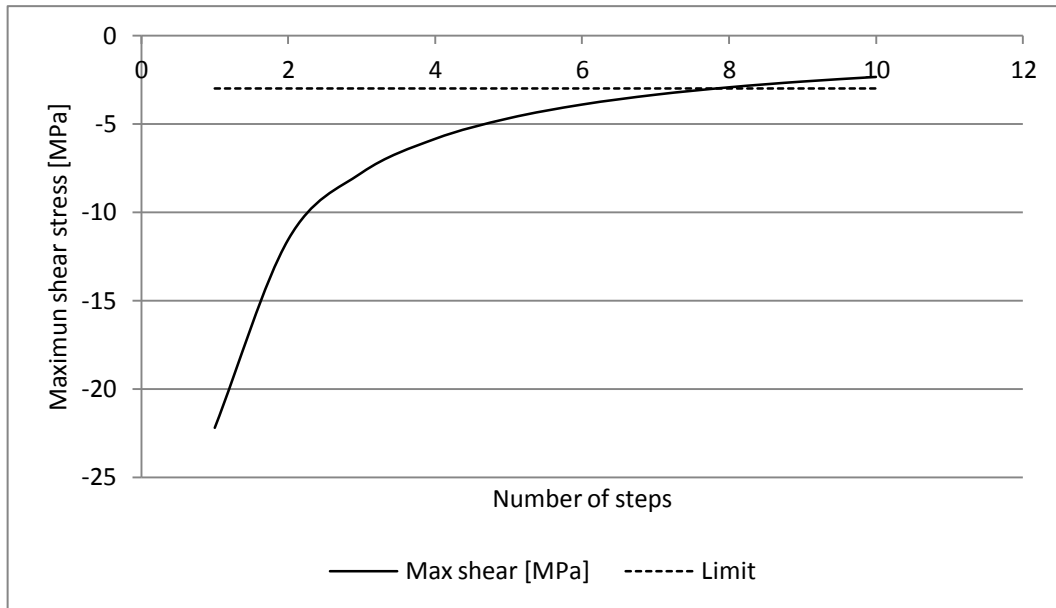


Figure 6.4 The maximum shear stress in the adhesive layer in relation to different number of steps.

By looking at the axial force in the laminate and how it increases it follows the principle of the stepwise prestressing concept very well. In Figure 6.5, the result from prestressing in eight steps and prestressing in one step is compared. Note that the dips in the graphs corresponds to the centre of each tab where the laminate strain is kept low and therefore only a small addition of axial force is taking place here. This is because the tabs and the laminate are merged together and the steel tabs add a lot to the stiffness and most of the force is transferred through the steel tabs. Bear in mind that this is only a result of how the interface between the tabs and the laminate is modelled.

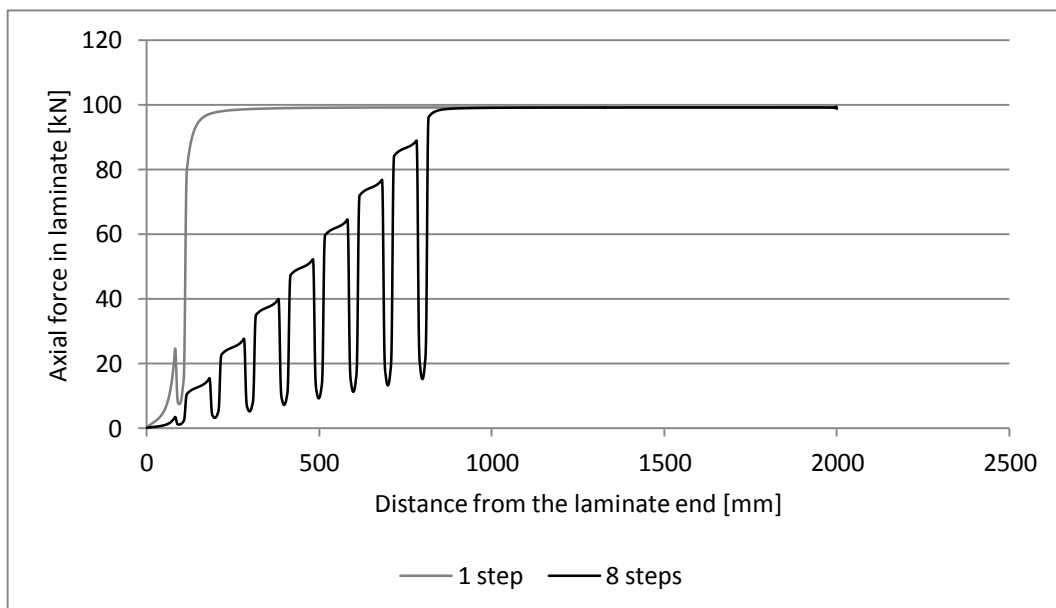


Figure 6.5 Comparison between axial force in CFRP laminate in one and eight steps with 100mm tab spacing.

### 6.1.2 Influence of adhesive stiffness

The stiffness of the adhesive layer bonding the laminate to the concrete has an effect on the maximum shear stiffness. This is because of that the anchorage length which is needed to transfer the force in one step is reduced with a higher stiffness of the adhesive. The adhesive stiffness is varied between four different values ranging from 4.5 to 7.0 GPa, see Figure 6.6, which is typical for adhesives actual for this type of strengthening and repair.

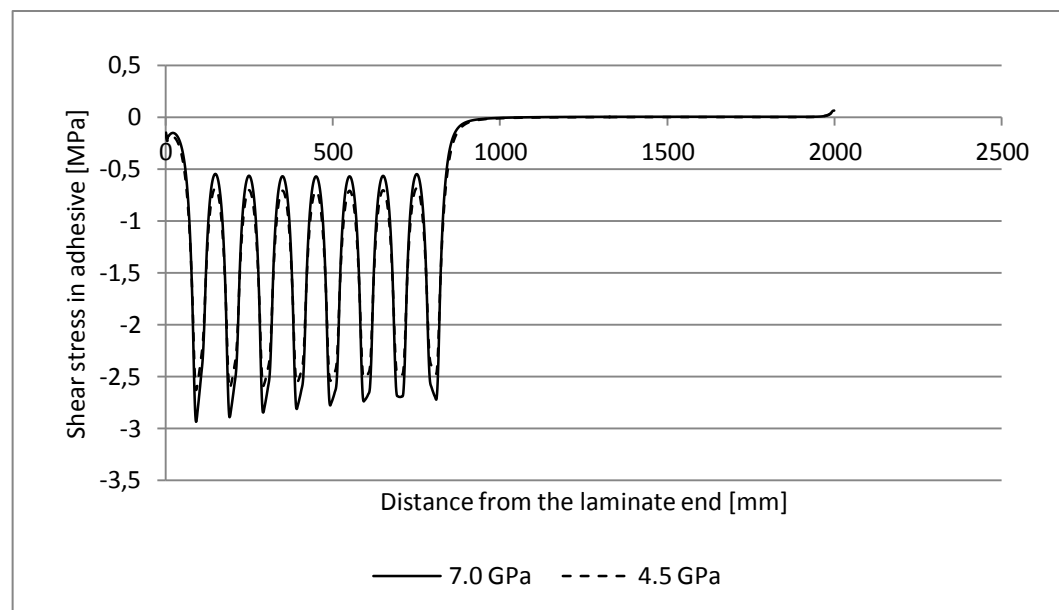


Figure 6.6 The shear stress distribution in the adhesive layer with different adhesive stiffness.

The impact the adhesive stiffness has on the shear stress in the adhesive itself is small, see Figure 6.7. A lower modulus adhesive will be beneficial with larger tab spacing as the anchorage length is longer. Another way to alter the stiffness of the adhesive layer that would give the same impact on the result would be to increase the adhesive thickness; a thicker layer would reduce shear stresses.

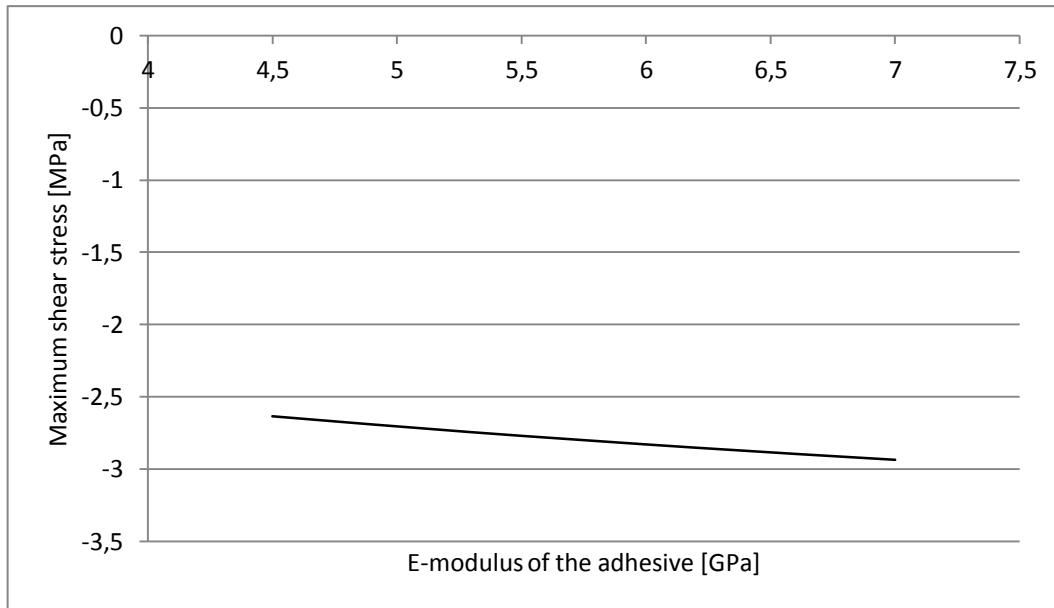


Figure 6.7 The maximum shear stress in the adhesive layer with different E-modulus of the adhesive.

### 6.1.3 Influence of the stiffness of the CFRP laminates

As with the adhesive the CFRP-laminates are also available with different properties where the modulus of elasticity is the parameter to be studied here as well. A laminate with a higher E-modulus have a lower strain at the same stress compared to a laminate with a lower one. As the shear stress in the adhesive is dependent on the strain difference between the substrate and the laminate, a stiffer laminate will result in lower shear stresses in the adhesive due to the smaller initial strain at the same prestressing level, see Figure 6.8.

Four different stiffness of the laminate is analysed, compared in Figure 6.9. The response was similar between the cases, as with the changing adhesive stiffness, and they differ only in magnitudes.

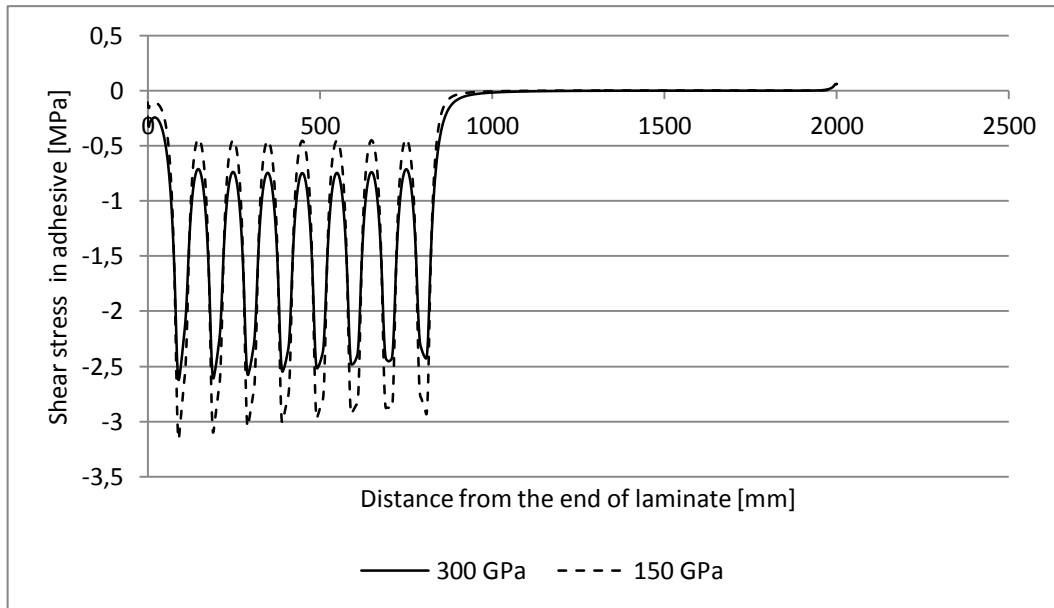


Figure 6.8 The shear stress distribution in the adhesive layer with different laminate stiffness.

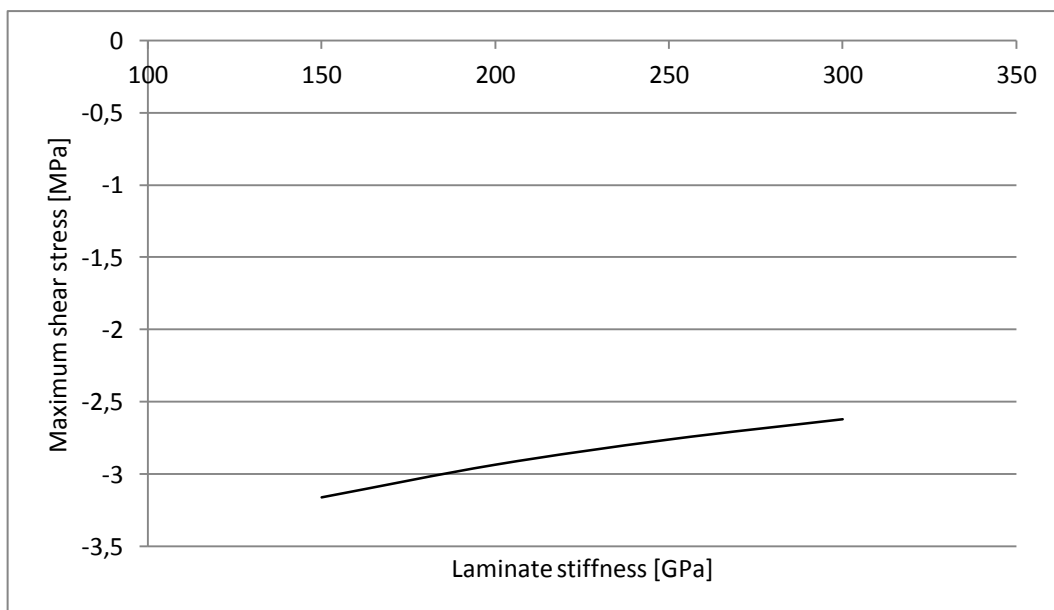


Figure 6.9 The maximum shear stress in the adhesive layer with different laminate stiffness.

#### 6.1.4 Influence of different tab spacing

As the shear is transferred over a certain length, the anchorage length, it is interesting to see how the spacing influences the high shear stresses. Five different spacing were analysed and it showed that a spacing of 100mm would be significant improvement over 50mm and a larger spacing than 100mm would not affect the shear stress much at all. In Figure 6.10, the interaction of anchorage zones are shown and in the 50mm case the total shear stress is increased by the anchorage zones interaction while in the 200mm case the whole anchorage length is able to fit in between the tabs.

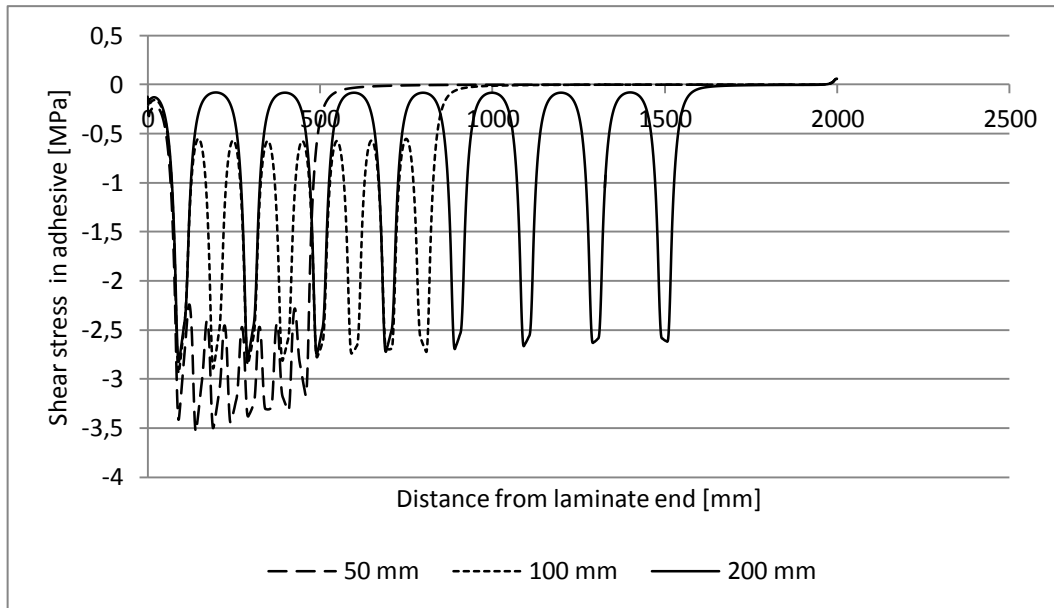


Figure 6.10 The shear stress in the adhesive layer when having three different tab spacing.

The result of changing the spacing between the tabs is an effective way to reduce the shear stress in the adhesive but only to the point where the anchorage length and the distance between the tabs are equal. The tab spacing is dependent on the number of steps in the way that if the number of steps is increased the tab spacing can be less as the force transferred in each step is smaller; requiring a smaller anchorage length, see Figure 6.11.

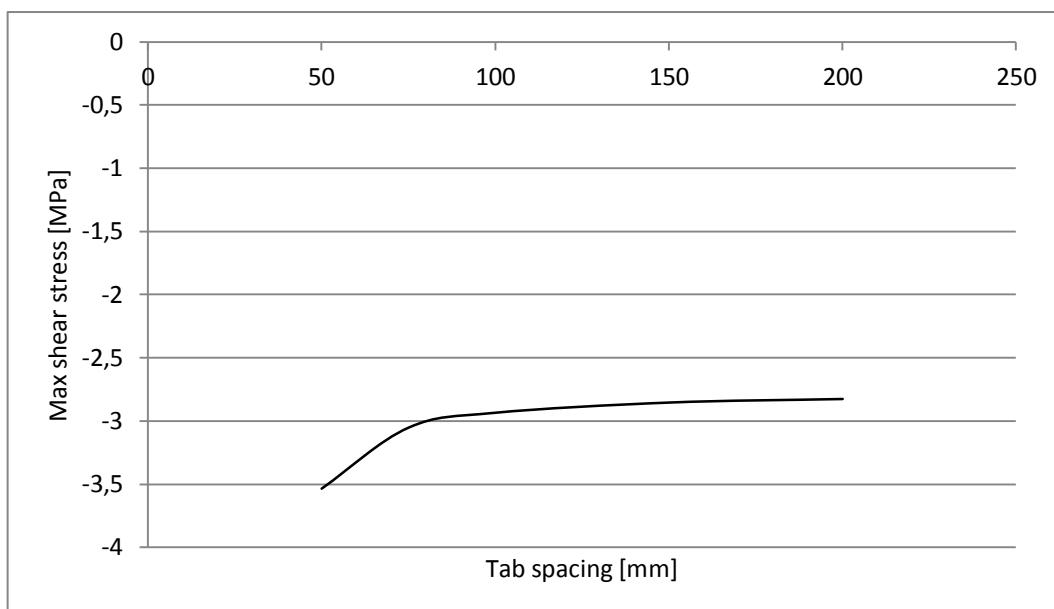


Figure 6.11 The maximum shear stress in the adhesive layer for different tab spacing.

### 6.1.5 Conclusions from the parametric study

After the parametric study it was concluded that the results obtained from each analysis corresponded very well to what was predicted. The parameter that had the

greatest influence on the shear stress was the number of steps in which the prestressing force was applied, i.e. how much the prestressing force was distributed over the laminate. The other parameters did influence the results but not as much as expected. As long as the tab spacing is kept at a distance over 100mm the spacing will not affect the result much at all. Changing from 50mm to 100mm gave a decrease of approx. 21% which is far more than the decrease given by changing from 100 mm to 200 mm. This is proof of that the benefit of increased anchorage length is utilized to its full potential around 100 mm.

By lowering the adhesive modulus the maximum shear was lowered. By comparing the change in modulus and maximum shear it was concluded that the adhesive stiffness affected the shear almost linearly. Changing the adhesive stiffness from 7.0 to 4.5GPa only gave a reduction of approx. 11%. In the same manner as for the adhesive stiffness, the laminate stiffness affected the shear stress almost linearly, although with opposite result i.e. higher laminate stiffness resulted in lower shear stress. Changing the stiffness of the laminate from 150 to 300GPa also gave a decrease of maximum shear stress of approx. 21%. Combining these different values would although result in a significant improvement over the worst scenario, see Figure 6.12.

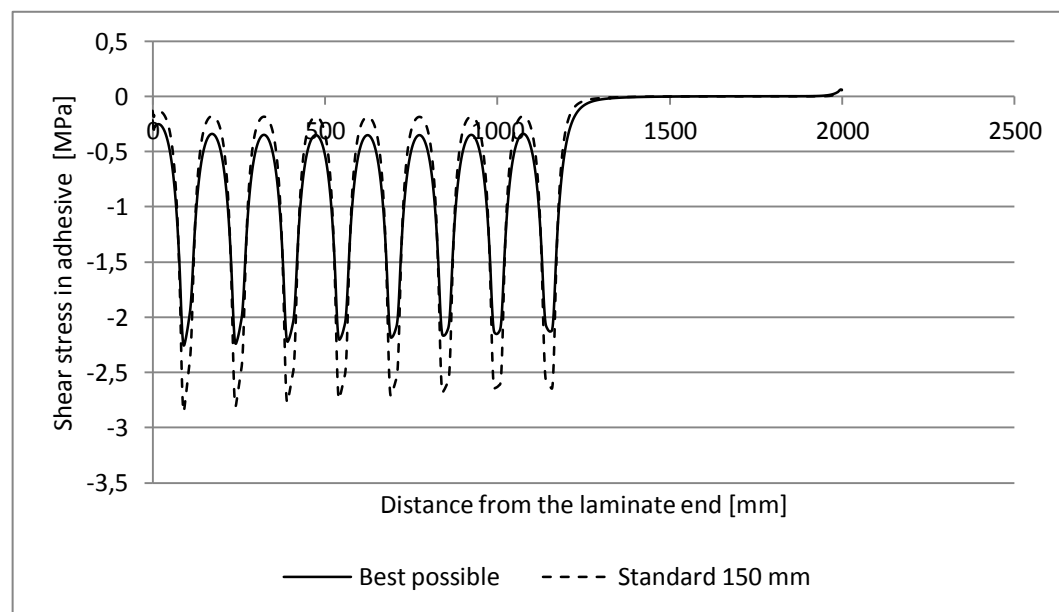


Figure 6.12 Comparison of the shear stresses in the adhesive layer with the best result (with 150mm tab spacing) and the “standard beam”.

## 6.2 FE-model of the concept without the prestressing device

A 3D solid FE-model is made to analyse the concept with more details after the conclusions made in the parametric study. The prestressing device is not included in the model in order not to add too much in one step to simplify in identifying potential issues. The main purpose of the model is to study the results of the added complexity and make conclusions based on that.

As the earlier experiments carried out at Chalmers resulted in that a GFRP plate with a steel plate molded inside was added on top of the CFRP laminate, this was added in the FE-model of the concept, see Figure 6.13.

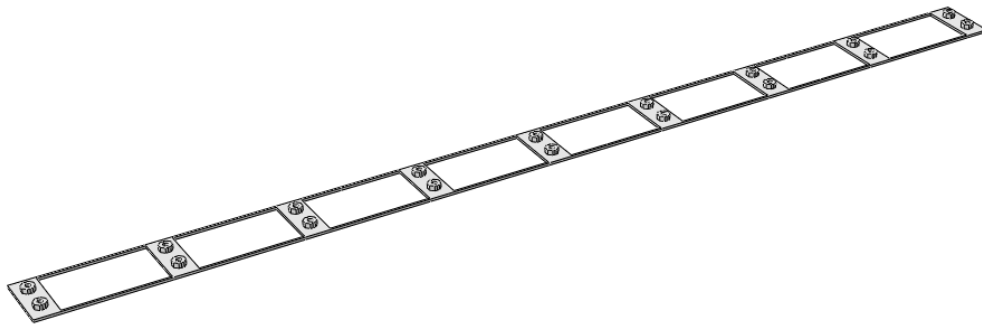


Figure 6.13 Illustration of the steel plate which is molded inside the GFRP plate to distribute the load over a larger area to avoid yielding of the GFRP.

To reduce the peeling effect and the stress concentration that would emerge at the transition in the adhesive between the GFRP plate end and the CFRP the termination of the GFRP laminate is reverse tapered and the adhesive between the GFRP and CFRP is also tapered, see Figure 6.14.

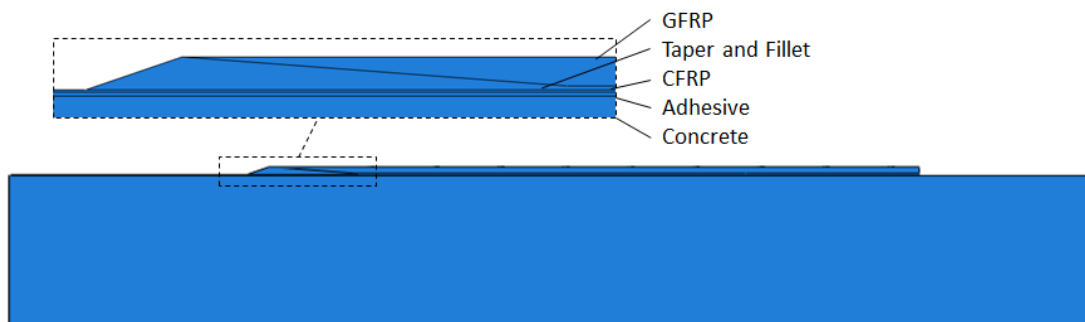


Figure 6.14 The tapering and the fillet between the GFRP plate and CFRP laminate.

To be able to study the response in the all of the parts of this new model, a 3D FE-model was created in ABAQUS using solid homogenous elements, see Figure 6.15.



Figure 6.15 The Abaqus FE-model without the prestressing device.



Material parameters which are used in this model are presented in the Table 6.3. The limit for the tensile strength of the concrete is based on the lowest concrete classes in EuroCode2. Class 12/15 have a tensile strength of 1.1MPa for the fifth percentile. Getting below this value would be optimal. The steel yield strength is based on the yield strength of S355 steel, i.e. 355MPa. Adhesive strength is assumed to be at least 60MPa, the lower end of the range of strength for epoxies in Table 2.2. Aluminium of grade 2011-T3 is assumed to reach yield strength of around 270 MPa [39].

Table 6.3 Material properties and dimensions of parts in the FE-model.

Part	E-modulus [GPa]	Poisson's ratio [-]	Width [mm]	Thickness [mm]
Concrete beam	20	0.3	250	350
Adhesive layer 1	7.0		80	2.0
CFRP laminate	200		80	1.2
Adhesive layer 2 (including fillet)	2.5		80	2.0 (17.0) <sup>*)</sup>
GFRP laminate	10		80	15
Steel	210		75	3

<sup>\*)</sup> Thickness of the fillet

As the GFRP plate is added to the concept there is reason to see how the distance between each step affects the shear stress distribution in the adhesive. The number of steps is also increased to nine steps as this concept is designed for a prestressing force of 100kN instead of 85kN as in the first concept and to get sufficient safety margin over the tensile strength of concrete and also to keep the length of the device reasonable.

The laminate is prestressed with a force of 100kN which represent 1040MPa, a prestressing level of 34% of the laminate ultimate capacity. The load is applied at the inner surface of the nuts in the embedded steel plate, to simulate the bolts that will transfer the load in reality. This is carried out using traction with a pressure on each nut corresponding to a total of 100kN.

The same three steps that are used in the parametric study to simulate the application of the prestressing force, adhesive curing and the release of the prestressing force are used in this model as well.

This model is primarily used to see the response in the beam together with the laminate, adhesive, GFRP, steel plate with nuts and the adhesive layer between GFRP and CFRP. A perfect distribution of the force, as in this model where the load is equally distributed between the nuts, is the optimal distribution to get an even shear flow through the bond line. All results are extracted from the undeformed model using paths, all starting ( $x = 0$  mm) at the support end of either the laminate or the concrete beam (for the case where the stress in the concrete underneath the adhesive layer is investigated).

### 6.2.1 Shear stress in the middle of the adhesive layer

The shear stress in the middle of the adhesive is the most important parameter to verify, it has to be below the tensile strength of the concrete (1.5MPa). Figure 6.16 show the shear stress measured in the middle of the adhesive layer.

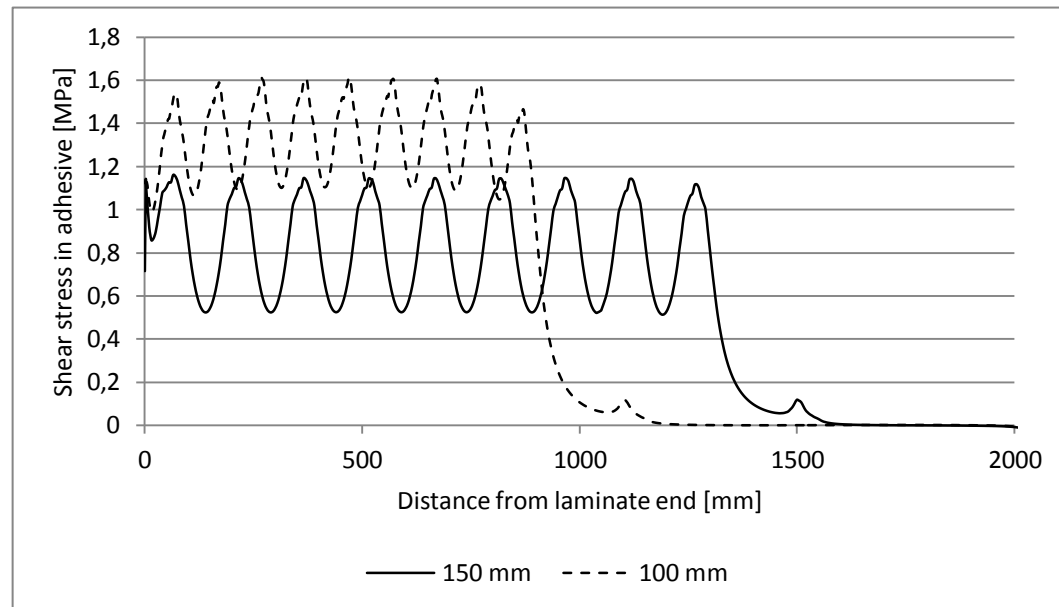


Figure 6.16 Comparison of shear stress distribution in the middle of the adhesive layer for nine tabs with 100mm spacing and 150mm spacing.

Compared to the parametric study where the GFRP layer was not included in the model the anchorage length in each step has become larger. With a larger anchorage length there is also benefitting with larger tab spacing. Therefore a comparison between a tab spacing of 100 mm and 150 mm is made showing that a spacing of 150 mm gives shear stresses around 30% lower than with 100 mm. Larger tab spacing than 150 mm is not investigated as a limit of the length and weight of the device is set.

### 6.2.2 Axial force in the laminate and effect of GFRP and tapering

With the added GFRP plate the axial force in the laminate is a bit different. The high peaks and low dips are smoothened out and the contribution from the tapering and filleting between the GFRP and the CFRP can easily be seen. In the graph below the axial force from three different cases are compared. Two curves are from the model used for the parametric study with nine steps, one as it was during the parametric study and one modified with added GFRP between the two laminates. The last curve is from the 3D FE-model without the device. This comparison is made to see what difference the different additions to the model contributed with.

It is interesting to see how the GFRP plate affects the axial force in the laminate. By adding the GFRP plate to the model from the parametric study it is easy to compare the axial force from between the different cases, see Figure 6.17.

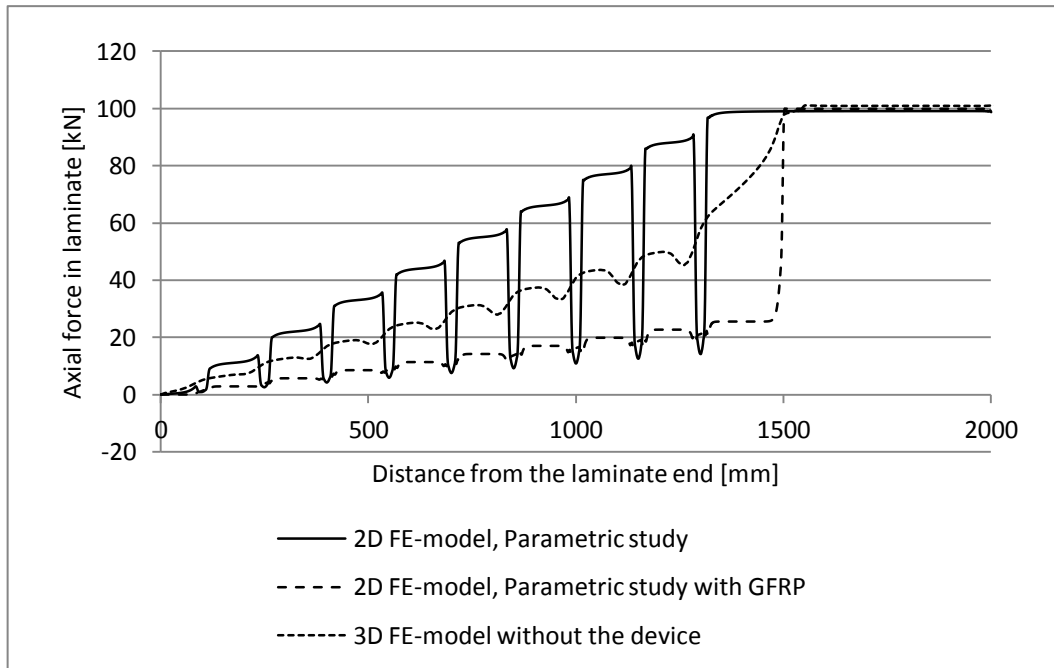


Figure 6.17 Comparison of axial force in the CFRP laminates in three different cases (for model with 9 tabs and 150mm spacing).

### 6.2.3 Shear stress in the concrete beneath the adhesive

The shear stress in the concrete is extracted from the analysis results along a path in the concrete layer centred underneath the adhesive. Two different paths are used to extract the stresses, one at 35mm and one at 10mm underneath the adhesive. As expected the shear stress is evened out down through the concrete with the maximum values a bit lower than it is in the adhesive layer, see Figure 6.18.

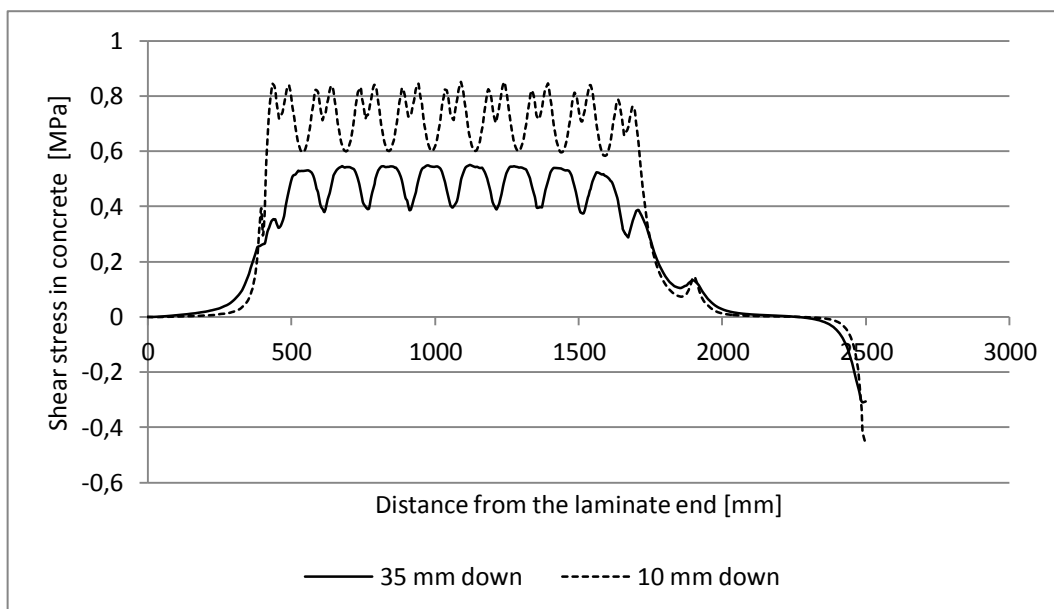


Figure 6.18 The shear stress in the concrete beneath the adhesive layer.

## 6.2.4 Stress in the adhesive between the CFRP and GFRP

The stress in the adhesive layer between the CFRP laminate and the GFRP plate is an important factor during the prestressing. It would be dangerous if the adhesive fail during the prestressing as it could result in serious injuries. As the von Mises stress reaches it maximum around 12 MPa, see Figure 6.19, it is important that the adhesive used has a capacity well above this limit.

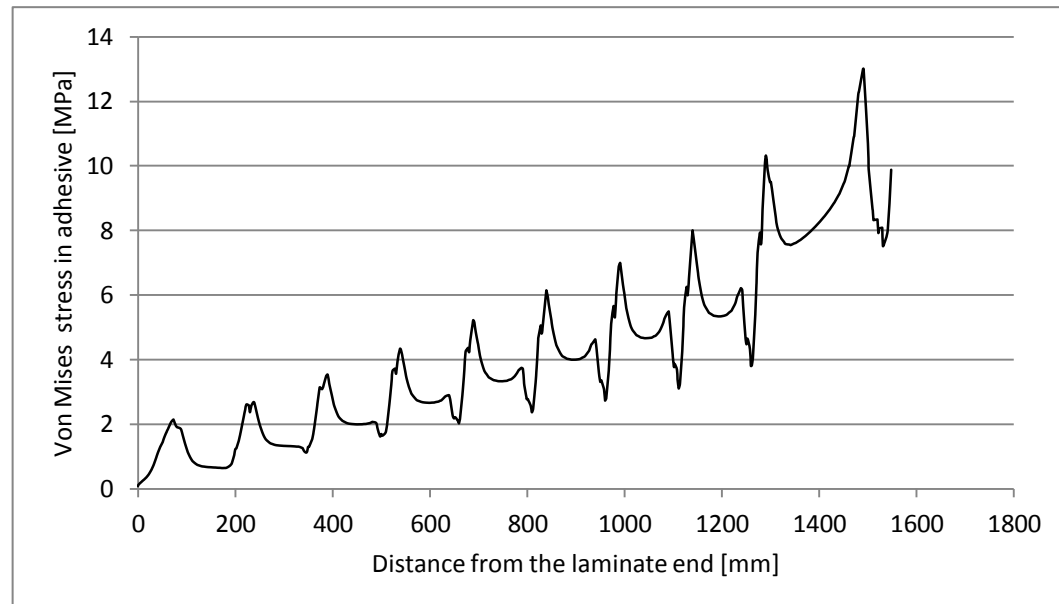


Figure 6.19 The von Mises stress distribution in the adhesive between the CFRP laminate and the GFRP plate.

## 6.2.5 Stress in the GFRP and steel plate in the middle of the GFRP

These verifications are carried out in order to ensure that none of the components of the concept are exposed to excessive stresses and yielding. In the layer of GFRP right above and right below the steel plate, note that the last bits of the graphs represent the adhesive filling of the tapered end of the GFRP plate. The stresses are as presented in Figure 6.20. Note that the strength of the GFRP is more than 100 MPa.

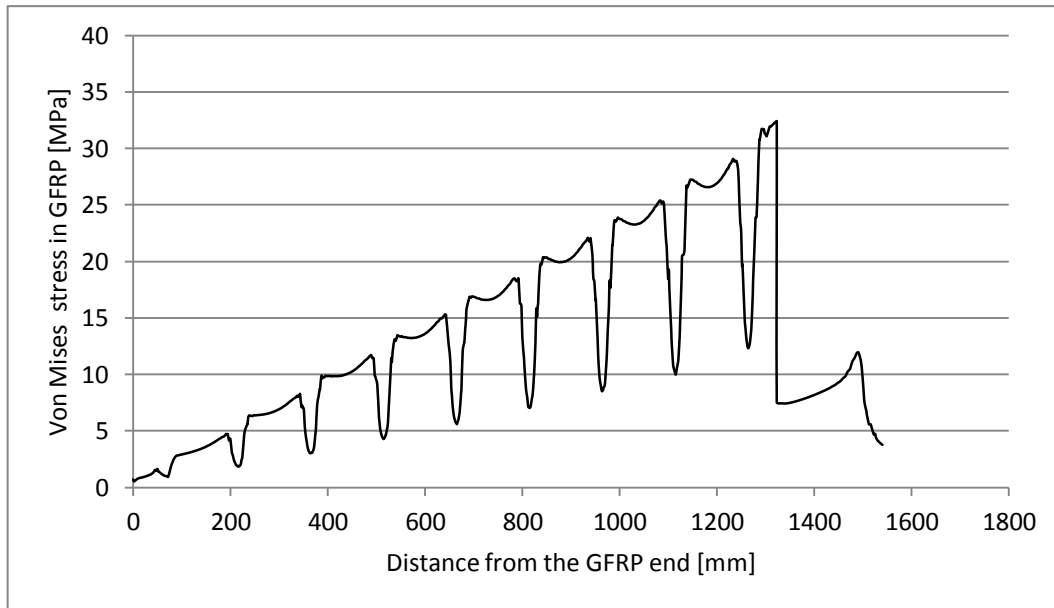


Figure 6.20 The von Mises stress in the GFRP plate.

In the middle of the GFRP plate the steel plate mentioned earlier is located. Its purpose is to distribute the prestressing force in each step and transfer the force between the nuts and the GFRP. The steel plate is also used to keep the nuts in place when manufacturing the GFRP plates. Figure 6.21 shows the maximum stress through the middle of the GFRP layer where the steel plate is located. Note that the last part of the graph is at the tapered end here as well as above and also that the stresses from the graph above match the stresses in between the steel plates in graph below.

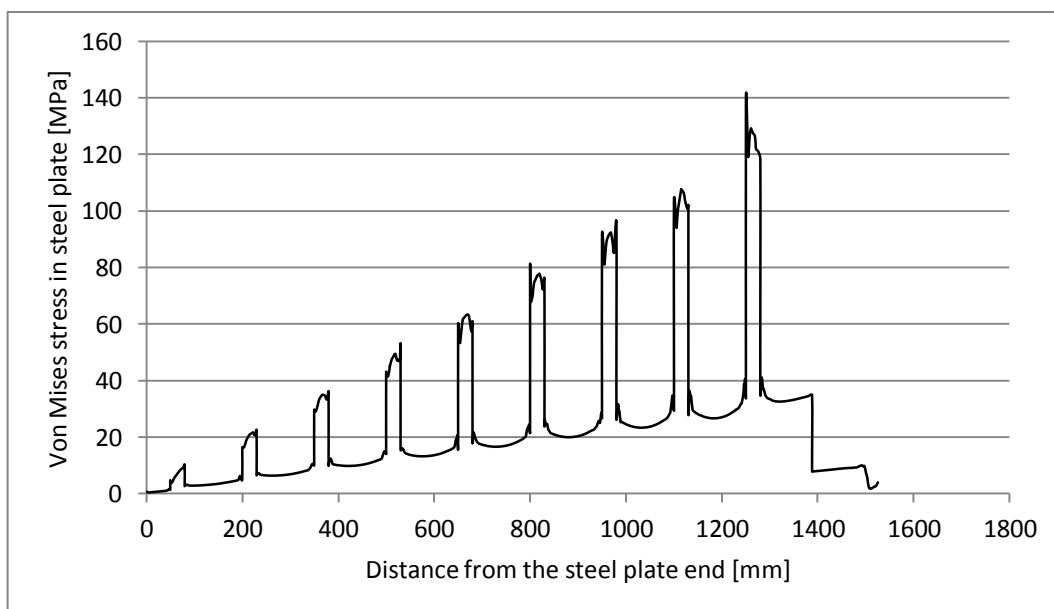


Figure 6.21 The von Mises stress in the steel plate in the middle of the GFRP laminate.

## 6.2.6 Stress in the steel nuts and steel plate

The maximum stress in the upper edge of the nuts and the GFRP in between them is presented in Figure 6.22. The path from where the results are extracted is running

from the edge of the first nut at the end of the laminate to the edge of the last nut toward the middle of the beam.

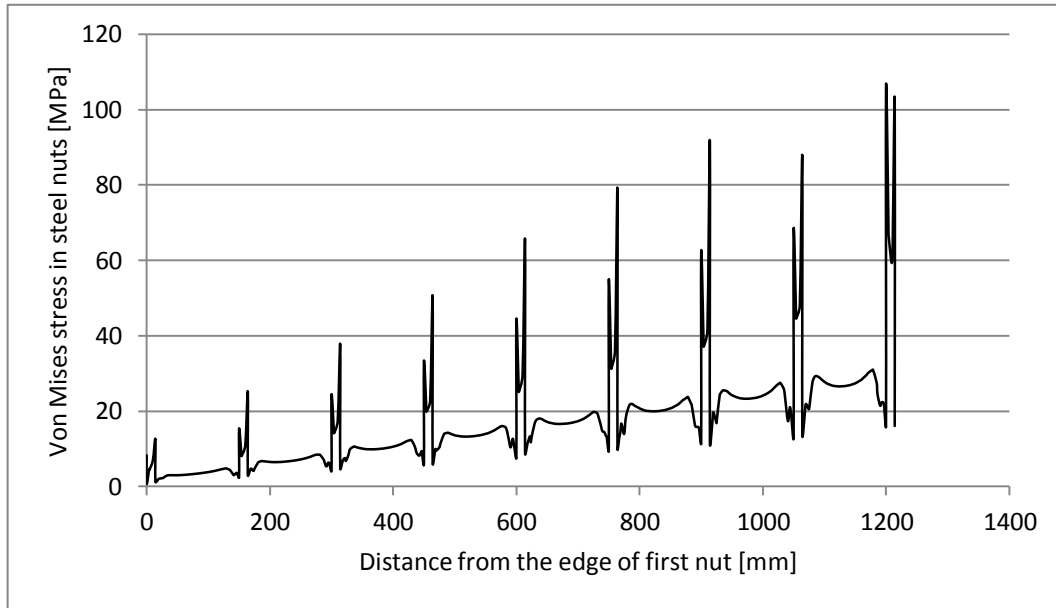


Figure 6.22 The von Mises stress in the top of the steel nuts.

The maximum stress in the middle of the GFRP plate running through the steel plate as well as the steel nuts is shown in Figure 6.23.

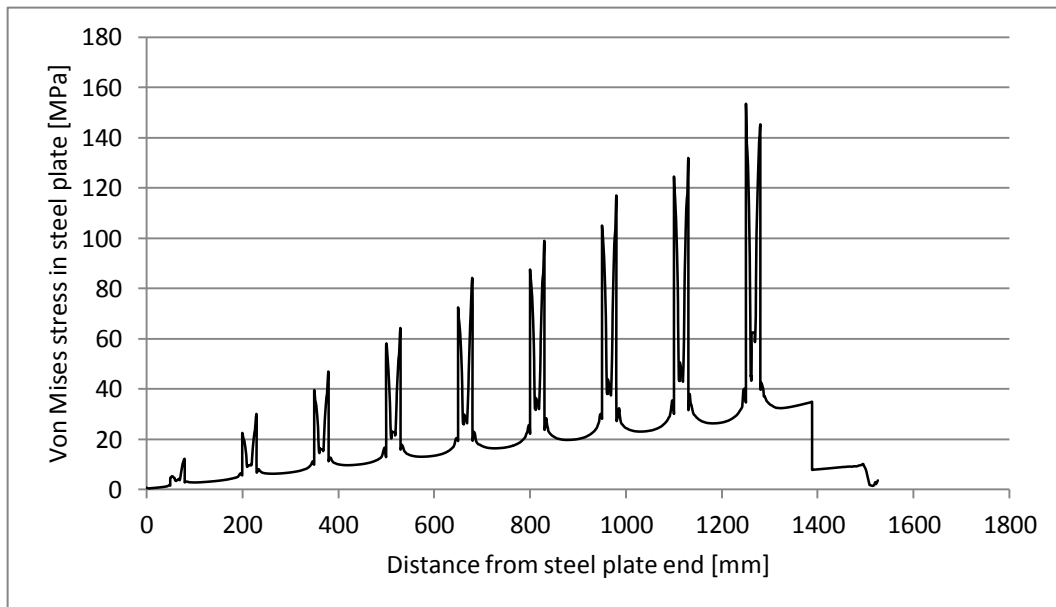


Figure 6.23 The von Mises stress through the steel plate and nuts.

The steel profiles that are there to hold the steel plates inside the GFRP together during manufacturing are subjected to stresses above their yield limit, see Figure 6.24. However, this will not be a problem as the force will redistribute to the GFRP and the plate is not meant to be used more than once.

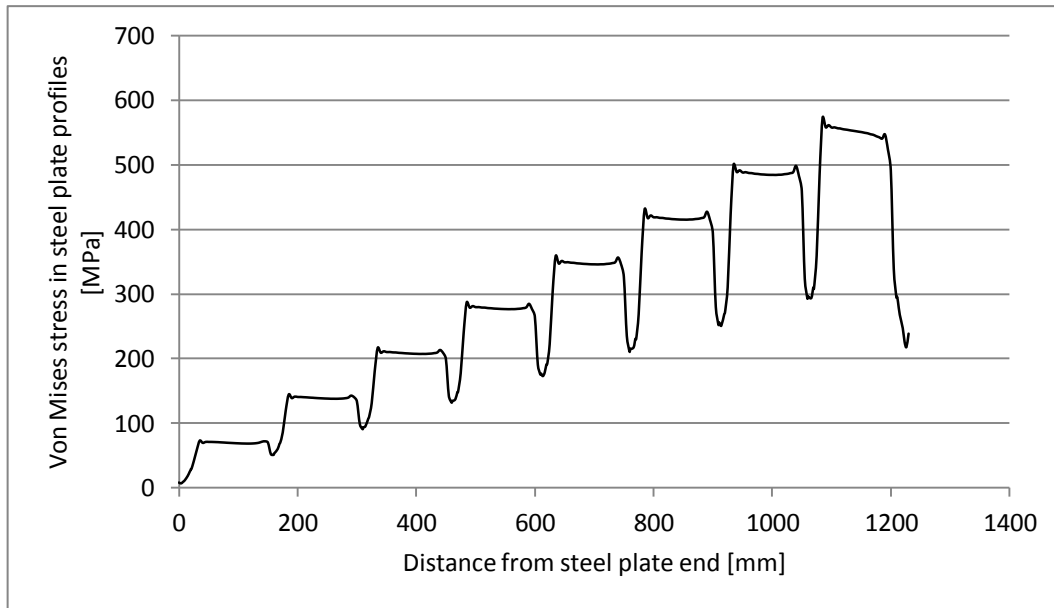


Figure 6.24 The von Mises stress in the steel profiles holding the steel plates together.

### 6.2.7 Changes made to the concept

The first concept that was used in the earlier experiments had a tab spacing of 100mm but with the added GFRP and the before mentioned benefits the tab spacing is increased to 150mm.

When studying the deformations of the FE-model without the device, it can be seen that the CFRP laminate is bent upwards in a bow, see exaggerated displacement in Figure 6.25. This phenomenon is due to the fact that the prestressing device is acting with an eccentricity causing a bending motion of the laminate. This behaviour is expected but not to the extent that was shown in the analysis. It will be necessary to prevent this large deformation in order to get an even adhesive layer and avoid the need of using large amounts of adhesive.

To cope with this problem a tenth tab is added to the prestressing device. This tenth tab is just added to keep the GFRP and CFRP down against the beam. It is not attached to the GFRP with bolts and will not transfer any of the prestressing force like the other tabs.

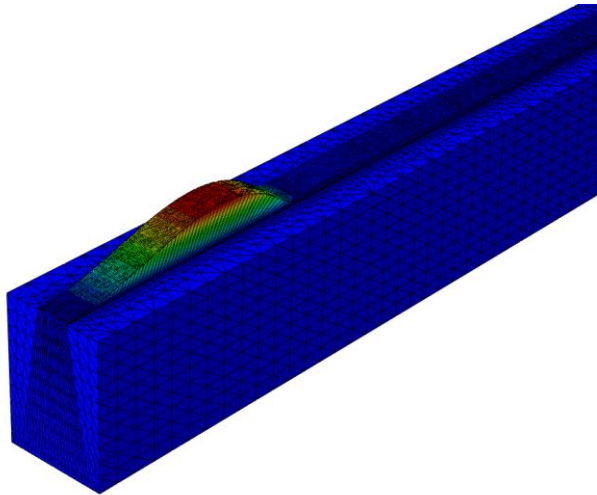


Figure 6.25 The deformations of the CFRP laminate caused by the eccentric loading from the prestressing device.

### 6.3 FE-model of the concept with the prestressing device

The third FE model is based on the solid FE-model in the chapter above but with the prestressing device added. This includes the prestressing device as well as the guiding bars and the aluminium holders which are used to keep the prestressing device in place and at the right distance from the concrete. The analyses presented through this section are carried out in order to identify and solve possible issues that arise with the prestressing device as well as verify its structural integrity.

The final model is based on the parameters found in Table 6.4. All materials are modelled with elastic material behaviour except for the steel plate inside the GFRP that exhibit elastic plastic properties in the analysis of the final design. The contact behaviour between the tabs and the guiding bars are considered frictionless. Note that there are changes made to the model during this phase based on how the actual prototype develops and the properties below are not valid for all analyses that have been carried out.

Table 6.4 Material properties of parts in the FE-model with the prestressing device.

Material	E-modulus [GPa]
Concrete	20
Adhesive layer (CFRP-Concrete)	7.0
CFRP laminate	200
Adhesive (CFRP-GFRP)	2.5
GFRP laminate	4.0
Steel <sup>*)</sup>	210
Aluminium <sup>**)</sup>	70



- \*) Steel in springs, first two tabs, guiding bars, plate inside GFRP
- \*\*) Aluminium in tabs and holders for the guiding bars

### 6.3.1 Removing the nuts on one side of the tabs in the device

Compared with the old concept, where the steel springs were manufactured in separate parts, the steel springs are manufactured in one single piece (except between the first two tabs). By doing this, each tab can move freely along the spring. The prestressing force is transferred between the spring and the tabs by putting a nut on the opposite of the pulling side of the tab. This is done in order to make it possible to release the prestressing force evenly at all tabs simultaneously. The old concept had the tabs fixed with nuts on both sides of each tab which resulted in stress remaining in the springs after release. This remaining stress had to be released by releasing a nut for each step of the prestressing device (i.e. for each spring), and if not done correctly it could possibly lead to forces in the laminate causing high shear stresses locally. Figure 6.26 illustrates the remaining stresses in the springs. To model the behaviour of the new solution where all tabs are released at the same time and no remaining stress is left in the device, the elements that are used to model the springs are removed in the third modelling step.

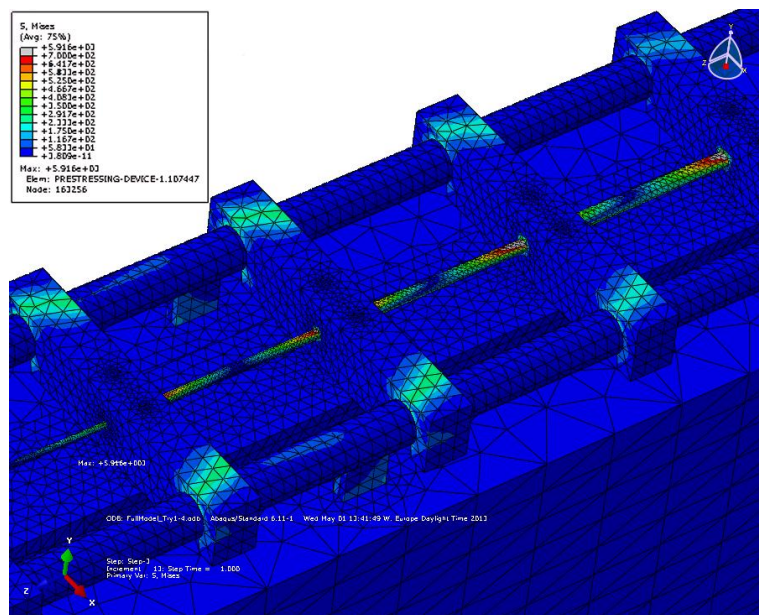


Figure 6.26 Remaining stress in the prestressing device based on the old device design.

### 6.3.2 Changing the first two tabs from aluminium to steel

The shear distribution in the adhesive in the first models resulted in higher stresses than expected, especially near the end of the laminate. In the original model of the device there were two springs between the first and the second tab. This is because if a single steel spring should be used it has to be so thick that it will not fit the tabs and the tabs cannot be higher because the eccentricity from the GFRP/CFRP will be too high. A model of the first two tabs was used to carry out analyses of the effects of how an uneven load distribution, due to different lengths of the first two springs, would affect the tabs. The results from this model instead showed very large deformations of the tabs and it was concluded that the first tabs were too weak and that the stiffness of the first step was affected to a large extent. Figure 6.27 show how

the first two tabs originally looked with two springs connecting them and under uneven load gives a clear picture of their large effect on the total stiffness of the step.

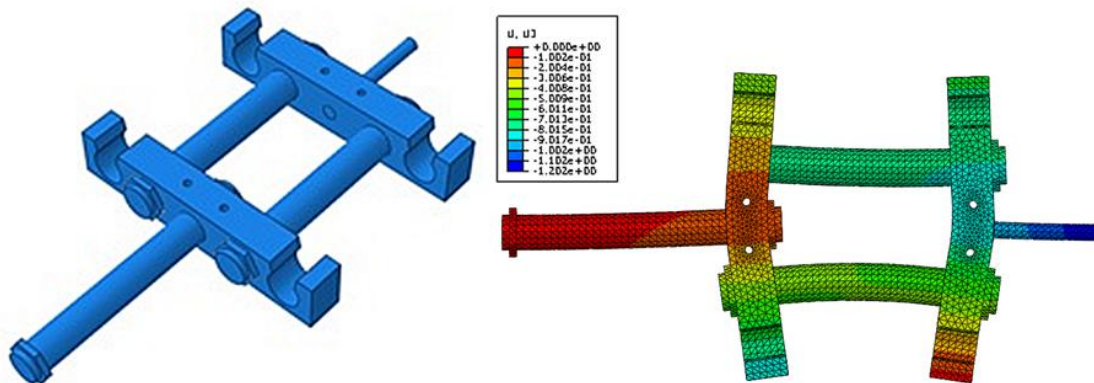


Figure 6.27 Model of the first two tabs in order to analyse the potential problem. Deformation of aluminium tabs under uneven load (uneven length of springs) with a scaling factor of 20x. This figure gives a clear picture of the stiffness problem due to the large deformations.

This is only a problem with the first two tabs because of the load eccentricity. Another problem with this configuration was the large stresses that were obtained in the tabs, see Figure 6.28.

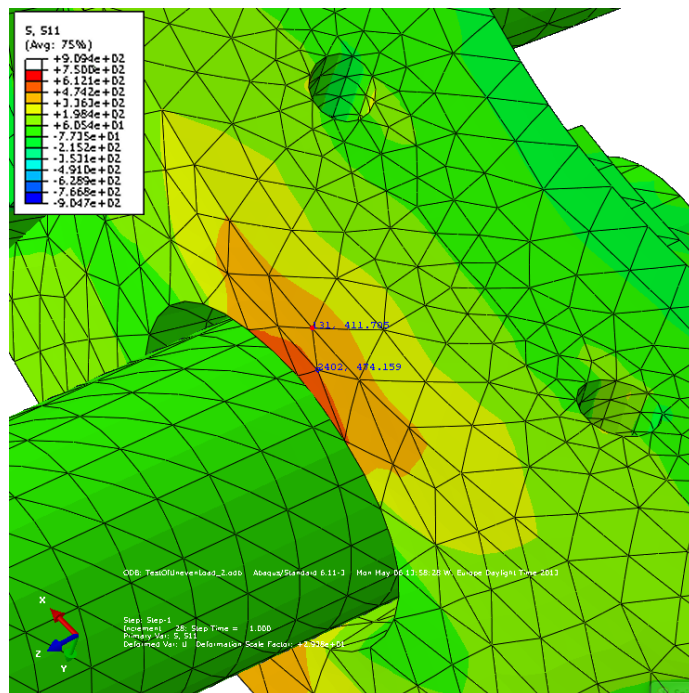


Figure 6.28 Stress in the front of the second aluminium tab, well over 400MPa.

To be able to determine how much the stiffness of the tabs affected the distribution of the prestressing force, and therefore shear stress distribution, the whole model was analysed with a higher modulus of elasticity for the first two tabs (800GPa instead of 70GPa). This resulted in a much more even shear stress curve, see Figure 6.29, and therefore it was decided to make a model with three springs and steel in the first two

tabs. Note that the peaks on the graphs around tab eight depends on large deflections of the guiding bars, this problem is dealt with and described below.

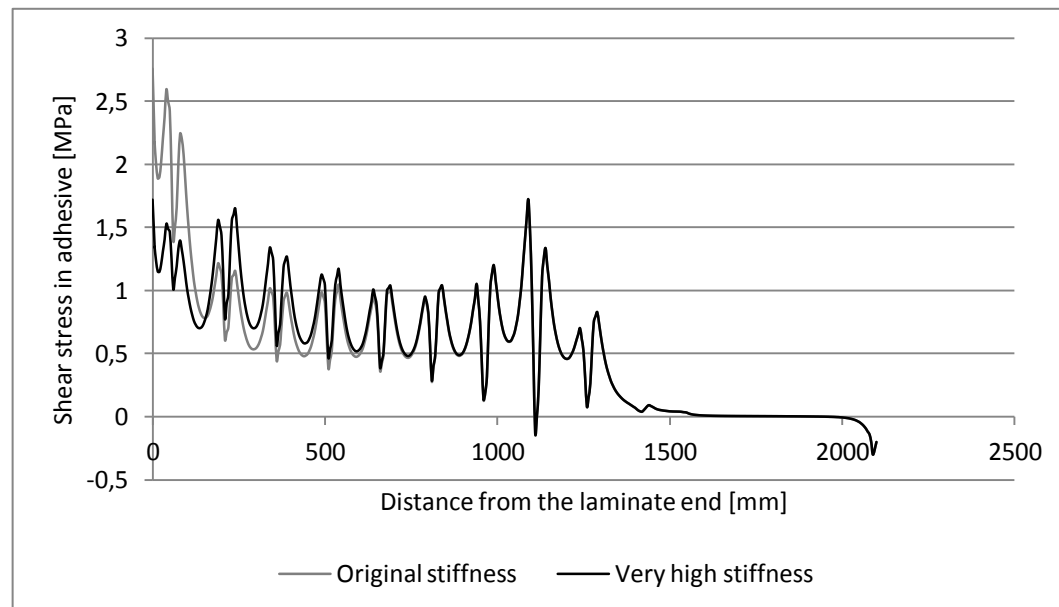


Figure 6.29 Shear stress in the adhesive: Comparison of the original device with two springs and aluminium tabs and a model where the first two tabs had an increased stiffness.

The first two tabs of aluminium were changed to steel and also widened with 10 mm to cope with the high stresses. These changes improved the results, but not to the extent required to ensure that the stiffness of the spring of the first step is high enough.

### 6.3.3 Three springs

To solve the problem with deformations of the first two tabs due to dual springs a solution with only one single spring would be optimal. The problem with this is that the spring has to have a diameter that is too large for the tabs as mentioned earlier.

A compromise would be to have three springs, one larger in the middle and two smaller on the sides. This will greatly reduce the bending effect on the tabs and there will not be any issues with large stresses and deformations. With three springs the final design is to have the first two tabs made of steel with a width of 35mm. With this solution the influence of the tabs stiffness will be practically none.

The solution with three springs was implemented in the Abaqus FE-model including the prestressing device. Figure 6.30 shows the first two tabs and springs. The single spring in the middle has the same diameter as the spring between tab two and three, and the springs on each side of it has a diameter of 20.30 mm. This is resulting in the same spring stiffness as the previous two springs. Figure 6.31 show the difference in shear stress obtained due to the change from two springs to three.

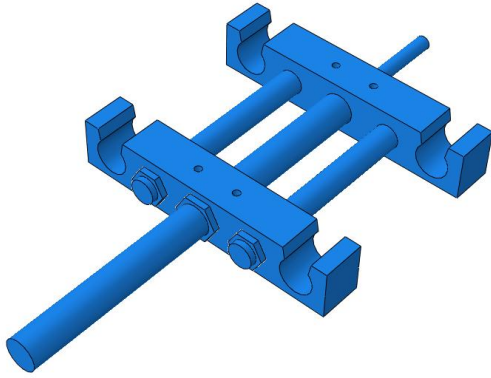


Figure 6.30 Prestressing device with three springs between the first and second tab which are 35mm wide and made of steel.

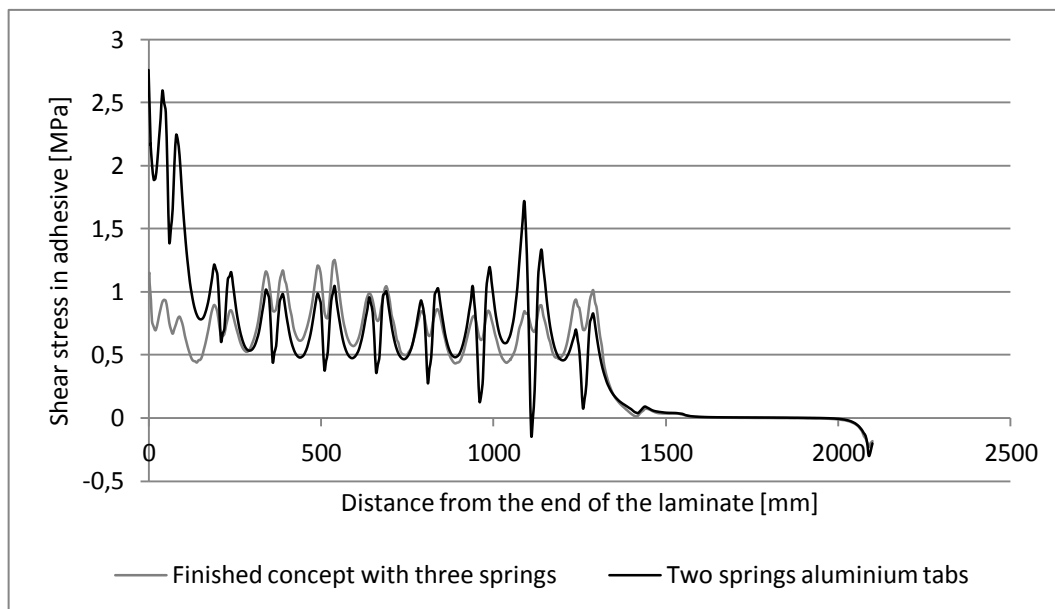


Figure 6.31 Difference between two and three springs.

### 6.3.3.1 Position of the aluminium holders

The aluminium holders that are keeping the guiding bars in place were originally positioned based on a simple two dimensional model at locations where the deformations were largest. The result of having them at these positions is that the guiding bars are subject to large deformations at the last tabs, see Figure 6.32. The prestressing device and the laminate were forced away from the beam at the end towards the middle of the beam.

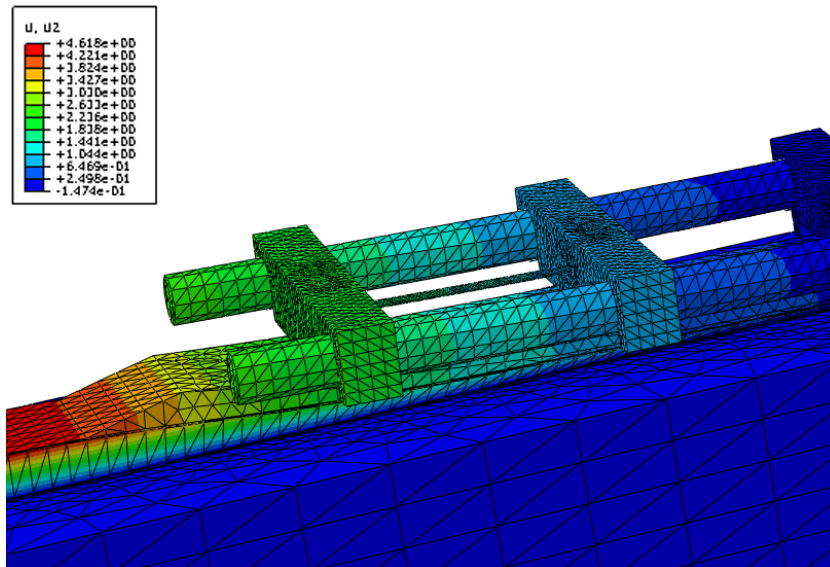


Figure 6.32 Deformation of the guiding bars, approximately. 2.4mm

To solve this, the guiding bars were turned around so that the aluminium holders end up closer to the tabs that bend away from the concrete beam. The end of the prestressing device close to the laminate end is forced in the opposite direction, against the concrete beam. When the guiding bars were turned the aluminium holders ended up further from the end causing the deformation to increase. However, this was solved by adding spacers that ensure an even adhesive layer. The turned guiding bars are shown in Figure 6.33.

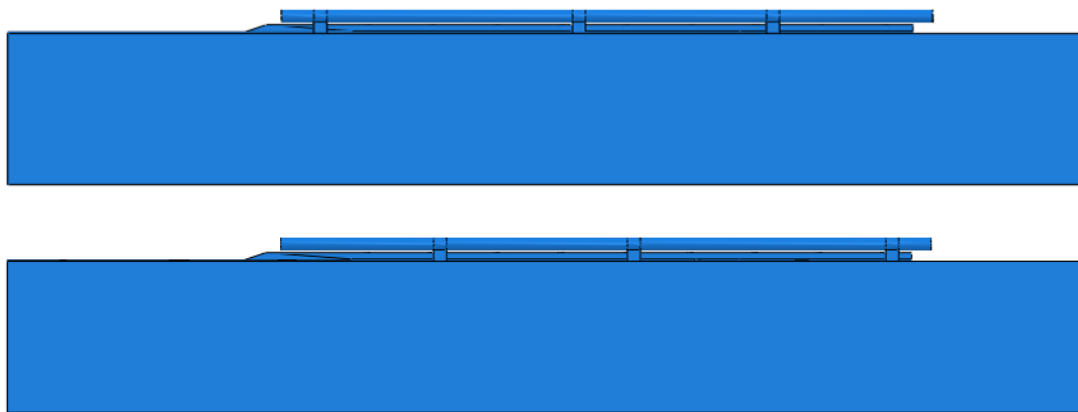


Figure 6.33 Position of the aluminium holders, new positions at the top and old positions at the bottom.

From the results of the initial design it was possible to see a deviation in the shear stress distribution curve where it differentiated around the holder closest to the longer free end. After that the guiding bars were turned around in the FE-model the deviation became a lot less as seen in Figure 6.34.

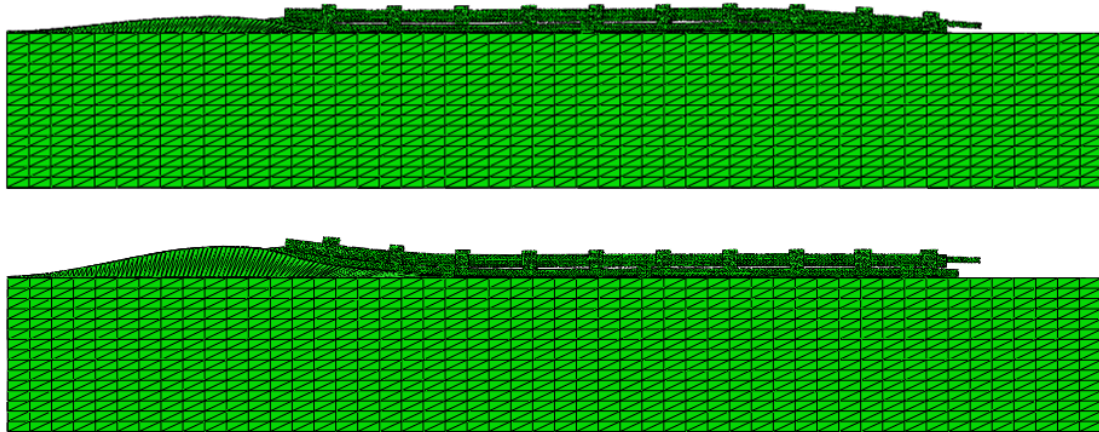


Figure 6.34 Comparison of the deformation between the different alternatives of holder placement. The bottom figure shows the old positioning with large upward deflections of the laminate.

### 6.3.4 Difference between locked and free ends of guiding bars

An analysis where the long free ends of the guiding bars are locked was carried out in order to investigate if it would be preferable to add an extra support. The shear force as well as the reaction force in each holder was investigated in order to see how large shear and withdrawal force that will act at the bolts mounted in the concrete. The stress in each holder was also verified to be well below yield limits. The shear stress in the adhesive is affected slightly negative by locking the free ends while the shearing force in the holders is reduced. A comparison of the shear stresses in the adhesive can be seen in Figure 6.35. The withdrawal and shear forces acting on the aluminium holders kept in place using bolts are considered to be more than manageable.

Table 6.5 Reaction force in the aluminium holders.

	Original FE-model (free ends)	FE-model with fixed ends
Deflection at the ends of the steel rods [mm]	1.3	0
Reaction force at fixed end [N]	-	2528
Reaction force at the holders [N] (pair):		
1	2474	-21
2	-1031	-12
3	-2237	-2311
Shear at holders [N] (pair):		
1	1778	-2331

2	-8364	-5206
3	713	1598
Maximum stress in holders [MPa] (left/right):		
1	63/40	35/20
2	37/61	8/12
3	55/30	51/38

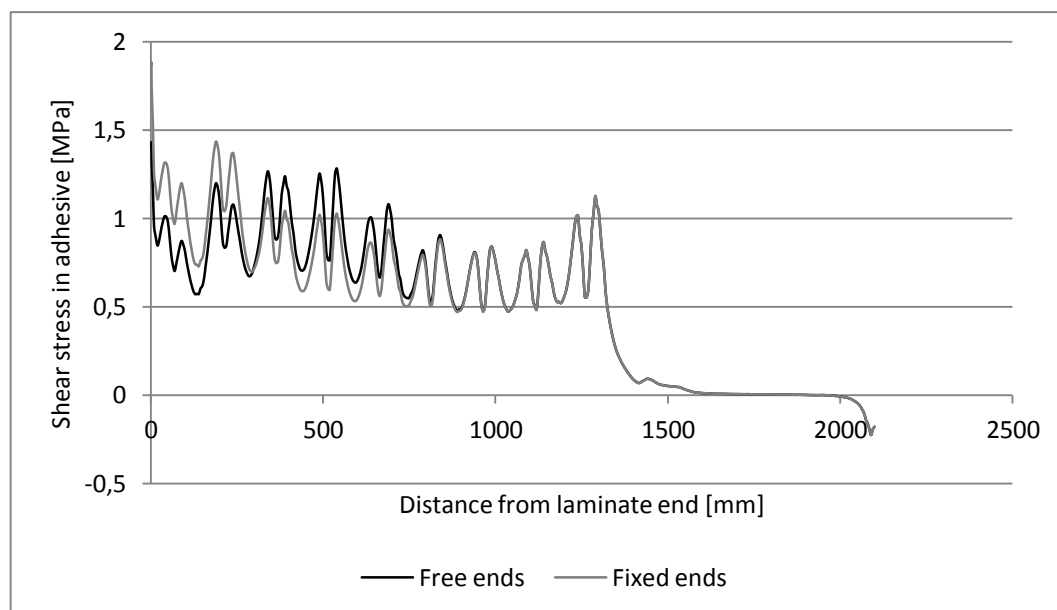


Figure 6.35 Difference between fixed and free ends: Graphs of shear stress comparison between fixed and free ends of guiding bars.

### 6.3.5 Effect of stiffness of the guiding bars

As an effort to see how much the guiding bars deflection affected the resulting shear stresses in the adhesive a model with very stiff guiding bars was made. The results can be seen in Figure 6.36, compared to the same model with regular steel guiding bars. Note that the ends of the guiding bars at the prestressing end are fixed as above mentioned though this will not affect the resulting conclusions of this comparison. The difference is small and there is no need to make any changes to their appearance as they meet their requirements.

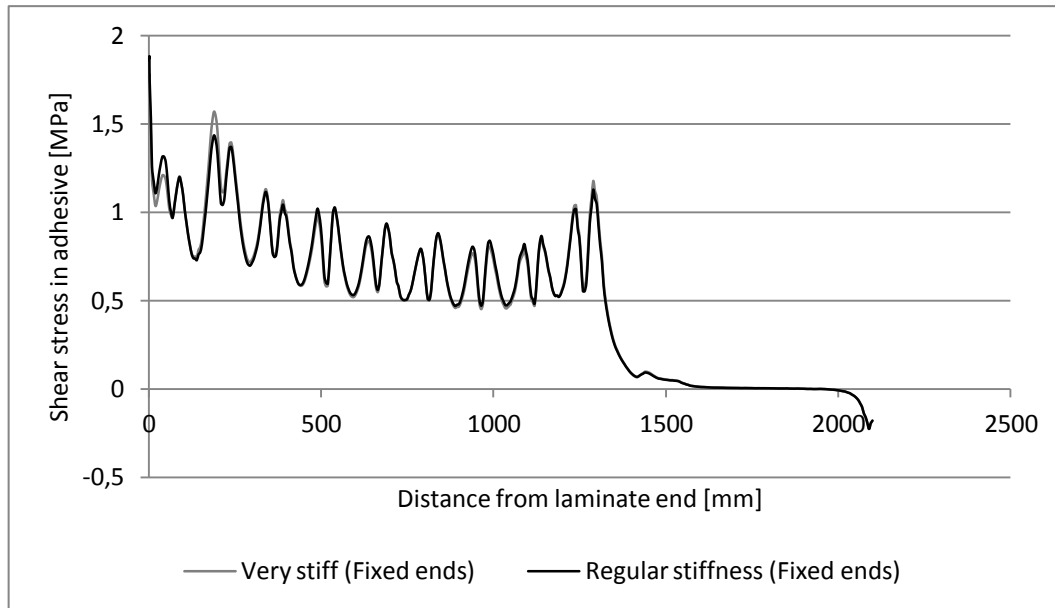


Figure 6.36 The influence of guiding bar stiffness on the shear stress in the adhesive.

### 6.3.6 Effect of stiffer GFRP laminate

The steel profiles in the GFRP layer were manufactured with a larger width than what was used in the original FE-model. The larger area of the steel profiles results in a stiffer GFRP layer. Therefore are the effects of how the GFRP laminate stiffness investigated. The total stiffness of the GFRP layer together with the steel plate inside it was added together aiming for a specific total stiffness. The GFRP stiffness can be varied in the manufactured concept while the steel is ordinary steel and therefore have the specific stiffness of steel.

At the same time, the steel stiffness is changed since the manufactured steel plates have a larger width of the thin profiles holding the plates together compared to the FE-model. In the FE-model the width is a fourth of the width of the manufactured concept so the area is increased with a factor of four so that the total  $E \cdot A$  is correct for the steel. The stiffness of the GFRP is then reduced to represent the smaller area of the GFRP with a stiffness of 10GPa. In Table 6.6, the calculation of the new stiffness for the steel and the GFRP is defined according to the GFRP and steel plate used in the concept.

Table 6.6 Table of areas and modulus of elasticity for the GFRP plate in the old models and the concept.

	Total E-modulus for the GFRP laminate, original FE-model			Total E-modulus for the GFRP laminate, manufactured concept.		
	E [GPa]	A [mm <sup>2</sup> ]	EA [GPa·mm <sup>2</sup> ]	E [GPa]	A [mm <sup>2</sup> ]	EA [GPa·mm <sup>2</sup> ]
Steel	210	15	3150	210	60	12600
GFRP	10	1185	11850	10	1140	11400



Total EA			15000			24000
Total E			12.5 [GPa]			20 [GPa]

Table 6.7 Modified modulus of elasticity for steel and GFRP used in the FE-model based on the properties and stiffness from the concept.

	E [GPa]	A [mm <sup>2</sup> ]	EA [GPa·mm <sup>2</sup> ]
Steel	840	15	12600
GFRP	9.62	1185	11400
Total EA			24000
Total E			20 [GPa]

As seen in Table 6.6 and Table 6.7, the new total stiffness is considerably larger than in the old model, this was predicted to give a lower shear stress as stiffer springs would transfer more of the load to the next tab and this could even out the shear stress curve. The result was the opposite; the first peak of the shear stress was higher before it evened out as seen in the Figure 6.37.

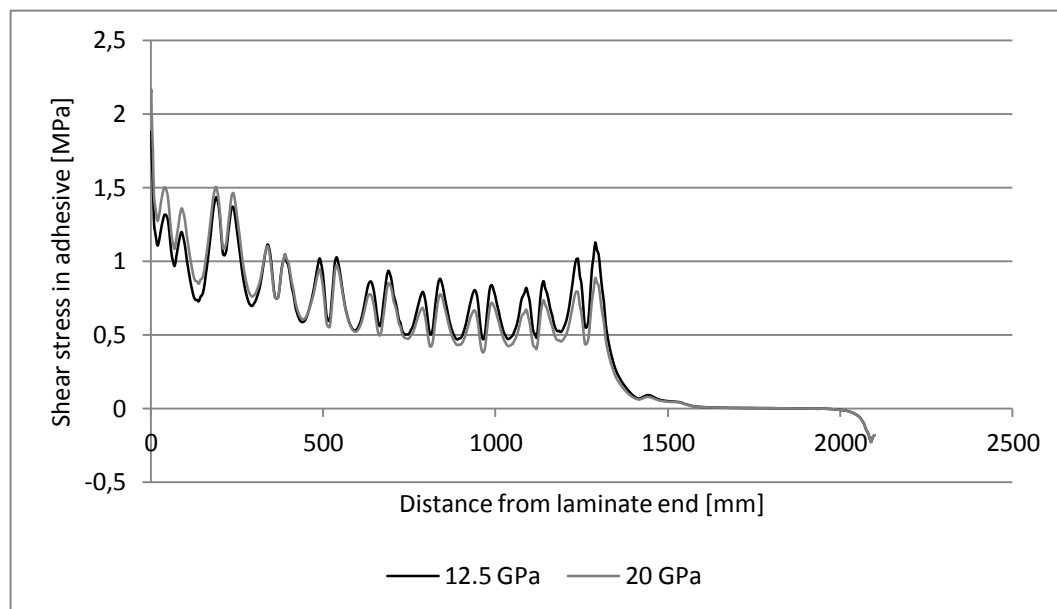


Figure 6.37 Graph showing the influence of the total stiffness of the GFRP layer, the result is the opposite of what was expected.

As the result of this change contradicts the expected result it illustrates the complex interaction between the stiffness of the prestressing device and the prestressed laminates. This is due to the fact the GFRP and steel plate is acting somewhere between the CFRP and the steel springs in the device.

This interaction is complex and the GFRP together with the steel plate is not working as pure springs, it works together with the CFRP as they are adhered together and the stiffness affects more than just the force transfer between the tabs but also the transfer to the CFRP.

To get a shear stress distribution that is closer to what it was before the steel area was increased the stiffness of the GFRP has to be lowered to lower the total stiffness of this layer. While aiming at the total stiffness as was before the GFRP cannot have that low stiffness and it is set at 4GPa which is a reasonable stiffness. In Table 6.8, the new stiffness of the materials is defined.

*Table 6.8 Adjusted modulus of elasticity for steel and GFRP used in the FE-model in order to lower to total stiffness of the layer.*

	Stiffness of the GFRP layer in the FE-model			Stiffness of the GFRP layer in the manufactured concept		
	E [GPa]	A [mm <sup>2</sup> ]	EA [GPa·mm <sup>2</sup> ]	E [GPa]	A [mm <sup>2</sup> ]	EA [GPa·mm <sup>2</sup> ]
Steel	840	15	12600	210	60	12600
GFRP	4.00	1185	4740	4.16	1140	4740
Total EA			17340			17340
Total E			14.45 [GPa]			14.45 [GPa]

### **6.3.7 The final resulting shear stress distribution**

A final FE-model was made with all parameters as close to the manufactured concept as possible. As the steel profiles holding the steel plates inside the GFRP yield, as mentioned above, this model use steel properties that allow yielding in order to ensure that this will not be an issue. Elastic-plastic properties of the steel used in the model are presented in Figure 6.38.

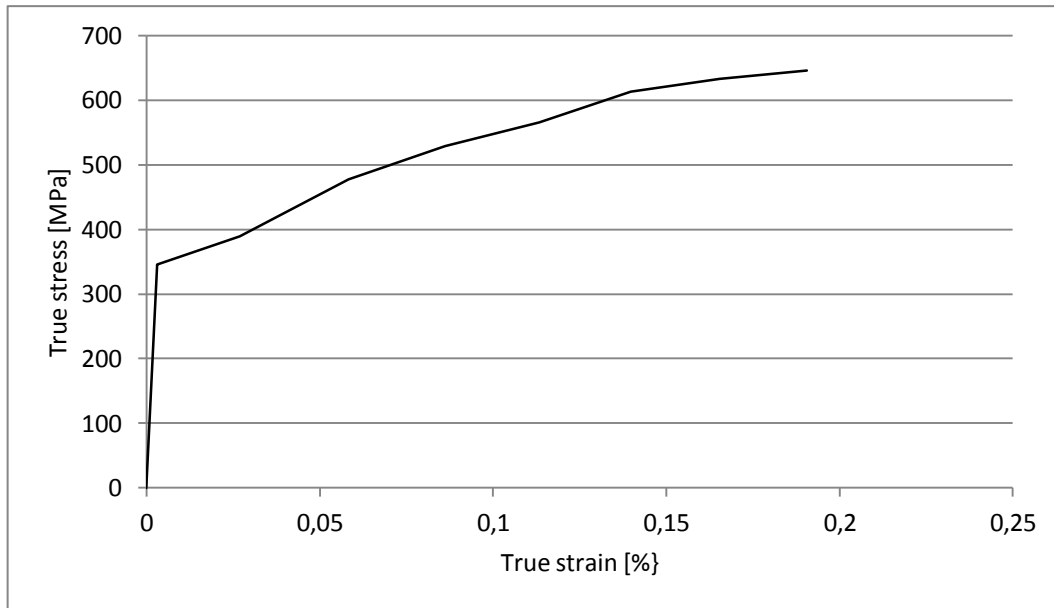


Figure 6.38 The plastic stress and strain behaviour for the steel in the plate.

The shear stress along the bond line is plotted in Figure 6.39 together with the mean shear stress over the bonded length which is around 0.75 MPa. The resulting shear stress distribution in the adhesive layer is approaching the ideal shear stress distribution seen in the results for the solid FE-model without the device.

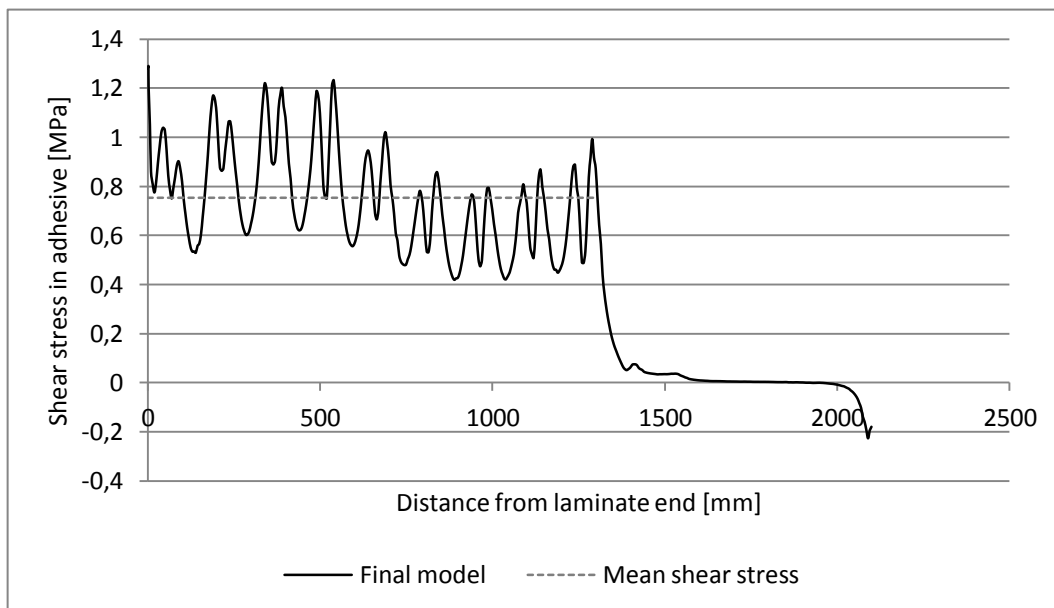


Figure 6.39 The shear stress distribution and mean shear stress in the adhesive layer from the final Abaqus model of the concept.

The final FE-model is also modelled with the force acting at the laminate, at the symmetry line, instead of the prestressing bar to simulate how the passive end will react. The shear stress in the adhesive is once again controlled and the largest difference is that there is a higher peak at the end of the laminate ( $x = 0$  mm), see Figure 6.40. This is reduced by adding an adhesive fillet on this side as well.

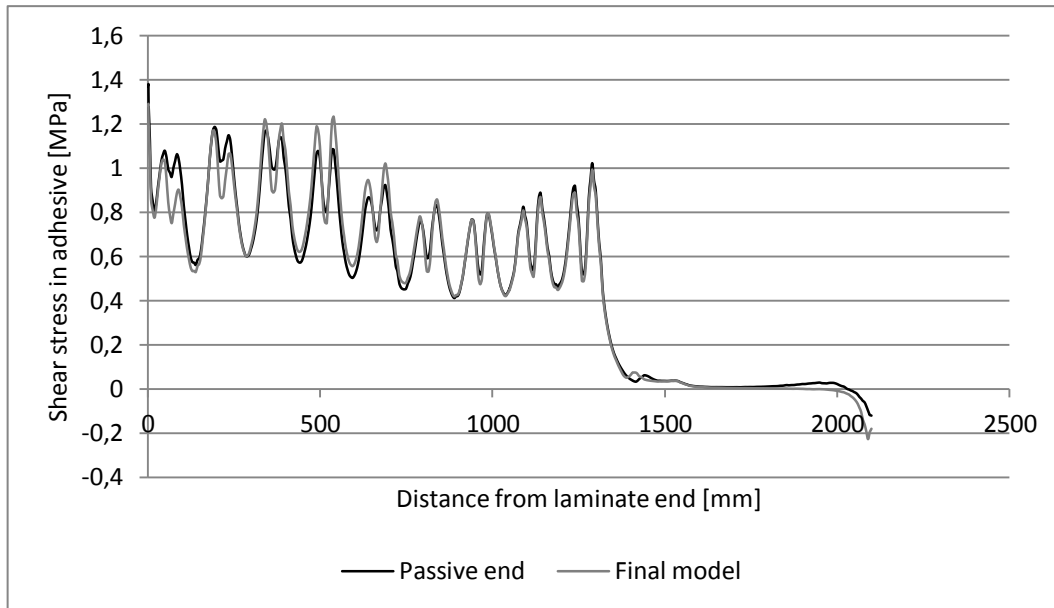


Figure 6.40 Final shear stress distribution.

In the analyses results there is consistently a peak in the shear stress in the adhesive at the end of the laminate. This peak is due to the fact the laminate ends very abruptly and that will not be the case when this method is carried out in reality. In reality the CFRP can be tapered in an easy manner just by sanding the last 20-30mm with a grit paper and also fillet of the adhesive would reduce the stresses a lot.

## 6.4 Modelling of details of the concept

The previous models were all carried out in order to verify and improve upon the main function of the concept, the prestressing device. Furthermore, several details are needed in order to be able to actually use the device in practice.

### 6.4.1 Temporary prestressing support

The anchor used as support for the hydraulic jack is based on the design of a rigid box of steel. It is temporary bolted to the concrete during the prestressing. The hydraulic jack that will be used is circular and 70mm in diameter.

The intention with the support is to make it have a small footprint, so that it will be lightweight and fit as many beams as possible. This is with regard to the minimum and maximum distances needed between the bolts and between the bolts and edges, but also with regard to the forces acting on the support. Distance requirement between the anchoring bolts is calculated according to EC5. The shear resistance and bearing resistance is checked by hand calculations found in Appendix C and show that four bolt with 20 mm diameter would be sufficient.

It is important that the support is stiff. With our 5m model beam with a total of 4.2m of laminate the total elongation is around 12mm when a prestressing force of 100kN is applied. This means that every tenth of an mm results in a prestress loss of approximately 1kN. The problem arises when tightening the locking nut. During the prestressing phase it is possible to compensate for a deflected box wall by prestressing more, but when the force is transferred from the deformed wall there the jack rest to the undeformed wall where the lock nut rest, it is really hard to compensate.

A deformation of around 0.2mm is considered good enough resulting in a 2kN loss which is easy to adjust in the prestressing phase just by prestressing 2kN more.

The aim was to make the support boxlike without stiffeners in order to make it as simple as possible. Though, this was not possible with regard to high stresses, seen in Figure 6.41 where the deformations were lowered by having thicker walls. Stiffeners had to be added to the design to lower the stresses. With stiffeners added a wall thickness of 10 mm is sufficient, the analysis results can be seen in Figure 6.42 which is showing how it could be designed. Both deformations and stresses are below limits but adding stiffeners is not preferred. Therefore, it was decided that the support manufactured for the concept will have the thicker, 20mm, loaded walls with the longer walls moved toward the middle of the box to add stiffness and support, as shown in Figure 6.43. A design which is in between the two concepts modelled.

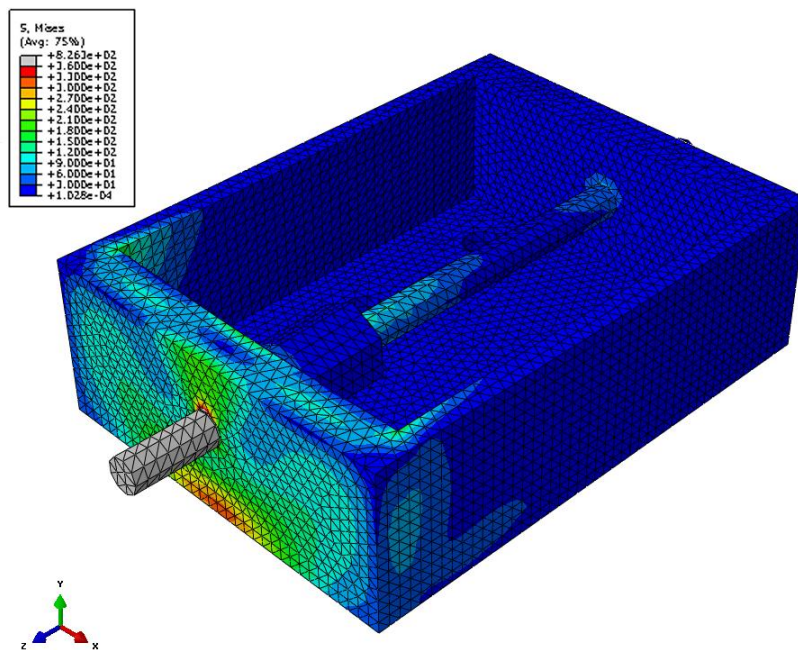


Figure 6.41 The temporary support box experience high stresses even with 20 mm thick walls.

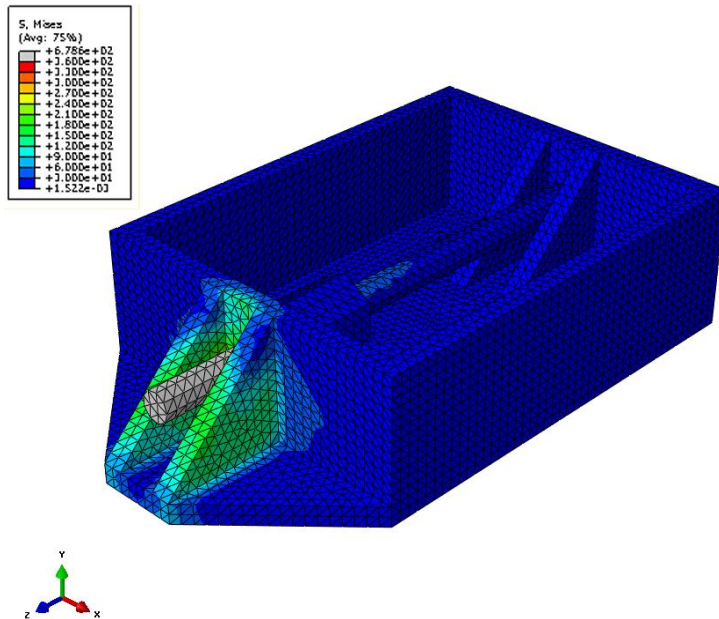


Figure 6.42 Adding stiffeners to the temporary support box lowered both the stresses and the deformations but increased complexity in manufacturing of the support.

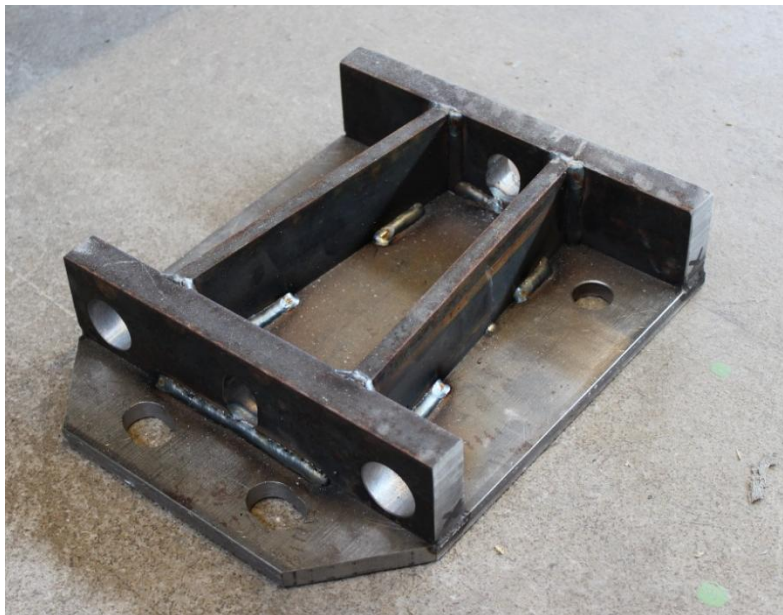


Figure 6.43 Manufactured temporary support

## 6.4.2 Holders for the guiding bars

The holders for the guiding bars are manufactured in two halves to make it possible to mount them around the guiding bars. This leaves a gap in the holder which will be subject to load and possibly large deformations. A model of only the holder and a part of the guiding bar is modelled with the guiding bar fixed while the load is acting on top of the holder. This simulates the withdrawal forces that the holders will be subjected to during prestressing. The load applied in the model is equal to 8kN and is well above the loads that the holders are subjected to in the full model. Figure 6.44 show how the holder will deform and the maximum deformation at the tip of the opening is around 0.01 mm which is very small, note that the scaling in this figure is very large. The maximum stresses in the holders are also very low.

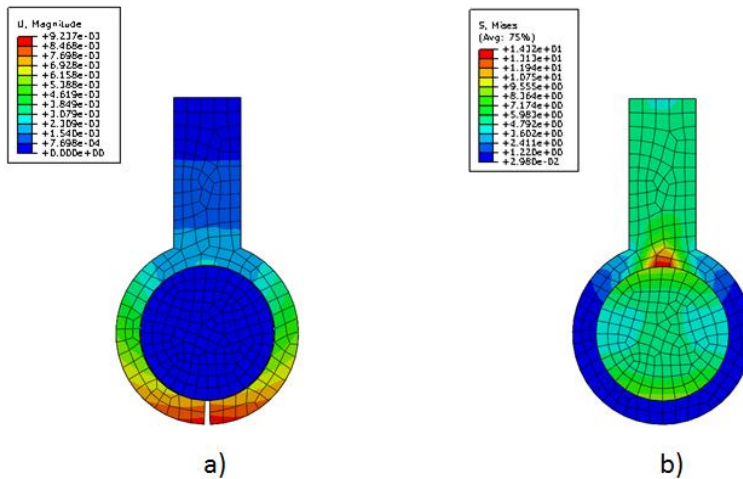


Figure 6.44 Figure showing the deformation, a), and stresses, b), in the holder for the guiding bars with a load of 8kN. The largest deformations are  $\sim 0.01\text{mm}$  and the largest stress is around 14.3MPa.

### 6.4.3 Aluminium tabs

The aluminium tabs in the device will be subjected to forces pulling them away from the guiding bars. This force will make the tabs deform to a certain extent. In order to verify that these deformations are within limits and not too extensive a model of half a tab is carried out. It is modelled with symmetry at the middle and a bit of the guiding bar running through the slot in the tab. The guiding bar is locked with boundary conditions and the load is applied to the tab as a pressure. A load of 8kN per slot is applied, i.e. a total of 16kN per tab.

The deformations and stresses can be seen in Figure 6.45. The deformations are a bit large but the load is also several times larger than what it will be in reality. While the deformations are considered a bit large the stresses are well below yielding and should not cause any problems during prestressing.

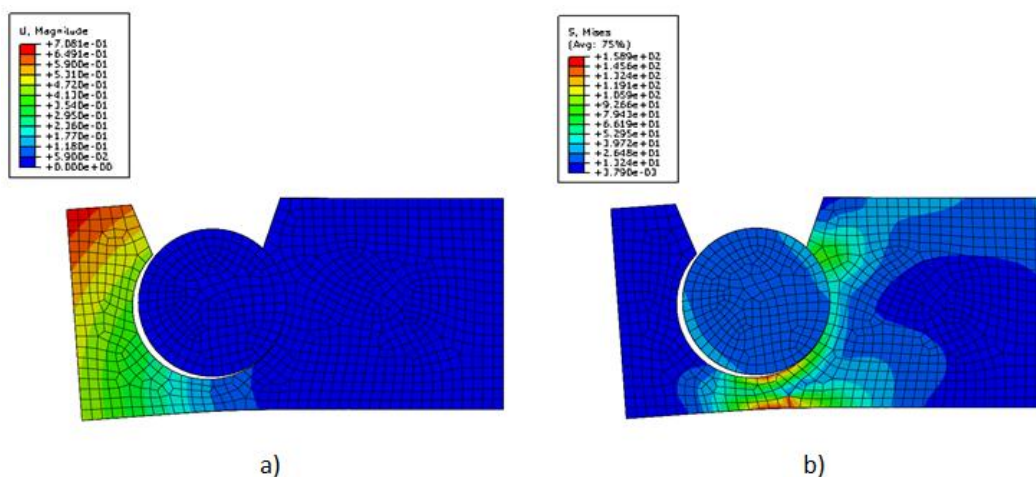


Figure 6.45 The deformation, a), and the stresses, b), of the aluminium tabs are controlled under a load of a total of 16kN per tab.

## 7 Experimental Verification of the Prestressing Device

In order to investigate if the new configurations of the prestressing device will work properly and is usable for a full scale case study, an experimental verification will be carried out. The refined model of the concept is based on a prototype already developed and verified with experiments at Chalmers. This chapter presents the experiments carried out for the concept baseline and prove that it is a working concept. Similar experiments are to be carried out using the refined prestressing device. Appendix D contains pictures and graphs obtained during the test.

### 7.1 Experiments carried out in advance at Chalmers

The first prototype was tested at Chalmers and is the base of the refined concept modelled though this report. The first prototype and the method were verified by testing three large scale beams with the configuration shown in Figure 7.1. A total number of four beams were ordered and manufactured and one of the beams were left for testing of the final prototype after the improvements made to the prestressing device.

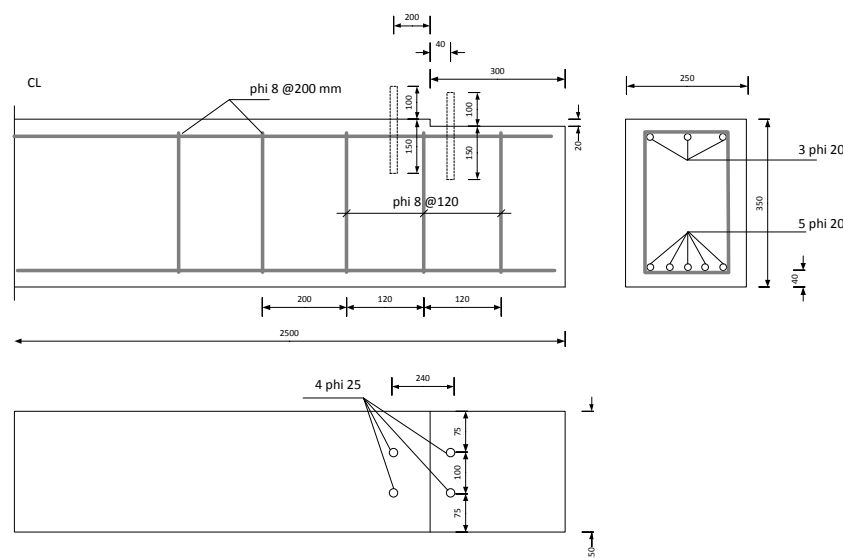


Figure 7.1 Schematic of the test specimen concrete beams.

The first prototype was tested by just pulling a laminate without adhesive. This was done with strain gauges to see that the correct force distribution was obtained in the laminate.

Then three beams were tested. One beam was strengthened with an unprestressed laminate to act as a reference. The second beam was strengthened with a laminate prestressed to 30kN and a third beam was pre-loaded and cracked and then strengthened with a laminate prestressed to 85kN. This was done to see the effect of prestressing on a cracked section.





Figure 7.2 Test setup with hydraulic jack mounted and using clamps to hold the device in place.



Figure 7.3 Test setup with four-point bending that was used.

Figure 7.2 show the prestressing phase for the first prototype which had to be clamped to the concrete while there were no guiding bars keeping the device in place. The beams were tested in four point bending and the test setup can be seen in Figure 7.3. Strain gauges and LVDT's were mounted to monitor displacements and strains during the tests.

### 7.1.1 Effect on Serviceability Limit State

The tests shows the promising effects that prestressing have on the service limit state. In the Figure below it is possible to see the load-deflection curves for the different beams. Table 7.1 provides SLS load levels for the beams which indicate consequent improvement of the SLS performance with increased prestressing. The improvements in SLS load level means that a larger load is needed to provide the same deflection. It should also be noted that the beam prestressed to 85kN is pre-cracked and this clearly demonstrates the effectiveness of this strengthening method.

Table 7.1 Serviceability Limit State load for different beams.

Configuration	SLS* load [kN]	Improvement with regard to reference beam [%]
---------------	----------------	---

Unstrengthened beam (reference)	108	-
Strengthened unprestressed	121	12
Strengthened – prestressed 30kN	130	20
Strengthened (repaired) 85kN	162	50

\*The limit for SLS was considered to be  $L/300 = 14\text{mm}$

### 7.1.2 Efficiency of strengthening and failure mode

As prestressing is a method to utilize more of the available capacity in the CFRP laminates debonding failure is not favourable as it utilize less than 100% of the capacity. Full utilization of the laminate is reached only if the failure is by laminate rupture. In Table 7.2, the failure modes for the different beams are provided.

Table 7.2 Failure mode of the different beams.

Configuration	Failure mode
Unstrengthened beam (reference)	Yield in steel reinforcement
Strengthened – unprestressed	Debonding of the laminate
Strengthened – prestressed 30kN	Debonding of the laminate
Strengthened (repaired) – prestressed 85kN	Rupture of the laminate

The unprestressed laminate failed and the laminate prestressed with 30kN failed by laminate debonding but the pre-cracked beam strengthened with a laminate prestressed to 85kN failed by laminate rupture which is what was aimed for.

### 7.1.3 Improved stiffness

By prestressing with 85kN both the stiffness and the load level where the internal reinforcement yield are improved. By comparing the stiffness with one of the unstrengthened beam it can be seen that it is improved with 39% and this indicates the great capability in restoring lost stiffness using this method.

## 8 Discussion

Results are discussed in each section of the report where results are obtained. Though, there are a few topics that can be discussed a bit further.

Due to the versatility of CFRPs, they can be tailored into a suitable material for strengthening and by choosing and combining different fibres and matrix materials. Properties such as durability, strength and elasticity can be emphasized. Care must be taken so that appropriate material properties are used in combination with the prestressing device in order to ensure safe usage and durability over time.

Some conceivable negative aspects to discuss concerning the use of strengthening with CFRP laminates might appear aesthetically displeasing on the strengthened member. The necessary addition of the GFRP plate, which is permanently attached to the CFRP laminate, increases the build height of the strengthened member drastically compared to the thickness of a single CFRP laminate. Even if it is just a couple of centimetres it will require more work to be covered. Furthermore, it might affect the aesthetics negatively and be the reason that the laminate need to be covered.

Using the prestressing device on a slightly concave or convex surface might be troublesome. Mounting of the tools, like the guiding bars, will be problematic and the adhesive layer will have a varying thickness. This might be a limitation of the prestressing device, although it is not unique for this device and other techniques are limited by this as well.

Alignment of the prestressing device, i.e. the guiding bars and the prestressing support, is necessary. Slightest misalignment will generate large forces that could break and destroy the equipment and potentially be dangerous. Of this reason it is of great importance to ensure that the tool is correctly aligned before prestressing.

Even after all changes and improvements that were made to the concept through the project, the results of the analyses are still not matching the theoretical stress distribution. As seen in the results even the slightest change to the design, i.e. properties or geometry, will make a noticeable difference to the outcome. The prestressing device is obviously complex and it would have been impossible to reach such results without the analyses done. It was not always easy to predict how and what would affect the results and in what way.

The analyses of the tool are made assuming frictionless contact between the guiding bars and the tabs. This surface will be greased to reduce the friction but it will never be completely frictionless. This assumption was based on reducing the influential factors of the results and to limit the complexity of the analysis, i.e. computational time.

There will always be room for improvement, but it is necessary to decide whether it is worth the effort and where to put it. As the already promising results of the prestressing device have been proved, focus might be put into making it more effective and easier to use. Improvement would of course be necessary if higher prestressing forces are to be obtained. This could be acquired by increasing the number of steps and the length of the prestressing device but that would affect the appearance and make the tool more ungainly. Though, the weight and size limit is based on a hunch and the only way to know if it is reasonable is by using the device. Furthermore, improvement of the device could also be achieved with a slightly more refined design of the GFRP plate.

One of the main selling points of the prestressing device is that it should be a; simple to use system that should be easy to operate and maintain. No problems should arise from the tool itself. Therefore it is important not to overcomplicate things and to strive for simplicity that generates predictable and consistent results.

The prestressing device should resist the wear and tear that is seen in the industry with its harsh environments. Parts of the prestressing device are fragile and wear and tear of e.g. the guiding bars or aluminium tabs would affect the friction and hence the function. Similarly, the steel rods acting as springs might suffer from hits and large forces if not handled with care. It is impossible to predict how careful and if careful handling is enough to ensure a long lifetime of the device. Luckily all parts are possible and quite easily replaced and thus should not be a major problem, but could lead to changes in the design. Time will also tell if it is easy to operate, that includes the size and weight of the prestressing device itself. It would be of great value if the tool could be operated without lifting aid. This is an area where it could be valuable to optimize the design, with regard to weight and size, e.g. using FRP materials in the tool as well.

## 9 Final Remarks

In this chapter, conclusions on the master's thesis work in its entirety are presented, followed by suggestions on future research.

### 9.1 Conclusions

As Europe is full of structures in need of strengthening and repairs with increasing demands on standard, there is a large need for development in this area of civil engineering. Clients demand solutions that require less effort that are time efficient and reduces future need for inspection and maintenance, all this in order to reduce traffic disruptions which are expensive.

The use of unprestressed FRP materials has a lot of advantages over other conventional methods. They can be used for strengthening in shear and compression of walls, floor slabs, columns and beams in all structures. As these materials are costly and methods with unprestressed laminates have a low utilization ratio there is need for inducing prestressing in the laminates. Prestressing has many good effects but there is one main problem with prestressing and that is the high shear stresses that appear at the laminates ends. This problem is usually solved with mechanical anchors and all commercial systems available at present time uses mechanical anchors. In order to overcome the disadvantages with mechanical anchors, a system based on stepwise prestressing without mechanical anchors is developed. The only way to eliminate the need of mechanical anchors is to transfer the force over a length of the laminate, e.g. in steps. The method developed by Meier showed promising results but was impractical and needed improvement to become feasible in practice. The work carried out on the concept prior to and through this report has certainly taken a giant leap towards a practical and viable solution. This system should be versatile, easy to operate, and "fast" to apply.

CFRPs ability to retain its capacity and withstand both creep and relaxation in tough environment makes it very useful within the field of repair and strengthening. Compared with steel it should be in less need of inspection and should be able to meet the requirements for the designed lifetime without the need of any major maintenance. The low density combined with its high strength and the possibility of manufacturing and transporting large quantities and dimensions, installation and expected workload is far less than for equally strong quantities of steel. Their brittle behaviour makes them vulnerable to impact and this is one of their major disadvantages and in a lot of cases they need to be protected in order to not jeopardize safety.

All of the reports read during the literature study showed that the possibilities and capabilities to restore lost stiffness and prestress and also increase both service life and ultimate state capacity are promising. When anchoring is done correctly, prestressed CFRP laminates have a great potential.

The parametric study showed that the most effective way of reducing the high shear stresses were to increase the number of steps and to increase the distance between each load point. Also, measures to increase the anchorage length are important as it efficiently reduce the peak shear stresses in the adhesive as it evens out the load distribution. In order to increase the anchorage length and make shear stress distribution even and as close to constant as possible it is beneficial to use a material with low stiffness, e.g. GRFP, to transfer the prestressing force.

From the FE-modelling of the concept, it was concluded that an even distribution of the load in at each step along the laminate is the best way to get an even shear flow. To achieve this with the prestressing device when it acts together with the laminate the only way to improve the distribution is by FE-modelling as the combined behaviour is complex.

In order to reduce deflections, stresses and strains in all components required for mounting and prestressing great care is needed in the designing of the details.

The previous experiments show that the concept works and that it improves both SLS and ULS behaviour of damaged and strengthened concrete beams. It shows that a prestressing force of 85kN is enough to reach laminate rupture, even though higher prestressing is favourable. To continue with this concept there are things that need to be changed with the system but the major issue is to solve practical issues regarding the system to be used outside the lab.

Even though a lot of changes were made to the concept during the time it was developed there are still a lot of uncertainties with the practical use of the concept. These issues appeared during the experimental work and sometimes this is the only way to actually realize where there is a problem. More detailing and changes are to be expected in order to develop a fully functional system, although as with most designs there will always be room for improvement and strive to reach perfection.

## 9.2 Suggestions on future research

The theory of the concept has been proved to work and further research should focus on practical issues when using and handling the device, consider potential sources of error and further improve upon the design.

The FE-model is considered to be detailed but there was not time to perform a proper mesh-convergence study or to increase the mesh density enough in all regions. Computing power is always a limiting factor and sub-modelling or locally increased mesh density would be preferred to investigate areas with insufficient mesh density further.

Details like the dimensions of the added adhesive fillets are not examined in detail, and though their additions are improvements to the design their configurations could be investigated further.

One of the things that had the most effect on decreasing the high shear stress peaks was the addition of the GFRP layer. It was added to enable so that the device could be attached to the CFRP and carry out the prestressing. Since this part had such an impact on the results by increasing the anchorage length, it would be of great interest to look into and find an ideal design. Especially since it adds both to the complexity of the design and the aesthetics.

The FE-model assumed an adhesive layer between both the GFRP and CFRP with a perfectly even thickness. Even if the preparations are done carefully there are always global and local variations in concrete surfaces, especially for old structures. Deviations in the thickness in these layers will have an impact on the results. It would be interesting to see the effect of this.

Another assumption is that the guiding bars are completely straight; when these are mounted in reality it is crucial to achieve this. The effect of a slight misalignment is

necessary to predict, though this could generate high resistance in form of friction and could possibly harm both equipment and affect the resulting prestress negatively.

Investigate the possibility to use the prestressing device with another prestressing method, e.g. it could be done by prestressing against an external beam, the independent beam system, to overcome the difficulties that can occur when mounting the guiding bars and prestressing support.

Finally, extensive testing of the prestressing device should be performed in reality to confirm the results of the FE-model.

## 10 References

- [1] P. Domone and J. Illston, *Construction materials: their nature and behaviour*. 2010.
- [2] PANTURA, “D5.3: Needs for maintenance and refurbishment of bridges in urban environments,” 2011.
- [3] B. Åkesson, *Fatigue Life of Riveted Steel Bridges*. CRC Press, 2010, p. 170.
- [4] R. El-Hacha, R. Wight, and M. Green, “Prestressed carbon fiber reinforced polymer sheets for strengthening concrete beams at room and low temperatures,” *J. Compos. ...*, no. February, pp. 3–13, 2004.
- [5] R. . Quantrill and L. . Hollaway, “The flexural rehabilitation of reinforced concrete beams by the use of prestressed advanced composite plates,” *Compos. Sci. Technol.*, vol. 58, no. 8, pp. 1259–1275, Aug. 1998.
- [6] R. El-Hacha, R. Wight, and M. Green, “Prestressed fibre-reinforced polymer laminates for strengthening structures,” *Prog. Struct. Eng. Mater.*, vol. 3, no. 2, pp. 111–121, Apr. 2001.
- [7] R. El-hacha, R. G. Wight, and M. F. Green, “Innovative System for Prestressing Fi ber-Reinforced Polymer Sheets,” no. 100, 2004.
- [8] S. T. Smith and J. G. Teng, “Interfacial stresses in plated beams,” *Eng. Struct.*, vol. 23, no. 7, pp. 857–871, Jul. 2001.
- [9] R. Haghani, “Analysis of geometrically modified adhesive joints in steel beams strengthened with composite laminates,” 2008.
- [10] B. Täljsten, *FRP Strengthening of Existing Concrete Structures: Design Guidelines*. 2002.
- [11] H. Nordin, “Strengthening structures with externally prestressed tendons Strengthening structures with Literature review,” 2005.
- [12] J. Cadei, T. Stratford, L. Hollaway, and W. Dcukett, “Strengthening metallic structures using externally bonded fibre-reinforced polymers,” 2004.
- [13] L. C. Hollaway and M. B. Leeming, *Strengthening of reinforced concrete structures*. Woodhead Publishing Limited, 1999.
- [14] L. Bank, *Composites for construction: Structural design with FRP materials*. 2006.
- [15] Manoochehr Zoghi, Ed., *The International Handbook of FRP Composites in Civil Engineering*. CRC Press.



- [16] V. P. Karbhari and L. S. Lee, *Service life estimation and extension of civil engineering structures*. Cambridge: Woodhead Publishing, 2011.
- [17] *FRP Reinforcement in RC Structures: Technical Report*. FIB - Féd. Int. du Béton, 2007, p. 147.
- [18] A. Carolin, *Carbon Fibre Reinforced Polymers for*. 2003, pp. 1402–1544.
- [19] PANTURA, “D5.8 Annex 5: Strengthening and repair of concrete bridges,” 2012.
- [20] R. Haghani, *Behaviour and design of adhesive joints in flexural steel members bonded with FRP laminates*. 2010.
- [21] P. Balaguru, A. Nanni, and J. Giancaspro, *FRP Composites for Reinforced and Prestressed Concrete Structures: A Guide to Fundamentals and Design for Repair and Retrofit*. Taylor & Francis, 2008.
- [22] T. C. Triantafillou, “Strengthening of structures with advanced FRPs,” *Prog. Struct. Eng. Mater.*, vol. 1, no. 2, pp. 126–134, Jan. 1998.
- [23] T. H. Kang, J. Howell, S. Kim, and D. J. Lee, “A State-of-the-Art Review on Debonding Failures of FRP Laminates Externally Adhered to Concrete,” vol. 6, no. 2, pp. 123–134, 2012.
- [24] M. R. Aram, C. Czaderski, and M. Motavalli, “Debonding failure modes of flexural FRP-strengthened RC beams,” *Compos. Part B Eng.*, vol. 39, no. 5, pp. 826–841, Jul. 2008.
- [25] W. Xue and Y. Tan, “International Perspective : Experimental studies of concrete beams strengthened with prestressed CFRP laminates,” pp. 70–85, 2008.
- [26] L. N. Deng, P. Zhang, and H. Chen, “Flexural Behaviour of RC Beams Strengthened with Prestressed CFRP Plates : Comparisons of Bonded and Unbonded Method,” *Key Eng. Mater.*, vol. 480–481, pp. 283–287, 2011.
- [27] D.-S. Yang, S.-K. Park, and K. W. Neale, “Flexural behaviour of reinforced concrete beams strengthened with prestressed carbon composites,” *Compos. Struct.*, vol. 88, no. 4, pp. 497–508, 2009.
- [28] R. Kotynia, R. Walendziak, I. Stoecklin, and U. Meier, “RC Slabs Strengthened with Prestressed and Gradually Anchored CFRP Strips under Monotonic and Cyclic Loading,” no. April, pp. 168–180, 2011.
- [29] B. Engström, *Design and analysis of prestressed concrete structures*. Göteborg: Chalmers University of Technology, 2011.
- [30] Y.-C. You, K.-S. Choi, and J. Kim, “An experimental investigation on flexural behavior of RC beams strengthened with prestressed CFRP strips using a

- durable anchorage system,” *Compos. Part B Eng.*, vol. 43, no. 8, pp. 3026–3036, Dec. 2012.
- [31] S. Hong and S.-K. Park, “Effect of prestress levels on flexural and debonding behavior of reinforced concrete beams strengthened with prestressed carbon fiber reinforced polymer plates,” *J. Compos. Mater.*, vol. 91, pp. 640–650, 2012.
- [32] J.-G. Dai, W.-W. Wang, K. A. Harries, and Q.-H. Bao, “Prestress Losses and Flexural Behavior of Reinforced Concrete Beams Strengthened with Posttensioned CFRP Sheets,” Apr. 2012.
- [33] M. Al-Emrani and R. Kliger, “Analysis of interfacial shear stresses in beams strengthened with bonded prestressed laminates,” *Compos. Part B Eng.*, vol. 37, no. 4–5, pp. 265–272, Jun. 2006.
- [34] M. Brunner and M. Schnueriger, “Timber Beams Strengthened by Attaching Prestressed Carbon FRP Laminated with a Gradiented Achnoring Device,” no. Bbfs, pp. 465–472, 2005.
- [35] W. Figeys, E. Verstrynghe, K. Brosens, L. Van Schepdael, J. Dereymaeker, D. Van Gemert, and L. Schueremans, “Feasibility of a novel system to prestress externally bonded reinforcement,” *Mater. Struct.*, vol. 44, no. 9, pp. 1655–1669, Mar. 2011.
- [36] “Sika Group | Sika AG.” [Online]. Available: <http://www.sika.com/>. [Accessed: 18-Mar-2015].
- [37] “Neoxe Prestressing System.” [Online]. Available: [http://www.neoxe.com/index.php/TECHNOLOGIE/Neoxe\\_Prestressing\\_System/](http://www.neoxe.com/index.php/TECHNOLOGIE/Neoxe_Prestressing_System/). [Accessed: 11-Sep-2013].
- [38] I. Stöcklin and U. Meier, “Strengthening of concrete structures with prestressed and gradually anchored CFRP strips,” in *Proceeding of the sixth international symposium on FRP Reinforcement for Concrete Structures (FRPRCS-6)*, 2003, pp. 1321–1330.
- [39] “Aluminium Alloy - Commercial Alloy - 2011 T3 Rod and Bar.” [Online]. Available: [http://www.aalco.co.uk/datasheets/Aluminium-Alloy-2011-T3-Rod-and-Bar\\_3.ashx](http://www.aalco.co.uk/datasheets/Aluminium-Alloy-2011-T3-Rod-and-Bar_3.ashx). [Accessed: 06-Jan-2017].

## Appendix A

### Derivation of formulas for calculation of interfacial shear stress in the adhesive, axial force in the laminate, and bending moment of the strengthened beam

The following derivation of formulas for beams strengthened with prestressed laminates are from [33].

#### Notations

##### Roman upper case letters

$A_l$	cross-sectional area of the laminate
$A_b$	cross-sectional area of the beam
$B_l$	width of the laminate
$C_1$	constant
$C_2$	constant
$E_l$	modulus of elasticity of the laminate
$E_b$	modulus of elasticity of the beam
$G_a$	shear modulus of the adhesive
$G_b$	shear modulus of the beam
$I_b$	second moment of area of the beam
$L$	laminate length
$M_b$	bending moment in the beam due to prestressing
$P_0$	initial prestressing force in the laminate
$P_l$	residual prestressing force in the laminate after bonding and releasing
$P_b$	axial force in the beam due to prestressing

##### Roman lower case letters

$h$	beam depth
$t_a$	thickness of the adhesive layer
$t_l$	thickness of the laminate

##### Greek lower case letters

$\delta_l$	displacement in the laminate
$\delta_b$	displacement in the outermost fibres in tensile strain of the beam
$\varepsilon_l$	strain in the laminate

$\varepsilon_b$	strain in the outermost fibres in tensile of the beam
$\tau$	shear stress in the adhesive layer
$\omega$	constant

## A.1 Shear stress distribution in the adhesive

The loss of prestressing force in the laminates is (A.1)

$$\Delta P_l = P_0 - P_l \quad (\text{A.1})$$

Equilibrium requires that (A.2)

$$P_b = -P_l \quad (\text{A.2})$$

Consider now the compatibility of deformation at a distance  $x$  from the centre line of the composite beam. The change in the axial strain in the laminate due to the deformability of the steel beam can be related to the loss in the prestressing force as follows

$$\frac{d}{dx} \delta_l(x) = \Delta \varepsilon_l = \frac{\Delta P_l(x)}{A_l E_l} = \frac{P_0 - P_l(x)}{A_l E_l} \quad (\text{A.3})$$

The deformation of the beam at the outermost fibre of the lower flange is on the other hand related to the axial force and bending moment induced on the beam by the prestressing

$$\frac{d}{dx} \delta_b(x) = \varepsilon_b(x) = \frac{-P_b(x)}{A_b E_b} + \frac{-M_b(x)}{I_b E_b} \cdot \frac{h}{2} \quad (\text{A.4})$$

**Assumption 1:** Again, it is assumed that the laminate is thin so that its effect on the second-moment of area of the composite beam can be neglected.

The shear stress in the adhesive layer is directly related to the difference in deformation between the laminate and the lower flange of the steel beam (A.5)

$$\tau(x) = \frac{G_a}{t_a} (\delta_l(x) - \delta_b(x)) \quad (\text{A.5})$$

Differentiating Eq. (A.5) once

$$\frac{d}{dx} \tau(x) = \frac{G_a}{t_a} \left( \frac{d}{dx} \delta_l(x) - \frac{d}{dx} \delta_b(x) \right) \quad (\text{A.6})$$

Inserting the expressions (A.3) and (A.4) yields

$$\frac{d}{dx} \tau(x) = \frac{G_a}{t_a} \left( \frac{P_0}{A_l E_l} - \frac{P_l(x)}{A_l E_l} + \frac{P_b(x)}{A_b E_b} + \frac{M_b(x)}{I_b E_b} \cdot \frac{h}{2} \right) \quad (\text{A.7})$$

Consider a segment in the composite beam with an infinitesimal length  $dx$  at a distance  $x$  from the beam centre line.

Equilibrium of forces requires that

$$\frac{d}{dx} P_b(x) = b_l \tau(x) \quad (\text{A.8})$$

$$\frac{d}{dx} P_l(x) = -b_l \tau(x) \quad (\text{A.9})$$

And

$$\frac{d}{dx} M_b(x) = b_l \frac{h}{2} \tau(x) \quad (\text{A.10})$$

Differentiating Eq. (A.7) again with respect to  $x$  gives

$$\frac{d^2}{dx^2} \tau(x) = \frac{G_a}{t_a} \left( \frac{-1}{A_l E_l} \frac{d}{dx} P_l(x) + \frac{1}{A_b E_b} \frac{d}{dx} P_b(x) + \frac{h}{2 I_b E_b} \frac{d}{dx} M_b(x) \right) \quad (\text{A.11})$$

Inserting Equations (A.8) - (A.10) results in

$$\frac{d^2}{dx^2} \tau(x) = \frac{G_a}{t_a} \left( \frac{b_l}{A_l E_l} + \frac{b_l}{A_b E_b} + \frac{b_l h^2}{4 I_b E_b} \right) \tau(x) \quad (\text{A.12})$$

Or

$$\frac{d^2}{dx^2} \tau(x) = \omega^2 \tau(x) \quad (\text{A.13})$$

In which:

$$\omega^2 = \frac{G_a}{t_a} \left( \frac{b_l}{A_l E_l} + \frac{b_l}{A_b E_b} + \frac{b_l h^2}{4 I_b E_b} \right) \quad (\text{A.14})$$

The differential equation (A.13) has the following general solution

$$\tau(x) = C_1 e^{\omega x} + C_2 e^{-\omega x} \quad (\text{A.15})$$

Where  $\omega$  is defined in Eq. (A.14) and the constants  $C_1$  and  $C_2$  are to be determined from the boundary conditions:

### Boundary 1

Due to symmetry, all displacements at the middle of the composite beam are zero:

$$\delta_l(x=0) = \delta_s(x=0) = 0 \quad (\text{A.16})$$

Which, substituted in Eq. (A.5), yields

$$\tau(x=0) = 0 \quad (\text{A.17})$$

Together with Eq. (A.15):

$$C_1 = -C_2 \quad (\text{A.18})$$

### Boundary 2

At the end of the laminate:

$$P_l\left(x = \frac{L}{2}\right) = P_b\left(x = \frac{L}{2}\right) = M_b\left(x = \frac{L}{2}\right) = 0 \quad (\text{A.19})$$

Inserting in Eq. (A.7) gives:

$$\frac{d}{dx}\tau(x) = \frac{G_a P_0}{t_a A_l E_l} \quad (\text{A.20})$$

Differentiating Eq. (A.15) once and substituting Eq. (A.20) yields

$$C_1 = -C_2 = \frac{G_a P_0}{t_a A_l E_l} \frac{1}{2\omega \cosh\left(\frac{\omega L}{2}\right)} \quad (\text{A.21})$$

Eq. (A.21) inserted in Eq. (A.15) gives the distribution of **shear stress along the bond line**:

$$\tau(x) = \frac{G_a P_0}{t_a A_l E_l} \frac{\sinh(\omega x)}{\omega \cosh\left(\frac{\omega L}{2}\right)} \quad (\text{A.22})$$

The maximum shear stress at the end of the laminate can be found for  $x = L/2$ :

$$\tau_{\max} = \frac{P_0}{A_l E_l} \frac{G_a}{t_a} \frac{\tanh\left(\frac{\omega L}{2}\right)}{\omega} \quad (\text{A.23})$$

## A.2 Axial force distribution in the laminate

The distribution of the axial force in the laminate can be found by differentiating Eq. (A.22) once and substituting the left- hand side in Eq. (A.7):

$$\frac{G_a P_0}{t_a A_l E_l} \frac{\cosh(\omega x)}{\cosh\left(\frac{\omega L}{2}\right)} = \frac{G_a}{t_a} \left( \frac{P_0}{A_l E_l} - \frac{P_l(x)}{A_l E_l} + \frac{P_b(x)}{A_b E_b} + \frac{P_l(x)}{I_b E_b} \cdot \frac{h^2}{2} \right) \quad (\text{A.24})$$

Using

$$P_l(x) = -P_b(x) \quad (\text{A.25})$$

And

$$M_b(x) = -P_l(x) \frac{h}{2} \quad (\text{A.26})$$

Gives:

$$P_l(x) = \frac{P}{A_l E_l} \left[ 1 - \frac{\cosh(\omega x)}{\cosh\left(\frac{\omega L}{2}\right)} \right] \frac{1}{\left( \frac{1}{A_l E_l} + \frac{1}{A_b E_b} + \frac{h^2}{4E_b I_b} \right)} \quad (\text{A.27})$$

## A.3 Bending moment distribution along the strengthened length of the beam

It was assumed in Eq. (A.26) that the height of the beam is very large in comparison to the thickness of the laminate and the adhesive layer, which allows neglecting the thicknesses when calculating the bending moment.

The distribution of bending moment along the strengthened length of the beam then becomes:

$$M_b(x) = -P_0 \frac{h}{2} \frac{\left[ 1 - \frac{\cosh(\omega x)}{\cosh\left(\frac{\omega L}{2}\right)} \right]}{\left( 1 + \frac{A_l E_l}{A_b E_b} + \frac{A_l E_l h^2}{4 E_b I_b} \right)} \quad (\text{A.28})$$



## **Appendix B**

### **Calculations of a reinforced concrete beam strengthened with CFRP laminate**

Appendix B contains calculations of a reinforced concrete (RC) beam strengthened with CFRP laminates. The calculations were used to learn more about the behaviour of the CFRP laminate when strengthened and the effects on the RC beam.

This document estimates the amount of CFRP laminates that required in order to reach a user specified capacity after strengthening of a RC beam with arbitrary dimensions. The calculations are based on the book “FRP strengthening of existing concrete structures” by Björn Täljsten [10]. To be able to predict the amount of CFRP laminates that is needed to reach desired capacity of a RC beam section in need of strengthening, the section has to be analysed. The amount needed for a certain increase in strength and stiffness is based on the combination of the initial design of the cross-section and desired final capacity.

By following the method suggested in [10] the strength prediction, the design method, the amount of CFRP as well as the most probable failure mode can be predicted.

The program Mathcad is used as an aid to carry out the calculations following the steps in the book. By entering the amount of reinforcement and dimensions of an arbitrary cross-section of reinforced concrete the amount of CFRP material which is needed is calculated based on desired capacity. Also the expected failure mode will be given. The calculations can further be used for more detailed calculations of prestressed CFRP laminates following the principles of prestressed concrete.

## Appendix B: Reinforced Concrete (RC) beam with prestressed Carbon Fibre-Reinforced Polymer (CFRP) laminates

This document estimates the need of prestress force and amount of CFRP-laminates in a reinforced concrete beam with arbitrary dimensions.

### DIMENSIONS AND MATERIAL DATA

#### **Table of Contents:**

- Dimensions of the RC beam
- Material properties
  - Concrete C30/37
  - Shear Reinforcement: Reinforcing steel stirrups B500B
  - Bottom Reinforcement: Reinforcing steel B500B in bending (tension)
  - Top Reinforcement: Reinforcing steel B500B in bending (compression)
  - CFRP laminates
  - Adhesive

#### **Dimensions of the RC beam:**

Length of the span/beam:

$$l_{\text{beam}} := 10\text{m}$$

Cross section:

Height of cross-section:

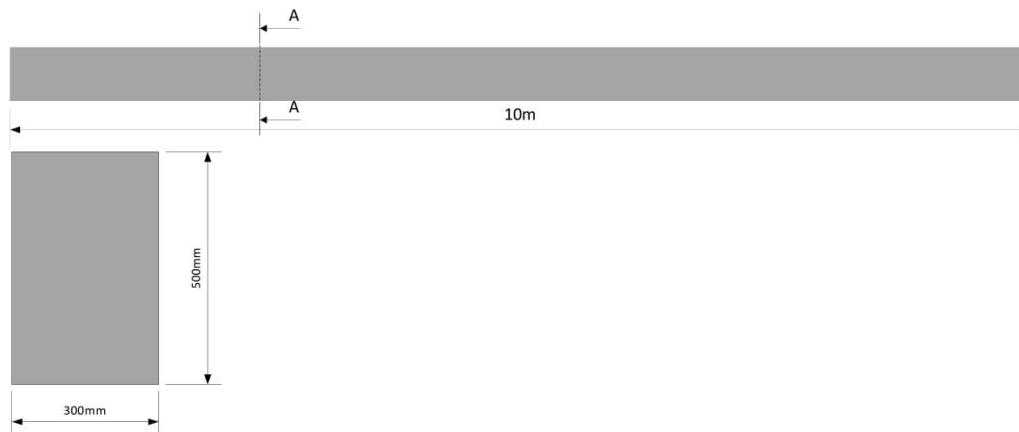
$$h := 500\text{mm}$$

Width of cross-section:

$$b := 300\text{mm}$$

Area of concrete section:

$$A_c := h \cdot b = 0.15 \text{ m}^2$$



Section A-A

**FIGURE 1: Chosen beam dimensions**

#### **Material properties:**

Concrete C30/37

Parameters for the compression zone of the concrete (depends on concrete class):

$$\alpha_c := 0.81$$

$$\beta_c := 0.416$$

Partial safety coefficient:

$$\gamma_{M1} := 1.5$$

Creep coefficient:

$$\varphi := 2.0$$

Strength:

Characteristic value:

$$f_{ck} := 30\text{MPa}$$

$$f_{ctm} := 2.9\text{MPa}$$

$$f_{ct} := 3.2\text{MPa} \quad \text{Splitting strength}$$

Design value:

$$f_{cd} := \frac{f_{ck}}{\gamma_{M1}} = 20\text{MPa}$$

$$f_{ctd} := \frac{f_{ctm}}{\gamma_{M1}} = 1.933\text{MPa}$$

Modulus of elasticity:

$$E_{cm} := 33\text{GPa}$$

With creep:

$$E_{cme} := \frac{E_{cm}}{1 + \varphi} = 11\text{GPa}$$

Ultimate strain:

$$\varepsilon_{cu} := 0.35\%$$

Density:

$$\rho_c := 2400 \frac{\text{kg}}{\text{m}^3}$$

Cover thickness:

$$\text{cover} := 30\text{mm}$$

### Shear Reinforcement: Reinforcing steel stirrups B500B

Partial safety coefficient:

$$\gamma_{\text{steel}} := 1.15$$

Strength:

Characteristic value:

$$f_{yk} := 500\text{MPa}$$

Design value:

$$f_{ywd} := \frac{f_{yk}}{\gamma_{\text{steel}}} = 434.783\text{MPa}$$

Modulus of elasticity:

$$E_{sw} := 200\text{GPa}$$

Diameter:

$$\phi_w := 8\text{mm}$$

Area of one stirrup (i.e. two bars):

$$A_{sw} := 2 \left( \frac{\phi_w}{2} \right)^2 \cdot \pi = 100.531 \cdot \text{mm}^2$$

Distance between stirrups (C-C):

$$s_w := 200\text{mm}$$

Number of stirrups along the beam:

$$\frac{10\text{m} - \text{cover} \cdot 2 - \left( \frac{\phi_w}{2} \right) \cdot 2}{200\text{mm}} = 49.66$$

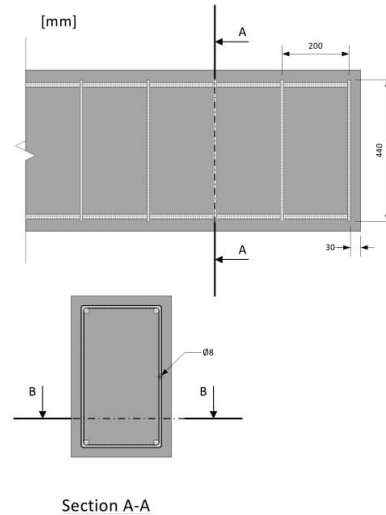


FIGURE 2: Reinforcement stirrups

Bottom Reinforcement: Reinforcing steel B500B in bending (tension)

Strength:

Characteristic value:

$$f_{yk} := 500\text{MPa}$$

Design value:

$$f_{yd} := \frac{f_{yk}}{\gamma_{\text{steel}}} = 434.783 \cdot \text{MPa}$$

Modulus of elasticity:

$$E_s := 200\text{GPa}$$

Yield strain:

$$\epsilon_{sy} := \frac{f_{yd}}{E_s} = 2.174 \times 10^{-3}$$

Density:

$$\rho_s := 7800 \frac{\text{kg}}{\text{m}^3}$$

Diameter:

$$\phi := 16\text{mm}$$

Area of one bar:

$$A_{si} := \left( \frac{\phi}{2} \right)^2 \cdot \pi = 201.062 \cdot \text{mm}^2$$

Number of reinforcement layers:

$$\text{layers}_{\text{bottom}} := 2$$

Number of bars:

$$n_{\text{layer1.bottom}} := 4$$

$$n_{\text{layer2.bottom}} := 4$$

$$n_{\text{layer3.bottom}} := 0$$

$$n := n_{\text{layer1.bottom}} + n_{\text{layer2.bottom}} + n_{\text{layer3.bottom}} = 8$$

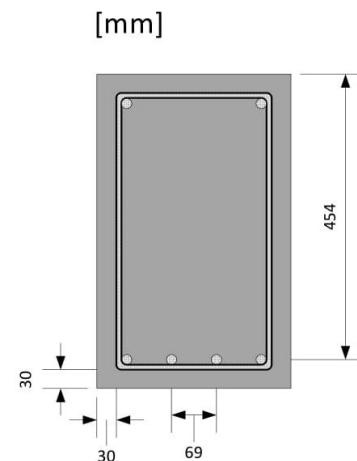


FIGURE 3: Bottom reinforcement

Total area of reinforcement:

$$A_s := n \cdot A_{si} = 1.608 \times 10^3 \cdot \text{mm}^2$$

Distance to tensile reinforcement from top of the cross-section:

$$d_{1,\text{bottom}} := \frac{\phi}{2} + \text{cover} + \frac{\phi}{2} = 46 \cdot \text{mm}$$

$$d_{2,\text{bottom}} := d_{1,\text{bottom}}$$

$$tp_{2\text{layers},\text{bottom}} := \left( \frac{d_{1,\text{bottom}}}{2} \right) \cdot \frac{n_{\text{layer1},\text{bottom}} + n_{\text{layer2},\text{bottom}}}{n} = 23 \cdot \text{mm}$$

$$tp_{3\text{layers},\text{bottom}} := \left( \frac{d_{1,\text{bottom}} + d_{2,\text{bottom}}}{2} \right) \cdot \frac{n_{\text{layer1},\text{bottom}} + n_{\text{layer2},\text{bottom}} + n_{\text{layer3},\text{bottom}}}{n} = 46 \cdot \text{mm}$$

$$d := \begin{cases} h - \text{cover} - \frac{\phi}{2} - \phi_w & \text{if } \text{layers}_{\text{bottom}} = 1 \\ h - \text{cover} - \frac{\phi}{2} - \phi_w - tp_{2\text{layers},\text{bottom}} & \text{if } \text{layers}_{\text{bottom}} = 2 \\ h - \text{cover} - \frac{\phi}{2} - \phi_w - tp_{3\text{layers},\text{bottom}} & \text{if } \text{layers}_{\text{bottom}} = 3 \\ \text{break otherwise} \end{cases} = 431 \cdot \text{mm}$$

C-C distance between rebars:

$$cc_{\text{bottom}} := \frac{\left( b - \text{cover} \cdot 2 - \frac{\phi}{2} \cdot 2 - \phi_w \cdot 2 \right)}{(n - 1)} = 29.714 \cdot \text{mm}$$

Top Reinforcement: Reinforcing steel B500B in bending (compression)

Strength:

Characteristic value:

$$f'_{yk} := 500 \text{MPa}$$

Design value:

$$f'_{yd} := \frac{f'_{yk}}{\gamma_{\text{steel}}} = 434.783 \cdot \text{MPa}$$

Modulus of elasticity:

$$E'_s := 200 \text{GPa}$$

Yield strain:

$$\epsilon'_{sy} := \frac{f'_{yd}}{E'_s} = 0.217 \cdot \%$$

Diameter:

$$\phi' := 16 \text{mm}$$

Area of one bar:

$$A'_{si} := \left(\frac{\phi'}{2}\right)^2 \cdot \pi = 201.062 \cdot \text{mm}^2$$

Number of reinforcement layers:

$$\text{layers} := 1$$

Number of bars:

$$n_{\text{layer1}} := 4$$

$$n_{\text{layer2}} := 0$$

$$n_{\text{layer3}} := 0$$

$$n' := n_{\text{layer1}} + n_{\text{layer2}} + n_{\text{layer3}} = 4$$

Total area of reinforcement:

$$A'_s := n' \cdot A'_{si} = 8.042 \times 10^{-4} \text{ m}^2$$

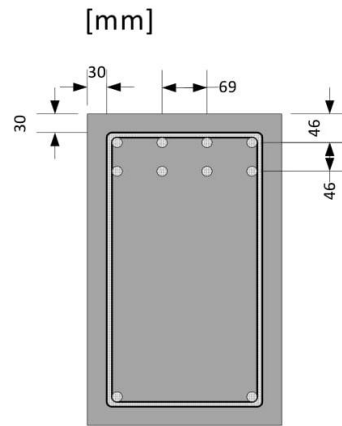


FIGURE 4: Top reinforcement

Distance to compressive reinforcement from top of the cross-section:

$$d_1 := \frac{\phi'}{2} + \text{cover} + \frac{\phi'}{2} = 46 \cdot \text{mm}$$

$$d_2 := d_1$$

$$tp_{2\text{layers}} := \left(\frac{d_1}{2}\right) \cdot \frac{n_{\text{layer1}} + n_{\text{layer2}}}{n'} = 23 \cdot \text{mm}$$

$$tp_{3\text{layers}} := \left(\frac{d_1 + d_2}{2}\right) \cdot \frac{n_{\text{layer1}} + n_{\text{layer2}} + n_{\text{layer3}}}{n'} = 46 \cdot \text{mm}$$

$$d' := \begin{cases} \text{cover} + \phi_w + \frac{\phi'}{2} & \text{if layers} = 1 \\ \text{cover} + \phi_w + \frac{\phi'}{2} + tp_{2\text{layers}} & \text{if layers} = 2 \\ \text{cover} + \phi_w + \frac{\phi'}{2} + tp_{3\text{layers}} & \text{if layers} = 3 \\ \text{break} & \text{otherwise} \end{cases} = 46 \cdot \text{mm}$$

## CFRP laminates

Partial safety coefficient/factor:

$$\gamma_f := 1.0$$

Thickness:

$$t_f := 1.2 \text{ mm} \quad (\text{Usually between } 1.2 - 2.0 \text{ mm})$$

Width:

$$b_f := 50 \text{ mm} \quad (\text{Usually between } 50 - 80 \text{ mm})$$

Cross-sectional area of one laminate:

$$A_{if} := t_f \cdot b_f = 60 \cdot \text{mm}^2$$

Strength:

Characteristic value:

$$f_f := 3000 \text{ MPa} \quad (\text{Usually between } 3000\text{-}3200 \text{ MPa})$$

Design value

$$f_{fd} := \gamma_f \cdot 3000 \text{ MPa} = 3 \times 10^3 \cdot \text{MPa}$$

Modulus of elasticity:

$$E_f := 180 \text{ GPa} \quad (\text{Usually between } 165\text{-}200 \text{ GPa})$$

Ultimate strain:

$$\epsilon_{fu} := 1.5\% \quad (\text{Usually between } 2.5\text{-}3\%)$$

Distance from top of concrete to center of CFRP:

$$d_f := h + \frac{t_f}{2} = 500.6 \cdot \text{mm}$$

Ratio of Elastic modulus:

Steel:

$$\alpha_s := \frac{E_s}{E_{cm}} = 6.061$$

CFRP:

$$\alpha_f := \frac{E_f}{E_{cm}} = 5.455$$

Density:

$$\rho_f := 1800 \frac{\text{kg}}{\text{m}^3} \quad (\text{Usually between } 1750 - 1950 \text{ Kg/m}^3)$$

## Adhesive

Modulus of elasticity:

$$E_a := 5 \text{ GPa}$$

Poisson's ratio:

$$\nu := 0.3$$

Shear modulus:

$$G_a := \frac{E_a}{1 + 2 \cdot \nu} = 3.125 \cdot \text{GPa}$$

☐ DIMENSIONS AND MATERIAL DATA

☑ LOADS AND LOAD COMBINATIONS

### **Table of Contents:**

- Loads from dead-weight
- Live load
- Design load in ULS and SLS
- Resulting design moment and shear force

### **Loads from dead-weight**

Loads that are acting on the beam. A variable part is added to the dead-weight which could represent e.g. a slab.

Load from the beam itself:

$$g_{\text{beam}} := h \cdot b \cdot \rho_c \cdot g = 3.53 \cdot \frac{\text{kN}}{\text{m}}$$

Load from e.g. slab:

$$g_{\text{var}} := 5 \frac{\text{kN}}{\text{m}}$$

### Live load

Distributed load:

$$q := 1 \frac{\text{kN}}{\text{m}}$$

### Design load in ULS and SLS

Load combination of the loads with partial coefficients

Partial coefficients:

$$\gamma_g := 1.35$$

$$\gamma_q := 1.5$$

Design load (ULS):

$$q_{\text{dULS}} := \gamma_g \cdot (g_{\text{beam}} + g_{\text{var}}) + \gamma_q \cdot q = 13.016 \cdot \frac{\text{kN}}{\text{m}}$$

Design load (SLS):

$$q_{\text{dSLS}} := g_{\text{beam}} + g_{\text{var}} + q = 9.53 \cdot \frac{\text{kN}}{\text{m}}$$

### Resulting design moment and shear force

Ultimate Limit State:

$$M_{\text{EdULS}} := \frac{q_{\text{dULS}} \cdot l_{\text{beam}}^2}{8} = 162.7 \cdot \text{kN} \cdot \text{m}$$

$$V_{\text{EdULS}} := \frac{q_{\text{dULS}} \cdot l_{\text{beam}}}{2} = 65.08 \cdot \text{kN}$$

Serviceability Limit State:

$$M_{\text{EdSLS}} := \frac{q_{\text{dSLS}} \cdot l_{\text{beam}}^2}{8} = 119.13 \cdot \text{kN} \cdot \text{m}$$

$$V_{\text{EdSLS}} := \frac{q_{\text{dSLS}} \cdot l_{\text{beam}}}{2} = 47.652 \cdot \text{kN}$$

LOADS AND LOAD COMBINATIONS

REINFORCED CONCRETE

CAPACITY OF THE CONCRETE BEAM STRENGTHENED WITH REINFORCING STEEL ONLY

## Capacity of the RC beam in bending

### Assumed failure mode 1:

Crushing of concrete as well as yielding in the compression steel reinforcement.

Horizontal equilibrium to find x:

Given

$$x_{\text{guess}} := 0.2\text{m}$$

$$\alpha_c \cdot f_{\text{cd}} \cdot b \cdot x_{\text{guess}} + A'_s \cdot f'_{\text{yd}} = A_s \cdot f_{\text{yd}}$$



$$x_{fm1} := \text{Find}(x_{\text{guess}})$$

$$x_{fm1} = 71.949 \cdot \text{mm}$$

Moment equilibrium:

$$M_{Rd1} := A'_s \cdot f'_{yd} \cdot (\beta_c \cdot x_{fm1} - d') + A_s \cdot f_{yd} \cdot (d - \beta_c \cdot x_{fm1}) = 274.867 \cdot \text{kN} \cdot \text{m}$$

$$x := \begin{cases} x & \text{if } x > 0 \\ 0.000001 \text{m} & \text{if } x = 0 \end{cases}$$

$$x_{\text{check}} := \begin{cases} x_{fm1} \cdot (-1) & \text{if } x_{fm1} < 0 \\ x_{fm1} & \text{if } x_{fm1} > 0 \\ 0.000001 \text{m} & \text{if } x_{fm1} = 0 \end{cases}$$

$$x_{fm1} = 0.072 \text{ m}$$

$$x_{\text{check}} = 0.072 \text{ m}$$

Check whether the assumptions are correct:

Condition 1: Yielding in the bottom (tensile) reinforcement

$$\epsilon_{s, fm1} := \frac{d - x_{\text{check}}}{x_{\text{check}}} \cdot \epsilon_{cu} = 1.747 \cdot \%$$

$$\epsilon_{s, fm1} \geq \epsilon_{sy} = 1$$

1 means that it's correct, i.e. that  $\epsilon_s$  is smaller or equal to  $\epsilon_{sy}$ .  
1 = condition fulfilled  
0 = condition unfulfilled.

Condition 2: Yielding in the top (compression) reinforcement

$$\epsilon'_{s, fm1} := \frac{x_{\text{check}} - d'}{x_{\text{check}}} \cdot \epsilon_{cu} = 0.126 \cdot \%$$

$$\epsilon'_{s, fm1} \geq \epsilon_{sy} = 0$$

If these two conditions are not true check below.

$$M_{Rd1} = 274.867 \cdot \text{kN} \cdot \text{m} \quad (\text{From moment equilibrium})$$

$$M_{Rd1 \text{ new}} := \left( \begin{cases} M_{Rd1} & \text{if } \epsilon_{s, fm1} \geq \epsilon_{sy} \wedge \epsilon'_{s, fm1} \geq \epsilon_{sy} \\ 0 & \text{if } \epsilon_{s, fm1} \leq \epsilon_{sy} \vee \epsilon'_{s, fm1} \leq \epsilon_{sy} \end{cases} \right) = 0 \cdot \text{kN} \cdot \text{m}$$

Ductility check:

$$\text{ductility} := \frac{x_{\text{check}}}{d} = 0.167$$

$$\text{ductility} < 0.45 = 1 \quad (\text{Should be less than 0.45})$$

### Assumed failure mode 2:

Crushing of concrete without yielding in the compression steel reinforcement

Horizontal equilibrium to find x:

Given

$$x_{\text{guess, fm2}} := 0.1 \text{m}$$

$$\alpha_c \cdot f_{cd} \cdot b \cdot x_{\text{guess, fm2}} + A'_s \cdot \left( \frac{x_{\text{guess, fm2}} - d'}{x_{\text{guess, fm2}}} \right) \cdot \epsilon_{cu} \cdot E'_s = A_s \cdot f_{yd}$$

$$x_{fm2} := \text{Find}(x_{\text{guess, fm2}})$$

$$x_{fm2} = 88.363 \cdot \text{mm}$$

compared to  $d' = 0.046\text{m}$

$$x_{\text{check, fm2}} := \begin{cases} x_{\text{fm2}} \cdot (-1) & \text{if } x_{\text{fm2}} < 0 \\ x_{\text{fm2}} & \text{if } x_{\text{fm2}} > 0 \\ 0.000001\text{m} & \text{if } x_{\text{fm2}} = 0 \end{cases}$$

Moment equilibrium:

$$M_{\text{Rd2}} := A'_s \cdot f'_{\text{yd}} (\beta_c \cdot x_{\text{fm2}} - d') + A_s \cdot f_{\text{yd}} (d - \beta_c \cdot x_{\text{fm2}}) = 272.479 \cdot \text{kN}\cdot\text{m}$$

Check if the assumption is correct

Condition 1: Yielding in the bottom (tensile) reinforcement

$$\epsilon_{\text{s, fm2}} := \frac{d - x_{\text{fm2}}}{x_{\text{fm2}}} \cdot \epsilon_{\text{cu}} = 1.357\%$$

$$\epsilon_{\text{s, fm2}} \geq \epsilon_{\text{sy}} = 1$$

Condition 2: Yielding in the top (compression) reinforcement

$$\epsilon'_{\text{s, fm2}} := \frac{x_{\text{fm2}} - d'}{x_{\text{fm2}}} \cdot \epsilon_{\text{cu}} = 1.678 \times 10^{-3}$$

$$\epsilon'_{\text{s, fm2}} \geq \epsilon_{\text{sy}} = 0$$

Moment resistance

$$M_{\text{Rd2}} = 272.479 \cdot \text{kN}\cdot\text{m} \quad (\text{From moment equilibrium})$$

$$M_{\text{Rd2new}} := \begin{cases} 0 & \text{if } M_{\text{Rd1new}} > 0 \\ M_{\text{Rd2}} & \text{if } M_{\text{Rd1new}} = 0 \end{cases} = 272.479 \cdot \text{kN}\cdot\text{m}$$

$$M_{\text{Rd}} := \max(M_{\text{Rd1}}, M_{\text{Rd2}}) = 274.867 \cdot \text{kN}\cdot\text{m}$$

Ductility check:

$$\text{ductility}_{\text{fm2}} := \frac{x_{\text{fm2}}}{d} = 0.205$$

$$\text{ductility}_{\text{fm2}} < 0.45 = 1 \quad (\text{Should be less than 0.45})$$

## Shear capacity of RC beam

Shear failure categories:

Web shear failure

Bending shear failure

Compressive failure in web

For yielding shear reinforcement:

$$V_{\text{Rd,s}} = n \cdot f_{\text{ywd}} \cdot A_{\text{sw}} = \frac{z \cdot \cot(\theta)}{s_w} \cdot f_{\text{ywd}} \cdot A_{\text{sw}}$$

Design value for steel stirrups (defined previously):

$$f_{\text{ywd}} = 434.783 \cdot \text{MPa}$$

Cross-section area of steel stirrup (defined previously):

$$A_{\text{sw}} = 100.531 \cdot \text{mm}^2$$

$$z := d - d' = 385 \cdot \text{mm}$$

$$s_w = 200 \text{ mm}$$

$$\theta := 45 \text{ deg} \quad \text{Chosen value between 21.8-45 degrees}$$

$$V_{Rd,s} := \frac{z \cdot \cot(\theta)}{s_w} \cdot f_{ywd} \cdot A_{sw} = 84.14 \cdot \text{kN}$$

### Compressive failure in web

According to EC2 the shear capacity for compressive failure in the web:

$$V_{Rd,max} = \alpha_{cw} \cdot b_w \cdot z \cdot v_1 \cdot f_{cd} \cdot \frac{1}{\cot(\theta) + \tan(\theta)}$$

with:

$$\alpha_{cw} := 1.0 \quad \text{No compressive normal force}$$

$$b_w := b \quad \text{Smallest cross section width between compressive and tensile zone}$$

$$v_1 := 0.6 \cdot \left( 1 - \frac{f_{ck}}{250 \text{ MPa}} \right) = 0.528$$

$$z := 0.9d = 0.388 \text{ m}$$

$$F_{cw} := \frac{\sigma_{cw} \cdot b_w \cdot 0.9 \cdot d}{\sqrt{2}}$$

$$V_{Rd,max} := \alpha_{cw} \cdot b_w \cdot z \cdot v_1 \cdot f_{cd} \cdot \frac{1}{\cot(\theta) + \tan(\theta)} = 614.434 \cdot \text{kN}$$

$$V_{Ed,ULS} = 65.08 \cdot \text{kN}$$

### Check minimum amount of shear reinforcement

$$\rho_{w,min} := 0.08 \cdot \frac{\sqrt{\frac{f_{ck}}{\text{MPa}}}}{f_{yk} \cdot \frac{1}{\text{MPa}}} = 8.764 \times 10^{-4}$$

$$\alpha := 90 \text{ deg}$$

$$\rho_w := \frac{A_{sw}}{s_w \cdot b_w \cdot \sin(\alpha)} = 1.676 \times 10^{-3}$$

$$\rho_w \geq \rho_{w,min} = 1$$

### Check maximum distance between stirrups (shear reinforcement)

$$s_{l,max} := 0.75 \cdot d \cdot (1 + \cot(\alpha)) = 0.323 \text{ m}$$

$$s_w \leq s_{l,max} = 1$$

$$s_{t,max} := \min(0.75d, 600 \text{ mm}) = 0.323 \text{ m}$$

$$s_t := b - 2 \text{ cover} = 0.24 \text{ m}$$

$$s_t \leq s_{t,max} = 1$$

$$V_{Rd} := \min(V_{Rd,s}, V_{Rd,max}) = 84.14 \cdot \text{kN}$$

## CRACKING LOAD & MOMENT OF INERTIA STATE I & II

Simple calculation of cracking load:

$$I_I := \frac{b \cdot h^3}{12} = 3.125 \times 10^{-3} \text{ m}^4$$

$$M_{cr} := \frac{f_{ctd} \cdot I_I}{\frac{h}{2}} = 24.167 \cdot \text{kN} \cdot \text{m}$$

$$f_{ctd} = 1.933 \cdot \text{MPa}$$

$$\sigma_c := \frac{M_{cr}}{I_I} \cdot \frac{h}{2} = 1.933 \times 10^6 \text{ Pa}$$

$$\sigma_m := \left( 0.6 + \frac{0.4}{\sqrt{\frac{h}{m}}} \right) \cdot f_{ctm} = 3.119 \times 10^6 \text{ Pa}$$

$$M_{EdULS} = 162.7 \cdot \text{kN} \cdot \text{m}$$

Moment of inertia in state II

To find x:

Given

$$x_{guess} := 0.1 \text{ m}$$

$$b \cdot x_{guess} \cdot \frac{x_{guess}}{2} + A'_s \cdot (\alpha_s - 1) \cdot (x_{guess} - d') = \alpha_s \cdot A_s \cdot (d - x_{guess})$$

$$x := \text{Find}(x_{guess})$$

$$x = 131.084 \cdot \text{mm} \quad x_{sls} := x = 0.131 \text{ m}$$

Moment of inertia.

$$I_{II} := \frac{b \cdot x^3}{12} + b \cdot x \cdot \left( \frac{x}{2} \right)^2 + (\alpha_s - 1) \cdot A'_s \cdot (x - d')^2 + \alpha_s \cdot A_s \cdot (d - x)^2 = 1.105 \times 10^{-3} \text{ m}^4$$

## STRESSES AND STRAINS AT MOMENT OF STRENGTHENING

The bending moment that is acting on the beam during the strengthening  
Here it is just set to a third of the service limit load

$$M_{02} := M_{EdSLs} \cdot 0.3 = 35.739 \cdot \text{kN} \cdot \text{m}$$

Stress & strain in the tensile steel:

$$\sigma_s := \alpha_s \cdot \frac{M_{02}}{I_{II}} \cdot (d - x) = 58.766 \cdot \text{MPa}$$

$$\epsilon_s := \frac{\sigma_s}{E_s} = 2.938 \times 10^{-4}$$

Stress & strain in the compressive steel:

$$\sigma'_s := \alpha_s \cdot \frac{M_{02}}{I_{II}} \cdot (x - d') = 16.671 \cdot \text{MPa}$$

$$\epsilon'_s := \frac{\sigma'_s}{E'_s} = 8.336 \times 10^{-5}$$

Stress & strain in the compressed concrete

$$\sigma_{c,over} := \frac{M_{02}}{I_{II}} \cdot x = 4.238 \cdot \text{MPa}$$

$$\epsilon_{c,over} := \frac{\sigma_{c,over}}{E_{cm}} = 1.284 \times 10^{-4}$$

Stress & strain in the lower face of the beam - "fictive concrete" (it is cracked)

$$\sigma_{u0} := \frac{M_{02}}{I_{II}} \cdot (h - x) = 11.927 \cdot \text{MPa}$$

$$\epsilon_{u0} := \frac{\sigma_{u0}}{E_{cm}} = 0.036 \cdot \%$$

REINFORCED CONCRETE

UNPRESTRESSED CFRP

## NEED OF CFRP TO REACH DESIRABLE STRENGTH

### *A rough estimation of the amount of CFRP needed*

The CFRP should be able to take up the following bending moment:

$$\Delta M = M - 0.9 \cdot d \cdot F_s = 0.9 \cdot h \cdot F_f$$

Old ULS limit and capacity of the beam:

$$M_{Rd} = 274.867 \cdot \text{kN} \cdot \text{m}$$

$$M_{EdULS} = 162.7 \cdot \text{kN} \cdot \text{m}$$

Should the beam be strengthened against the old limit or the old capacity, choose.

The beam should be stronger than the old beam capacity:

$$\Delta M := 30\% \cdot M_{Rd} = 8.246 \times 10^4 \text{ J}$$

New capacity:

$$M_{Rd,NEW} := M_{Rd} + \Delta M = 357.327 \cdot \text{kN} \cdot \text{m}$$

The beam should be

$$\Delta M := 30\% \cdot M_{EdULS} = \blacksquare \cdot \text{kN} \cdot \text{m}^{\blacksquare}$$

New capacity:

$$M_{Rd,NEW} := M_{EdULS} + \Delta M = \blacksquare \cdot \text{kN} \cdot \text{m}^{\blacksquare}$$

Set a limit for the laminate strain:

$$\epsilon_f := 0.5\%$$

Then the following CFRP area is obtained:

$$A_f := \frac{\Delta M}{0.9 \cdot h \cdot \epsilon_f \cdot E_f} = 2.036 \times 10^{-4} \text{ m}^2$$

Cross-sectional area of one laminate:

$$A_{if} = 60 \cdot \text{mm}^2$$

Number of laminates needed:

$$n_f := \text{ceil} \left( \frac{A_f}{A_{if}} \right) = 4$$

Total area of CFRP:

$$A_f := A_{if} \cdot n_f = 240 \cdot \text{mm}^2$$

## Determination of failure mode

Investigate which type of failure that is most likely to occur.

Assume if the compressive steel is going to yield, if it does - use  $\rho_{f1}$ , if it does not - use  $\rho_{f2}$

Also assume which mode it is going to be and calculate the corresponding strengthening ratios  $\rho_{fu}$ ,  $\rho_{fn}$ ,  $\rho_{fo}$  to check if the assumption is correct.

### ---- $\rho_{f1}$ ----

Strain compatibility for the cross-section gives strain in the laminate:

$$\epsilon_f := \frac{h-d}{d} \cdot \epsilon_{cu} + \frac{h}{d} \cdot \epsilon_{sy} - \epsilon_{u0} = 2.721 \times 10^{-3}$$

$$\alpha_c \cdot x_{\text{guess}} \cdot f_{cd} \cdot b = A_s \cdot f_{yd} - A'_s \cdot f'_{yd} + A_f \cdot \epsilon_f \cdot E_f$$

To be able to determine the type of failure mode which is governing, several comparative parameters,  $\rho_f$ , needs to be calculated.

$$v_1 := \frac{\epsilon_{cu}}{\epsilon_{cu} + \epsilon_{sy}} = 0.617$$

Reinforcement ratio:

$$\rho_s := \frac{A_s}{b \cdot d} = 0.012 \quad \rho'_s := \frac{A'_s}{b \cdot d} = 6.22 \times 10^{-3}$$

$$\rho_{f1} := \frac{\alpha_c \cdot v_1 \cdot f_{cd} - \rho_s \cdot f_{yd} + \rho'_s \cdot f'_{yd}}{\left[ \epsilon_{cu} \cdot \left( \frac{h}{v_1 \cdot d} - 1 \right) - \epsilon_{u0} \right] \cdot E_f} = 0.015$$

### ---- $\rho_{f2}$ ----

In the case where compression steel reinforcement does not yield, an equilibrium equation gives the following:

$$\alpha_c \cdot x \cdot f_{cd} \cdot b = A_s \cdot f_{yd} - A'_s \cdot \epsilon'_s \cdot E'_s + A_f \cdot \epsilon_f \cdot E_f$$

The strain in the compression steel reinforcement is expressed as the following:

$$\epsilon'_s := \left( 1 - \frac{d'}{d \cdot v_1} \right) \epsilon_{cu} = 0.289 \cdot \% \quad \epsilon_{sy} = 0.217 \cdot \%$$

$$\rho_{f2} := \frac{\alpha_c \cdot v_1 \cdot f_{cd} - \rho_s \cdot f_{yd} + \rho'_s \cdot \epsilon_{cu} \cdot \left( 1 - \frac{d'}{d \cdot v_1} \right) \cdot E'_s}{\left[ \epsilon_{cu} \cdot \left( \frac{h}{v_1 \cdot d} - 1 \right) - \epsilon_{u0} \right] \cdot E_f} = 0.017$$

### Strengthening ratios

Normally-reinforced strengthened cross-section

With normal or under-reinforced cross-sections, the composite sheet fails before the concrete is crushed. An equilibrium equation gives:

$$\alpha_c \cdot x \cdot f_{cd} \cdot b = A_s \cdot f_{yd} - A'_s \cdot f'_{yd} + A_f \cdot \epsilon_f \cdot E_f$$

To calculate the strengthening ratio an iterative process is necessary. Assume first a stress level in the compressed steel reinforcement and calculate the distance to the neutral layer. Verify the compressive steel strain using the equations for stress and strain below. Finally use the equation for  $\rho_{fu}$ .

$$f'_s := 163.27 \text{ MPa}$$

Given

$$x_{\text{guess}} := 0.1 \text{ m}$$

$$\alpha_c \cdot x_{\text{guess}} \cdot f_{cd} \cdot b = A_s \cdot f_{yd} - A'_s \cdot f'_s + A_f \cdot \epsilon_f \cdot E_f$$

$$x := \text{Find}(x_{\text{guess}})$$

$$x = 141.065 \cdot \text{mm}$$

From which the strengthening ratio  $\rho_{fu}$  can be expressed as:

$$\rho_{fu} := \frac{\alpha_c \cdot f_{cd} \cdot \frac{x}{d} - \rho_s \cdot f_{yd} + \rho'_s \cdot f'_{yd}}{\epsilon_f \cdot E_f} = 5.304 \times 10^{-3}$$

where the strain and stress in the compressed steel reinforcement can be verified by:

$$\epsilon'_s := \frac{x - d'}{h - x} \cdot (\epsilon_f + \epsilon_{u0}) = 0.082 \cdot \%$$

$$\epsilon'_{sy} = 0.217 \cdot \%$$

$$\sigma'_s := \epsilon'_s \cdot E_s = 163.27 \cdot \text{MPa}$$

Compare  $\sigma'_s = 163.27 \text{ MPa}$  with initial assumption

$$f'_s = 163.27 \text{ MPa}$$

### Balanced strengthened cross-section

With so-called balanced cross-sections, the concrete is crushed at the same time as the composite laminate fails. An equilibrium equation gives:

$$\alpha_c \cdot x \cdot f_{cd} \cdot b = A_s \cdot f_{yd} - A'_s \cdot \epsilon'_s \cdot E'_s + A_f \cdot \epsilon_f \cdot E_f$$

The term  $v_2$  which is needed for the expression for the compression steel:

Note that  $\epsilon_{fu}$  is used because the laminate is at the limit where it fails.

$$v_2 := \frac{\epsilon_{cu}}{\epsilon_{fu} + \epsilon_{u0} + \epsilon_{cu}} = 0.186$$

Strain in the compression steel reinforcement is expressed as:

$$\epsilon'_s := \left(1 - \frac{d'}{h \cdot v_2}\right) \cdot \epsilon_{cu} = 0.176 \cdot \% \quad \epsilon'_{sy} = 0.217 \cdot \%$$

$$\sigma'_s := \epsilon'_s \cdot E'_s = 352.95 \cdot \text{MPa}$$

$$\rho_{f1} := \frac{\alpha_c \cdot f_{cd} \cdot \frac{h \cdot v_2}{d} - \rho_s \cdot f_{yd} + \rho'_s \cdot \epsilon_{cu} \left(1 - \frac{d'}{h \cdot v_2}\right) \cdot E'_s}{\epsilon_{fu} \cdot E_f} = 1.015 \times 10^{-4}$$

### Over-reinforced strengthened cross-section

In and over-reinforced cross-section the concrete is crushed without the composite laminate failing. An equilibrium equation gives:

$$\alpha_c \cdot x \cdot f_{cd} \cdot b = A_s \cdot f_{yd} - A'_s \cdot \epsilon'_s \cdot E'_s + A_f \cdot \epsilon_f \cdot E_f$$

The laminate strain and the compression strain in the steel reinforcement can be expressed as:

$$v_3 := \frac{\epsilon_{cu}}{\epsilon_{cu} - \epsilon'_{sy}} = 2.639$$

$$\epsilon_f := \left( \frac{h}{d' \cdot v_3} - 1 \right) \cdot \epsilon_{cu} - \epsilon_{u0} = 0.011$$

$$\epsilon'_s := \epsilon_{cu} \left( 1 - \frac{1}{v_3} \right) = 0.217 \cdot \%$$

$$\rho_{f0} := \frac{\alpha_c \cdot f_{cd} \cdot \frac{d' \cdot v_3}{d} - \rho_s \cdot f_{yd} + \rho'_s \cdot \epsilon_{cu} \left( 1 - \frac{1}{v_3} \right) \cdot E'_s}{\left[ \epsilon_{cu} \left( \frac{h}{d' \cdot v_3} - 1 \right) - \epsilon_{u0} \right] \cdot E_f} = 9.787 \times 10^{-4}$$

#### 1. Failure in laminate with yielding in the compression steel reinforcement

$$\rho_{fu} \leq \rho_{f1} \leq \rho_{f0} = 0$$

#### 2. Failure in laminate without yielding in the compression steel reinforcement

$$\rho_{f2} \leq \rho_{fu} \wedge \rho_{f0} = 0$$

#### 3. Crushing of concrete as well as yielding in the compression steel reinforcement

$$\rho_{f1} \geq \rho_{f0} \wedge \rho_{f0} = 1$$

#### 4. Crushing of concrete without yielding in the compression steel reinforcement

$$\rho_{f0} \leq \rho_{f2} \leq \rho_{f0} = 0$$

## CAPACITY OF THE CONCRETE BEAM STRENGTHENED WITH BOTH STEEL AND CFRP (non-prestressed)

### The moment capacity depends on failure type

#### 1. Failure in laminate with yielding in the compression steel reinforcement

Horizontal equilibrium gives x:

$$x := \frac{A_s \cdot f_{yd} + \epsilon_{fu} \cdot E_f \cdot A_f - A'_s \cdot f'_{yd}}{\alpha_c \cdot f_{cd} \cdot b} = 0.205 \text{ m}$$



$$M_{Rd1} := A'_s \cdot f'_{yd} \cdot (\beta_c \cdot x - d') + A_s \cdot f_{yd} \cdot (d - \beta_c \cdot x) + \epsilon_{fu} \cdot E_f \cdot A_f \cdot (h - \beta_c \cdot x) = 524.134 \cdot \text{kN} \cdot \text{m}$$

Check if the assumption is correct

$$\epsilon'_s := \frac{x - d'}{h - x} \cdot \epsilon_{fu} = 8.107 \times 10^{-3}$$

$$\epsilon'_s \geq \epsilon_{sy} = 1$$

## 2. Failure in laminate without yielding in the compression steel reinforcement

Initial strain is needed:

$$\epsilon_{u0} = 3.614 \times 10^{-4}$$

Horizontal equilibrium to find x:

Given

$$x_{\text{guess}} := 0.1\text{m}$$

$$\alpha_c \cdot f_{cd} \cdot b \cdot x_{\text{guess}} + A'_s \cdot \left( \frac{x_{\text{guess}} - d'}{h - x_{\text{guess}}} \right) \cdot (\epsilon_{fu} + \epsilon_{u0}) \cdot E'_s = A_s \cdot f_{yd} + \epsilon_{fu} \cdot E_f \cdot A_f$$

$$x := \text{Find}(x_{\text{guess}})$$

$$x = 141.606 \cdot \text{mm} \quad \text{compared to } d' = 0.046\text{m}$$

Moment equilibrium:

$$M_{Rd2} := A'_s \cdot \left( \frac{x - d'}{h - x} \right) \cdot (\epsilon_{fu} + \epsilon_{u0}) \cdot E'_s \cdot (\beta_c \cdot x - d') + A_s \cdot f_{yd} \cdot (d - \beta_c \cdot x) \dots = 554.557 \cdot \text{kN} \cdot \text{m} \\ + \epsilon_{fu} \cdot E_f \cdot A_f \cdot (h - \beta_c \cdot x)$$

Check if the assumption is correct

$$\epsilon_s := \frac{d - x}{x} \cdot \epsilon_{cu} = 7.153 \times 10^{-3}$$

$$\epsilon_s \geq \epsilon_{sy} = 1$$

$$\epsilon_s := \frac{d - x}{h - x} \cdot \epsilon_{fu} = 0.012$$

## 3. Crushing of concrete as well as yielding in the compression steel reinforcement

Horizontal equilibrium to find x:

Given

$$x_{\text{guess}} := 0.2\text{m}$$

$$\alpha_c \cdot f_{cd} \cdot b \cdot x_{\text{guess}} + A'_s \cdot f'_{yd} = A_s \cdot f_{yd} + \left( \frac{h - x_{\text{guess}}}{x_{\text{guess}}} \cdot \epsilon_{cu} - \epsilon_{u0} \right) \cdot E_f \cdot A_f$$

$$x := \text{Find}(x_{\text{guess}})$$

$$x = 144.945 \cdot \text{mm}$$

Moment equilibrium:

$$M_{Rd3} := A'_s \cdot f'_{yd} \cdot (\beta_c \cdot x - d') + A_s \cdot f_{yd} \cdot (d - \beta_c \cdot x) \dots = 420.239 \cdot \text{kN} \cdot \text{m} \\ + \left( \frac{h - x}{x} \cdot \epsilon_{cu} - \epsilon_{u0} \right) \cdot E_f \cdot A_f \cdot (h - \beta_c \cdot x)$$

Check if the assumption is correct

$$\epsilon_s := \frac{d-x}{x} \cdot \epsilon_{cu} = 6.907 \times 10^{-3}$$

$$\epsilon_s \geq \epsilon_{sy} = 1$$

$$\epsilon'_s := \frac{x-d'}{x} \cdot \epsilon_{cu} = 2.389 \times 10^{-3}$$

$$\epsilon'_s \geq \epsilon_{sy} = 1$$

#### 4. Failure mode assumed: Crushing of concrete without yielding in the compression steel reinforcement

Horizontal equilibrium to find x:

Given

$$x_{\text{guess}} := 0.2\text{m}$$

$$\alpha_c \cdot f_{cd} \cdot b \cdot x_{\text{guess}} + A'_s \cdot \left( \frac{x_{\text{guess}} - d'}{x_{\text{guess}}} \right) \cdot E'_s = A_s \cdot f_{yd} + \left( \frac{h - x_{\text{guess}}}{x_{\text{guess}}} \cdot \epsilon_{cu} - \epsilon_{u0} \right) \cdot E_f \cdot A_f$$

$$x := \text{Find}(x_{\text{guess}})$$

$$x = 46.559 \cdot \text{mm} \quad \text{compared to } d' = 0.046\text{m}$$

Moment equilibrium:

$$M_{Rd4} := \left( \frac{x-d'}{x} \cdot \epsilon_{cu} \right) \cdot A'_s \cdot E'_s \cdot (\beta_c \cdot x - d') + A_s \cdot f_{yd} \cdot (d - \beta_c \cdot x) \dots = 987.947 \cdot \text{kN} \cdot \text{m} \\ + \left( \frac{h-x}{x} \cdot \epsilon_{cu} - \epsilon_{u0} \right) \cdot E_f \cdot A_f \cdot (h - \beta_c \cdot x)$$

Check if the assumption is correct

$$\epsilon_s := \frac{d-x}{x} \cdot \epsilon_{cu} = 0.029$$

$$\epsilon_s \geq \epsilon_{sy} = 1$$

$$\epsilon'_s := \frac{x-d'}{x} \cdot \epsilon_{cu} = 4.2 \times 10^{-5}$$

$$\epsilon_{cu} - \frac{d'}{d} \cdot (\epsilon_s + \epsilon_{cu}) = 4.2 \times 10^{-5}$$

$$\epsilon_f := \left( \frac{h-d}{d} \right) \epsilon_{cu} + \frac{h}{d} \cdot \epsilon_s - \epsilon_{u0} = 0.034$$

$$\epsilon_{cu} - \frac{d'}{h} \cdot (\epsilon_f + \epsilon_{cu} + \epsilon_{u0}) = 4.2 \times 10^{-5}$$

## CONTROL OF STRESSES AND STRAINS

Given

$$x_{\text{guess}} := 0.1\text{m}$$

$$b \cdot x_{\text{guess}} \cdot \frac{x_{\text{guess}}}{2} + A'_s \cdot (\alpha_s - 1) \cdot (x_{\text{guess}} - d') = \alpha_s \cdot A_s \cdot (d - x_{\text{guess}}) + \alpha_f \cdot A_f \cdot (h - x_{\text{guess}})$$

$$x := \text{Find}(x_{\text{guess}})$$

$$x = 139.746 \cdot \text{mm}$$

Area for the strengthened cross-section in state II:

$$A_{II} := b \cdot x + A'_s \cdot (\alpha_s - 1) + \alpha_s \cdot A_s + \alpha_f \cdot A_f = 0.057 \text{ m}^2$$

Moment of inertia for the strengthened cross-section in State II:

$$I_{II} := \frac{b \cdot x^3}{12} + b \cdot x \cdot \left(\frac{x}{2}\right)^2 + \alpha_s \cdot A_s \cdot (d - x)^2 + (\alpha - 1) \cdot A'_s \cdot (x - d)^2 \dots = 1.274 \times 10^{-3} \text{ m}^4$$

$$+ \alpha_f \cdot A_f \cdot (h - x)^2$$

$$M_{Rd} = 274.867 \cdot \text{kN} \cdot \text{m}$$

$$M_{02} := M_{Rd} \cdot 0.7 \cdot 1.5 - M_{EdSLS} = 169.481 \cdot \text{kN} \cdot \text{m}$$

$$\sigma_{co2} := \frac{M_{02}}{I_{II}} \cdot x = 18.593 \cdot \text{MPa}$$

$$\sigma_{s2} := \alpha_s \frac{M_{02}}{I_{II}} \cdot (d - x) = 234.86 \cdot \text{MPa}$$

$$\sigma_{f2} := \alpha_f \frac{M_{02}}{I_{II}} \cdot (h - x) = 261.45 \cdot \text{MPa}$$

The contribution from the remaining load must also be added i.e. the total stress in the reinforcement in the SLS becomes:

$$\sigma_{c,over} = 4.238 \times 10^6 \text{ Pa}$$

$$\sigma_{cotot} := \sigma_{co2} + \sigma_{c,over} = 22.831 \cdot \text{MPa}$$

$$\sigma_s = 5.877 \times 10^7 \text{ Pa}$$

$$\sigma_{s,tot} := \sigma_s + \sigma_{s2} = 293.626 \cdot \text{MPa}$$

$$\sigma_f := \sigma_{f2} = 261.45 \cdot \text{MPa}$$

The strain in the laminate in the service limit state can be calculated according to:

$$\epsilon_f := \epsilon_{cu} \left( \frac{h}{x} - 1 \right) - \epsilon_{u0} = 8.661 \times 10^{-3}$$

UNPRESTRESSED CFRP



## **Appendix C**

### **Hand calculations for the temporary prestressing support**

Appendix C contains hand calculations for the temporary prestressing support. The number and dimensions of the bolts that are needed to attach it to the concrete are investigated. Bolt spacing and edge/end distance, shear resistance, bearing resistance and also an approximate value for the anchorage force is calculated. This is done as a first step in the support design.

## Appendix C: Temporary prestressing support

### *How many bolts are needed (approximately based on yield strength)*

Applied load:  $F_{Ed} := 100\text{kN}$

Plate thickness:  $t_{\text{plate}} := 10\text{mm}$

Number of bolts:  $n_{\text{bolts}} := 4$

Diameter of bolt:  $d_{\text{bolts}} := 20\text{mm}$

Area of bolts:  $A_{\text{bolts}} := n_{\text{bolts}} \cdot \frac{\pi \cdot (d_{\text{bolts}})^2}{4} = 1.257 \times 10^3 \cdot \text{mm}^2$

Steel yield strength (S355):  $f_y := 355\text{MPa}$

$$f_{y,\text{shear}} := \frac{f_y}{\sqrt{3}} = 204.959 \cdot \text{MPa} \quad (\text{Shear strength})$$

Safety factor:  $\gamma_{\text{safety}} := 1.2$  (Is really = 1.0, but we increase it a bit)

Shear design capacity:  $f_{\text{shear.Rd}} := \frac{f_{y,\text{shear}}}{\gamma_{\text{safety}}} = 170.799 \cdot \text{MPa}$

Shear force capacity of all bolts:  $F_{\text{shear.capacity}} := f_{\text{shear.Rd}} \cdot A_{\text{bolts}} = 214.633 \cdot \text{kN}$

Safety factor:  $\frac{F_{\text{shear.capacity}}}{F_{Ed}} = 2.146$

Comments: Using 4 bolts with diameter = 20mm we get approximately double the capacity we need.

### **Minimum holes spacing and edge distance**

(See EC3 p.23: **3.5 Positioning of holes for bolts and rivets**)

Diameter of hole:  $d_0 := d_{\text{bolts}} + 2\text{mm} = 22 \cdot \text{mm}$  Adding 2mm to the hole to be able to accommodate the bolt during installation.

EC3 - Table 3.3:

**End distance  $e_1$ :**

$$\text{Min}_{e1} := 1.2 \cdot d_0 = 26.4 \cdot \text{mm}$$

Steel exposed to the weather or other corrosive influences:

$$\text{Max}_{e1} := 4 \cdot t_{\text{plate}} + 40 \text{mm} = 80 \cdot \text{mm}$$

Steel used unprotected:

$$\text{Max}_{e1.2} := \begin{cases} 8 \cdot t_{\text{plate}} & \text{if } 8t_{\text{plate}} > 125 \text{mm} \\ 125 \text{mm} & \text{otherwise} \end{cases} = 125 \cdot \text{mm}$$

$$e1_{\text{max}} := \max(\text{Max}_{e1}, \text{Max}_{e1.2}) = 125 \cdot \text{mm}$$

**Edge distance  $e_2$ :**

$$\text{Min}_{e2} := 1.2 \cdot d_0 = 26.4 \cdot \text{mm}$$

Steel exposed to the weather or other corrosive influences:

$$\text{Max}_{e2} := 4 \cdot t_{\text{plate}} + 40 \text{mm} = 80 \cdot \text{mm}$$

Steel used unprotected:

$$\text{Max}_{e2.2} := \begin{cases} 8 \cdot t_{\text{plate}} & \text{if } 8t_{\text{plate}} > 125 \text{mm} \\ 125 \text{mm} & \text{otherwise} \end{cases} = 125 \cdot \text{mm}$$

$$e2_{\text{max}} := \max(\text{Max}_{e2}, \text{Max}_{e2.2}) = 125 \cdot \text{mm}$$

**Spacing  $p_1$ :**

$$\text{Min}_{p1} := 2.2 \cdot d_0 = 48.4 \cdot \text{mm}$$

Steel exposed to the weather or other corrosive influences:

$$\text{Max}_{p1} := \begin{cases} 14 \cdot t_{\text{plate}} & \text{if } 14 \cdot t_{\text{plate}} < 200 \text{mm} \\ 200 \text{mm} & \text{otherwise} \end{cases} = 140 \cdot \text{mm}$$

Steel used unprotected:  $t_{\text{min}} := t_{\text{plate}}$

$$\text{Max}_{p1.2} := \begin{cases} 14 \cdot t_{\text{min}} & \text{if } 14 \cdot t_{\text{min}} < 175 \text{mm} \\ 175 \text{mm} & \text{otherwise} \end{cases} = 140 \cdot \text{mm}$$

$$p1_{\max} := \max(\text{Max}_{p1}, \text{Max}_{p1.2}) = 140 \cdot \text{mm}$$

### Spacing $p_2$ :

$$\text{Min}_{p2} := 2.4 \cdot d_0 = 52.8 \cdot \text{mm}$$

Steel exposed to the weather or other corrosive influences:

$$\text{Max}_{p2} := \begin{cases} 14 \cdot t_{\text{plate}} & \text{if } 14 \cdot t_{\text{plate}} < 200 \text{mm} \\ 200 \text{mm} & \text{otherwise} \end{cases} = 140 \cdot \text{mm}$$

Steel used unprotected:

$$\text{Max}_{p2.2} := \begin{cases} 14 \cdot t_{\min} & \text{if } 14 \cdot t_{\min} < 175 \text{mm} \\ 175 \text{mm} & \text{otherwise} \end{cases} = 140 \cdot \text{mm}$$

$$p2_{\max} := \max(\text{Max}_{p2}, \text{Max}_{p2.2}) = 140 \cdot \text{mm}$$

### Final dimensions of plate and box:

$$L_{\text{plate}} := e_1 + \left( \frac{n_{\text{bolts}}}{n_{\text{rows}}} - 1 \right) \cdot p_1 + e_1$$

End distance:  $\text{Min}_{e1} = 26.4 \cdot \text{mm}$   
 $e_1 := 30 \text{mm}$   
 $e1_{\max} = 125 \cdot \text{mm}$

Edge distance:  $\text{Min}_{e2} = 26.4 \cdot \text{mm}$   
 $e_2 := 30 \text{mm}$   
 $e2_{\max} = 125 \cdot \text{mm}$

Spacing  $p_1$ :  $\text{Min}_{p1} = 48.4 \cdot \text{mm}$   
 $p_1 := 140 \text{mm}$   
 $p1_{\max} = 140 \cdot \text{mm}$

Spacing  $p_2$ :  $\text{Min}_{p2} = 52.8 \cdot \text{mm}$   
 $p_2 := 90 \text{mm}$   
 $p2_{\max} = 140 \cdot \text{mm}$

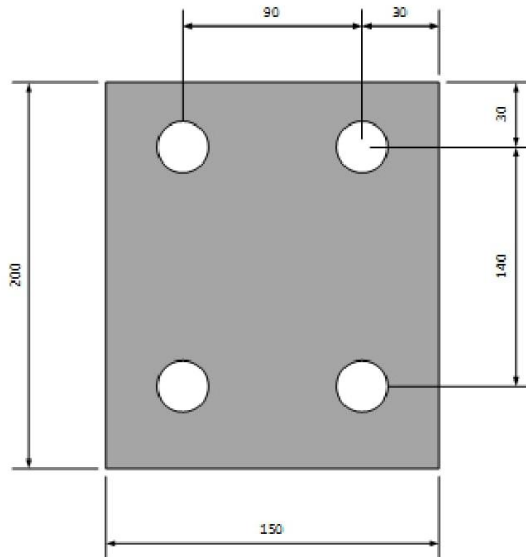
### Plate dimensions:

$$t_{\text{plate}} = 10 \cdot \text{mm}$$

$$b_{\text{plate}} := e_2 + p_2 + e_2 = 150 \cdot \text{mm}$$



$$L_{\text{plate}} := e_1 + p_1 \cdot \left( \frac{n_{\text{bolts}}}{2} - 1 \right) + e_1 = 200 \cdot \text{mm}$$



### Shear resistance according to EC3

(See EC3 p.27: **Table 3.4**)

Ultimate strength:  $f_{u,S355} := 520 \text{MPa}$

Safety factor:  $\gamma_{M2} := 1.25$

Formula:  $F_{V,Rd} = \frac{\alpha_V \cdot f_{ub} \cdot A}{\gamma_{M2}}$      $\alpha_V := 0.5$     to be on the safe side (  $0.5 < 0.6$  )

(index b in  $f_{ub}$  refers to "bolt")

Area of one bolt:  $A_{\text{tensilearea}} := \frac{\pi \cdot (d_{\text{bolts}})^2}{4} = 314.159 \cdot \text{mm}^2$

Shear resistance for one bolt:  $F_{V,Rd} := \frac{0.5 \cdot f_{u,S355} \cdot A_{\text{tensilearea}}}{\gamma_{M2}} = 65.345 \cdot \text{kN}$

Total shear resistance:  $F_{V,Rd,\text{tot}} := n_{\text{bolts}} \cdot F_{V,Rd} = 261.381 \cdot \text{kN}$

Safety factor:  $\frac{F_{V,Rd,\text{tot}}}{F_{Ed}} = 2.614$     even better than the estimated shear resistance calculated at the beginning.

### **Bearing resistance according to EC3**

(See EC3 p.27: **Table 3.4**)

$$\text{Formula: } F_{b,Rd} = \frac{k_1 \cdot \alpha_b \cdot f_u \cdot d \cdot t}{\gamma_{M2}}$$

$$\text{Same steel in plate as in bolt: } f_{ub} := f_{u,S355}$$

$$\alpha_d := \frac{f_{ub}}{f_{u,S355}}$$

$$\alpha_b := \begin{cases} \alpha_d & \text{if } \alpha_d < 1.0 \\ 1.0 & \text{otherwise} \end{cases} = 1$$

#### **Direction of load transfer:**

End bolts:

$$\alpha_{d1.1} := \frac{e_1}{3 \cdot d_0} = 0.455$$

$$\alpha_{b1.1} := \begin{cases} \alpha_{d1.1} & \text{if } \alpha_{d1.1} < 1.0 \\ 1.0 & \text{otherwise} \end{cases} = 0.455$$

Inner bolts:

$$\alpha_{d1.2} := \frac{p_1}{3 \cdot d_0} - \frac{1}{4} = 1.871$$

$$\alpha_{b1.2} := \begin{cases} \alpha_{d1.2} & \text{if } \alpha_{d1.2} < 1.0 \\ 1.0 & \text{otherwise} \end{cases} = 1$$

#### **Perpendicular to the direction of load transfer:**

Edge bolts:

$$k_{1,edge} := \begin{cases} \left( 2.8 \cdot \frac{e_2}{d_0} - 1.7 \right) & \text{if } \left( 2.8 \cdot \frac{e_2}{d_0} - 1.7 \right) < 2.5 \\ 2.5 & \text{otherwise} \end{cases} = 2.118$$

Inner bolts:

$$k_{1,inner} := \begin{cases} \left( 1.4 \cdot \frac{p_2}{d_0} - 1.7 \right) & \text{if } \left( 2.8 \cdot \frac{e_2}{d_0} - 1.7 \right) < 2.5 \\ 2.5 & \text{otherwise} \end{cases} = 4.027$$

**Edge bolt bearing resistance:**

$$\alpha_{b,edge} := \alpha_{b1.1} = 0.455$$

$$F_{b,Rd,edgebolt} := \frac{k_{1,edge} \cdot \alpha_{b,edge} \cdot f_{u,S355} \cdot d_{bolts} \cdot t_{plate}}{\gamma_{M2}} = 80.106 \cdot \text{kN}$$

If all bolts are edge bolts (conservative):

$$F_{b,Rd,edgebolt} \cdot n_{bolts} = 320.423 \cdot \text{kN}$$

**Inner bolt bearing resistance:**

$$\alpha_{b,inner} := \alpha_{b1.2} = 1$$

$$F_{b,Rd,innerbolt} := \frac{k_{1,inner} \cdot \alpha_{b,inner} \cdot f_{u,S355} \cdot d_{bolts} \cdot t_{plate}}{\gamma_{M2}} = 335.069 \cdot \text{kN}$$

***Anchorage length/Length of bolt embedded into the concrete (approximatly using shear area)***

Moment equilibrium (moment due to excentricity of prestressing force):

$$F_{Ed} \cdot e_{prestress} = 2F_{Rd,withdrawal} \cdot x_{bolt}$$

The bolts furthest away from rotation center will be subjected to the greatest moment.

$$x_{bolt} := L_{plate} - 2 \cdot e_1 = 140 \cdot \text{mm} \quad p_1 = 140 \cdot \text{mm}$$

$$\text{Excentricity: } e_{prestress} := t_{plate} + 30.2 \text{mm} = 40.2 \cdot \text{mm}$$

Estimated force which the bolt must resist (or rather the concrete must resist by holding the bolt in space):

$$F_{Rd,withdrawal} := \frac{F_{Ed} \cdot e_{prestress}}{2x_{bolt}} = 14.357 \cdot \text{kN}$$

Shear force acting on the concrete:

$$d_{bolts} = 0.02 \text{ m}$$

Depth of each hole:

$$h_{hole} := 0.15 \text{ m}$$

Area inside each hole:

$$A_{\text{hole}} := d_{\text{bolts}} \cdot \pi \cdot h_{\text{hole}} = 9.425 \times 10^{-3} \text{ m}^2$$

Shear stress:

$$\tau := \frac{F_{\text{Rd.withdrawal}}}{A_{\text{hole}}} = 1.523 \cdot \text{MPa}$$

## Appendix D

### Photographs and results from the experimental verification of the prestressing device

Appendix D contains pictures and results obtained during the experimental verification of the baseline concept of the prestressing device. It is included to prove the functionality and to show how a similar test will be carried out on the refined prestressing device design. At the beginning of the chapter are pictures taken during the experimental verification that show the test setup and failure of tested beams. At the end of the chapter load deflection curves are provided that emphasizes the increased bending stiffness.

#### G.1 Photographs of experiments carried out in advance at Chalmers



*Figure G.1* Picture showing the first prototype of the prestressing device together with the CFRP laminate with adhered steel tabs.



*Figure G.2* Test setup with hydraulic jack mounted and using clamps to hold the device in place.



*Figure G.3 Test setup with four-point bending that was used.*



*Figure G.4 Debonding of the laminate in strengthened beam with unprestressed laminate.*



*Figure G.5 Failure by laminate rupture in the strengthened beam with 85kN prestressing force.*

## **G.2 Results from experiments carried out in advance at Chalmers**

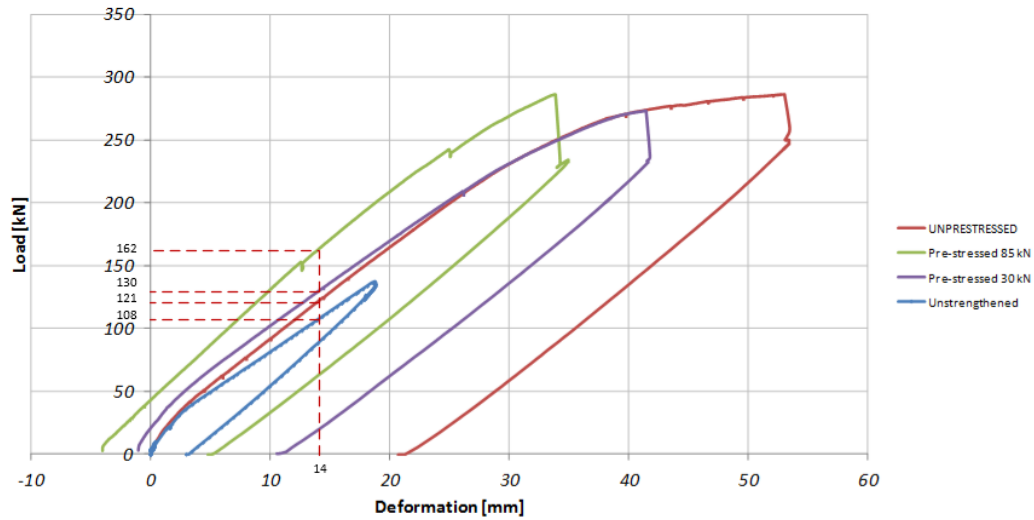


Figure G.6 Load – deflection diagram for the different test-specimens.

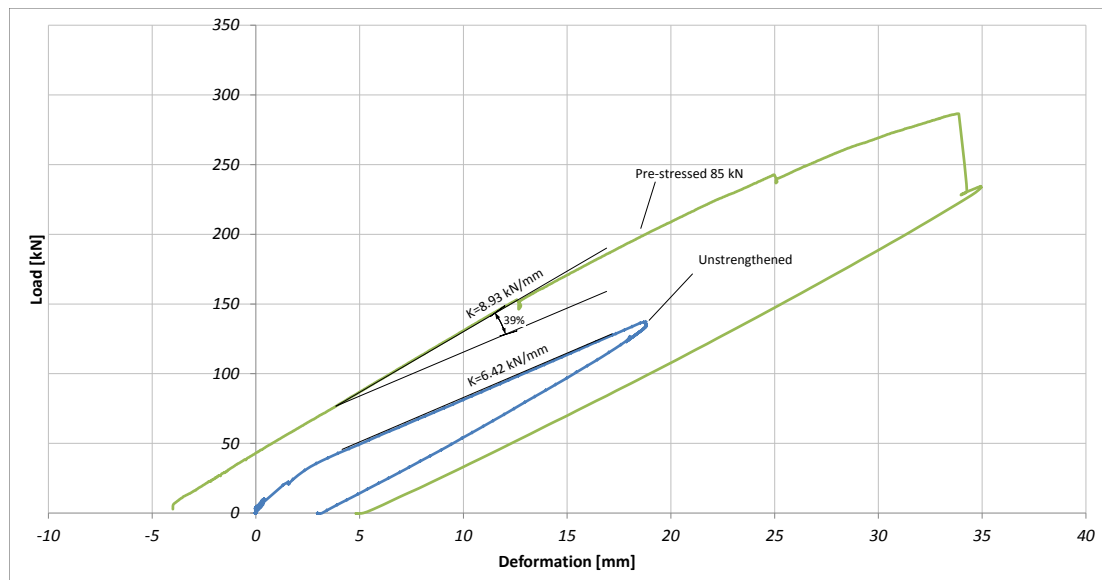


Figure G.7 Improvement of the stiffness in the prestressed beam with initial prestress of 85kN with regard to the unstrengthened beam.